Benchmarking Pavement Performance between Transit's LTPP and CAPTIF Programmes

T.F.P Henning, D.C. Roux and D. Alabaster
MWH New Zealand Ltd, Auckland

An important note for the reader

Acknowledgments

Contents

Executive summary

Introduction

This research project is the second report detailing findings from the NZ Long Term Pavement Performance (LTPP) programme. This programme includes the monitoring of 63 sections on the State Highways and 82 sections on local authority roads. This report details all work related to developing a rutting model for New Zealand conditions. Previous work highlighted some data limitations in the LTTP programme – some of this development work relied on the Transit CAPTIF accelerated pavement testing programme.

This research project also investigated a total new method of predicting rut changes over time including:

- a simplified model proposed for the initial rut/initial densification of the pavement;
- model formats considered for the prediction of the annual change in rutting progression; and
- an additional component to the rutting model added to predict the probable point when the accelerated rut stage starts.

Summary of the results

The results from this research are summarised in Table 1. Note that the results are presented in relation to the original expected outcomes during the initial stages of the project.

Table 1   Summary of results from this research.

Hypothesis	Outcome from this study
Hypothesis 1: Three distinct stages of rut rate progression exist: • initial densification, • stable rut rate progression, and • failure and/or accelerated deterioration.	**True.** The three phases were identified and used effectively in this study. However, bound and strong pavements have only two phases, initial densification and progression.
Hypothesis 2: No significant variables can predict rut progression in a robust manner.	**True.** Rut progression analysis was intensively investigated in this report and no satisfactory outcome was achieved with the current data.
Hypothesis 3: It is possible to find an alternative model to the HDM-4 model for predicting initial densification that uses data which are more readily available on network databases.	**True.** A simpler alternative model was established.
Hypothesis 4: A relationship between the initial densification and rate of rut change exists during the stable phase.	**False.** A relationship was noticed but no robust model could be developed that could predict the rate of rut change.
Hypothesis 5: The failure point in terms of rutting can be predicted based on two methods: For unbound/low volume pavements, the point of commencement of the accelerated rutting can be predicted. Bound and strong unbound pavements will not have an accelerated rut rate stage, but an unacceptable rut depth can be determined based on predictions from the rate of rutting.	**True.** A linear logistic model that yielded satisfactory results was developed.

The models that were developed for predicting rutting include:

<u>Predicting the initial densification rut</u>

$$Initial\ Rut = 3.5 + e^{(2.44 - 0.55SNP)}$$

Where:

    SNP is the structural number as being derived from the Falling Weight Data.

<u>Predicting the rut progression</u>

• For thin pavements (total layer thickness <150 mm), the rate is 0.5 mm per year.
• For thick pavements (total layer thickness ≥150 mm), the rate is 0.3 mm/year.

Predicting the initiation of accelerated rutting

$$p(Rutaccel) = \frac{1}{1 + e^{\left(-7.568\times10^{-6}\times ESA + 2.434\times snp - \left[(4.426, 0.4744) for\ thickness = (0,1)\right]\right)}}$$

Where:

ESA	Equivalent Standard Axles.
SNP	Pavement strength Structural Number.
Thickness	0 for base layer thickness <150 mm, 1 for base layer thickness >150 mm.

Further work

As with many research projects, this research was also limited to achieving only outcomes for which sufficient data were available. However, much was achieved, and using both the LTPP data and the CAPTIF data in the model development work gave excellent outcomes. But some holes in the data still prevented all the objectives from being achieved. In addition to this, the research needs to continue in order to test and expand the applicability of the model developed. A summary of the recommended further work is presented in Table 2.

Table 2   Summary of recommended further work.

Topic area	Description of recommended further work
General applicability of models	The models are data driven models and should therefore be tested on other data in New Zealand, such as network data.
Relative performance of different material types	This study only included thin-surfaced unbound pavements. Some work remains to be completed in order to understand the difference in behaviour between different material types such as dense graded and open graded porous asphalt pavements.
Urban environment	Most of the data included in the current research represented pavements from the rural environment. As the data become available on the Land Transport New Zealand and Local Authority LTPP database, these models should now be tested for local urban pavements.
Operational research	It should be realised that the LTPP programmes delivered a wealth of data for research into practical aspects such as data collection and maintenance practices. For example, the data can be used to validate some maintenance practices used to address rutting. Similarly, a number of aspects can be investigated regarding the data collection of rutting etc. These research areas should be encouraged in order to get the full benefit from the data collected to date.

Abstract

This report details the findings from research conducted on the Long Term Pavement Performance Programme (LTPP) and on the Transit New Zealand CAPTIF programme for accelerated pavement testing. The research was aimed at delivering a complete new model format to predict rut progression on New Zealand roads. It was based on earlier findings that suggested some limitations with the current approach using the World Bank's HDM rutting models.

A three-stage modelling approach is recommended:

- Firstly, a simpler model is proposed to predict the initial rutting or densification.
- Average progression rates are proposed for the annual increase of rutting during the normal life of the pavement since no satisfactory model could yield any results which were more accurate.
- Lastly, a probabilistic model is proposed to predict the probability or risk of a pavement undergoing accelerated rut progression caused by weak layers or overloading.

One benefit that the new proposed model promises is its simplistic format which makes it easy to adopt into a modelling system. Another is it is based on improved accurate pavement condition data. Further work in this area is recommended, mostly on the practical implications of these research findings, and on developing remaining models based on the LTPP programme and CAPTIF experiments.

1.   Introduction

1.1   Introduction to the research

New Zealand embarked on Long Term Pavement Performance (LTPP) studies in 2000 with the establishment of 63 LTPP sections on the State Highway Network. The LTPP sections were expanded to include a further 82 section established on local authority roads during 2003. The intent of the LTPP studies is to provide data for the calibration and development of pavement deterioration models specific to New Zealand conditions. Once successful, these models would be incorporated into the pavement deterioration modelling system (dTIMS) adopted for all levels of road maintenance management in New Zealand.

This research study was conducted as part of the Land Transport New Zealand research programme by MWH, Uniservices and Transit New Zealand (CAPTIF). It is the second major research study completed using the LTPP data. It is also the first study that used the CAPTIF data in conjunction with the LTPP data. The CAPTIF data was included in the study in order to have more data for the failure stages of the pavements, since the LTPP data is still limited in this regard. The first model attempting to use these two datasets is the rutting model. This document contains a full description of the work completed in the rut model development.

For more information on the LTPP programme or on research work completed earlier, the reader is referred to the following publications:

- Henning et al. 2006. A review of the HDM/dTIMS pavement models based on calibration site data. *Land Transport New Zealand Research Report number 907.*
- Henning, Dunn et al. 2004. *Long-term Pavement Performance (LTPP) Studies in New Zealand – Lessons, the Challenges and the Way Ahead.*
- Henning, Costello et al. (2004) The establishment of a long-term pavement performance study on the New Zealand state highway network. *ARRB Journal, Vol 13 No 2.*

1.2   Scope of the report

This report fully covers the model development for rut progression in thin-surfaced pavements in New Zealand. The research work has been documented according to the following sections.

The next part of the introduction provides all the current model details as used for HDM-4. Since the HDM-4 model is still being used widely in New Zealand, it will be used as a reference point for this research. Where applicable, all model outcomes are compared with this model.

Chapter 2 gives a full background to this study. This background includes a brief description of both the LTPP and CAPTIF programmes. A summary of findings from earlier research is presented, which sets the scene for the particular objectives defined for this study. The objectives are then further expanded into the definition of specific hypotheses for the analysis.

Chapters 3 to 6 contains the analyses, results and discussions on the findings.

Chapter Seven summarises the findings and lists areas where further work on rut development is required.

1.3 HDM-4 relationships

1.3.1 Model description

The HDM-4 rutting model consists of the following components:

- initial densification,
- structural deformation,
- plastic deformation, and
- wear from studded tyres.

Only the first three components of the rut progression are relevant to New Zealand conditions. Studded tyres are not used in New Zealand. The following paragraphs discuss the model formats in more detail.

1.3.2 Initial densification

The initial densification is given by::

$$RDO = K_{rid}\left[a_0\left(YE4x10^6\right)^{a_1+a_2DEF}\right]SNP^{a_3}COMP^{a_4} \qquad \text{Equation 1}$$

Where RDO = rutting caused by initial densification (mm)

K_{ri} = calibration coefficient for initial densification

$YE4$ = annual number of Equivalent Standard Axles (ESA)(millions/lane)

DEF = Maximum Benkelman Beam deflection (mm)

SNP = adjusted structural number of the pavement

$COMP$ = relative compaction (%)

a_i = model coefficients

(NDLI 1995)

1.3.3   Structural deformation

It is recognised by engineers that rutting is a very good indicator of structural health for a pavement. For example, rutting is one of the key performance indices used on performance specified maintenance contracts. It is expected that the rutting performance of networks will become more important in future as the understanding of this indicator increases.

HDM-4 provides two forms of rutting progression for cracked and uncracked sections (NDLI 1995):

- Structural deformation for uncracked sections

$$\Delta RDST_{uc} = K_{rst}\left(a_0 SNP^{a_1} YE4^{a_2} COMP^{a_3}\right)$$ Equation 2

- Structural deformation after cracking

$$\Delta RDST_{crk} = K_{rst}\left(a_0 SNP^{a_1} YE4^{a_2} MMP^{a_3} ACX^{a_4}\right)$$ Equation 3

Where:		
$\Delta RDST$	=	incremental increase in structural deformation in the analysis year (mm)
K_{rst}	=	calibration coefficient for structural deformation
$YE4$	=	annual number of ESA (millions/lane)
$COMP$	=	relative compaction (%)
MMP	=	mean monthly precipitation (mm/month)
SNP	=	adjusted structural number of the pavement
ACX	=	area of indexed cracking (% of total carriageway area)
a_i	=	model coefficients

1.3.4   Plastic deformation

The HDM-4 plastic deformation is presented as (NDLI 1995):

$$\Delta RDPD = K_{rpd} CDS^3 a_0 YE4 Sh^{a_1} HS^{a_2}$$ Equation 4

Where		
$\Delta RDPD$	=	is the incremental increase in plastic deformation in the analysis year (mm)
K_{rpd}	=	calibration coefficient for plastic deformation
$YE4$	=	annual number of ESA (millions/lane)
Sh	=	speed of heavy vehicles (km/h)
HS	=	total thickness of the bitumen surface
a_i	=	model coefficients

Default model coefficients are provided for both asphalt and chipseal pavements. The model format and the coefficients have to be validated for New Zealand roads, which often consist of multiple surfaced layers.

2. Background to the study

2.1 LTPP studies in New Zealand

While the asset management system in New Zealand was being implemented, the HDM models were adopted with the knowledge that they would require calibration once the appropriate data became available. The need for calibration has also been highlighted in a number of modelling reports completed for both Transit New Zealand (Transit) regions and local authorities. As a result, two LTPP programmes were initiated:

- Transit established 63 LTPP sections on the State Highways. An annual condition survey is performed on these sections, and during April 2006, these sections were surveyed for the fifth time.
- Land Transport New Zealand, in association with 21 local authorities, established 82 sections on typical local authority roads in both urban and rural networks.

This report documents the calibration results based on the 05/06 Land Transport New Zealand Research round. The analysis was mainly focused on developing a rutting model for New Zealand based on State Highway LTPP data and CAPTIF data.

2.2 The CAPTIF experiment

CAPTIF (Canterbury Accelerated Pavement Testing Indoor Facility) is located in Christchurch, New Zealand. It consists of a circular track, 58 m long (on the centreline) contained within a concrete tank 1.5 m deep and 4 m wide, so that the moisture content of the pavement materials can be controlled and the boundary conditions are known. A central platform holds the machinery and electronics needed to drive the system. A sliding frame is mounted on this platform, which can move horizontally by 1 m. This radial movement enables the wheelpaths to be varied laterally, and can be used to have the two 'vehicles' operating in independent wheelpaths. An elevation view is shown in Figure 2.1**Error! Reference source not found.**.

At the end of this frame, two radial arms connect to the Simulated Loading and Vehicle Emulator (SLAVE) units shown in Figure 2.2. These arms are hinged in the vertical plane so that the SLAVEs can be removed from the track during pavement construction, profile measurement, etc., and in the horizontal plane to allow for vehicle bounce.
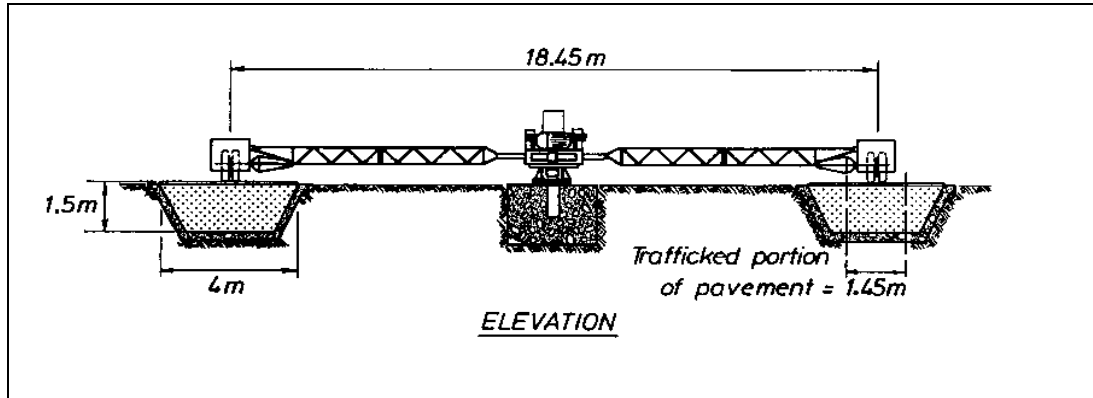
Figure 2.1   Elevation view of the CAPTIF testing equipment.
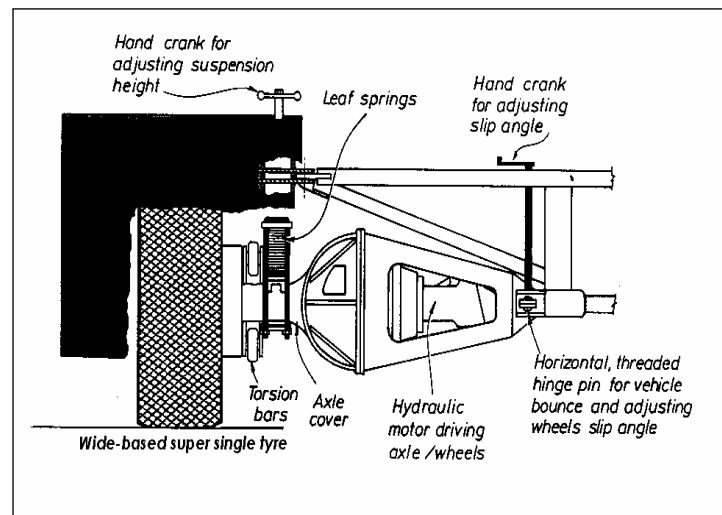
Figure 2.2   Diagram of the key components of the CAPTIF SLAVE unit.

2.3   Combining the LTPP and CAPTIF experiment

The original idea of combining the LTPP experiment with an accelerated pavement testing programme was taken from Martin (2003) and Martin et al. (2004). Martin used accelerated load testing in order to estimate the relative performance factors for all the maintenance treatments for rutting and roughness. Given that Martin's research gave reasonable results, this project included the CAPTIF data for developing pavement deterioration models. More specifically, the CAPTIF data was used since it contains data up to the point of pavement failure (taken as 15 mm rutting).

Some additional benefits from using the LTPP in conjunction with the CAPTIF data included:

- **Gaining a better understanding of the environmental impact on pavements:** The LTPP sections were subjected to normal climatic influences whereas the CAPTIF testing was conducted under controlled conditions. It is therefore possible to investigate the specific environmental impacts on pavement performance, something which is relatively complex to do based on LTPP work alone; and

- **Confirming CAPTIF life cycle and mass limit study results** with the LTPP performance data.

2.4 Findings from earlier research

2.4.1 Cracking

During the 2004/2005 research programme, a new cracking model was developed for New Zealand conditions. This model differs significantly from the original World Bank HDM-type model, since it forecasts the probability of a pavement being cracked as opposed to predicting crack initiation time and crack progression time (See Figure 2.3). This figure illustrates the probability of the pavement cracking in two possible scenarios. Firstly, if the pavement has cracked before resurfacing, the probability of it cracking again is high. However, for pavements that have not cracked prior to resurfacing, we observe much lower crack probabilities for corresponding seal ages.
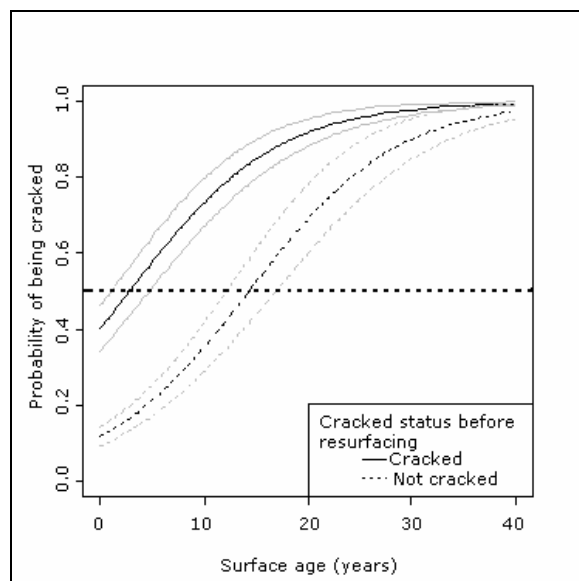
Figure 2.3   Probability of cracking for a given pavement and traffic loading (Henning et al. 2006).

Notes to Figure 2.3:

- Data plotted for**:**
  - annual average daily traffic (AADT) = 2500,
  - total surface thickness of all layers in a pavement (HTOT) = 60 mm,
  - SNP = 2.5.

- Confidence interval plotted for two standard deviations.

- Expected crack initiation where the probability = 0.5.

Developing the crack model development also contributed significantly towards the general understanding of pavement behaviour. Some items learned include:

- Pavement strength was not always a good indicator of pavement performance as explained by cracking.
- The number of surface layers has a significant impact on the performance of a road. It was established that surfaces on a pavement with a total thickness of more than 40 mm are significantly underperforming. A possible explanation for this observation is that with a high number of surface layers, layer stability may become an issue. Also, a higher number of surfaces may indicate an older pavement which performs poorly, and for which resurfacing does not address any failure mechanisms.
- With more and deeper understanding of the deterioration, the actual mathematical model becomes simpler and easier to apply.

2.4.2   Rutting

Previous data analysis suggested that the incremental rut change is relatively small (see Figure 2.4). From the figure, we can make the following observations:

- The majority of incremental rut changes are within plus or minus 1 mm per year.
- Negative rut changes were observed at sections which had either some main-tenance or some measurement errors within the specification of the contract.
- Any sections with rut changes above, say, 1 mm per year were assumed to be in an accelerated deterioration phase. Further queries confirmed that most of these sections have subsequently been rehabilitated.
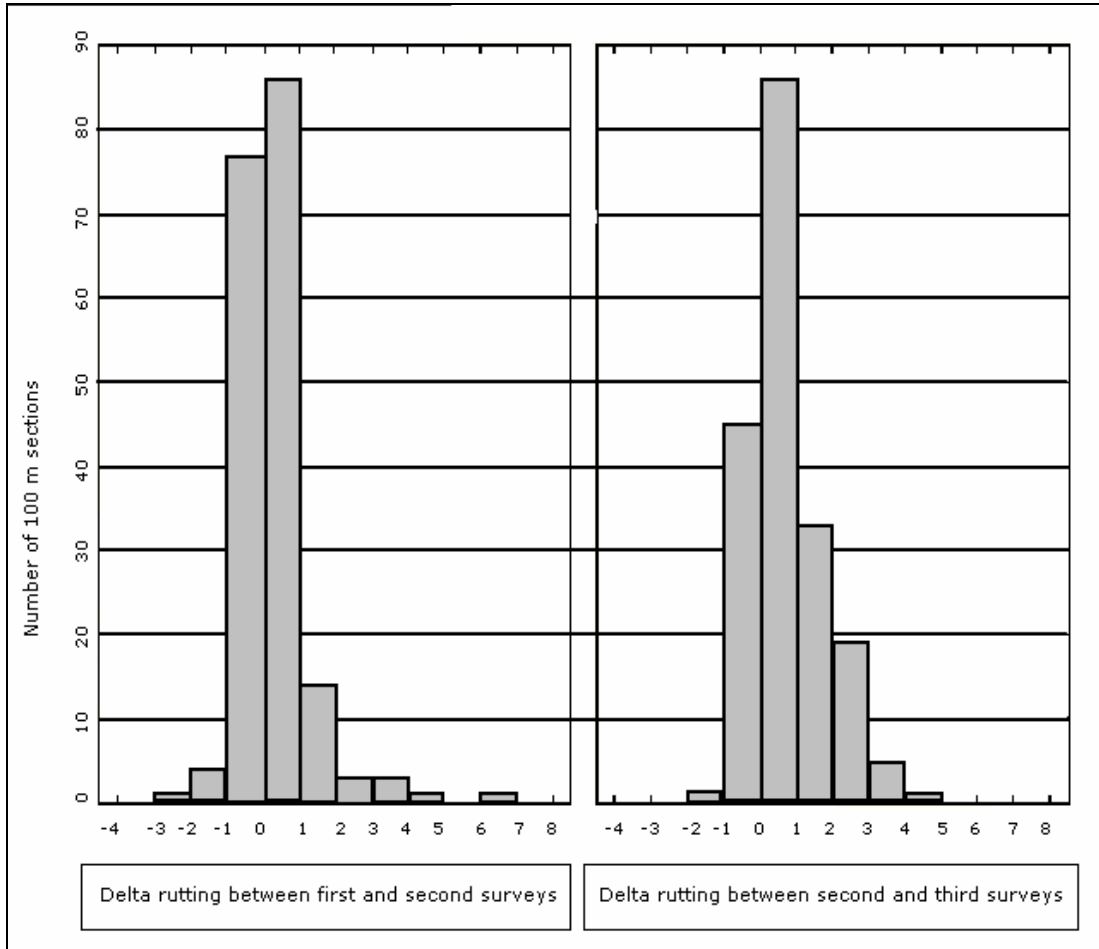
Figure 2.4   Observed incremental rut change during the first three years of the LTPP programme.

Henning et al. (2006) document the rut model calibration according to two stages. Stage 1 consisted of calibrating the model (i.e. adjusting the calibration coefficient) according to an error minimisation method. Note that both the HDM-III and HDM-4 model forms were calibrated. The outcome of this process suggested an unacceptable outcome (low correlation), showing the need to review the model format completely. Stage 2 involved the development of a new model format in order to predict the incremental rut change. This analysis also resulted in an unacceptable outcome (low correlation), for which the following applied:

- The data displayed an overall agreement with the theoretical HDM model format in terms of the two phases of rut progression being an initial densification and a progression phase (this trend is assumed for unbounded base layers and chipseal surfacing).
- No specific independent variable stood out as being a strong moderator of incremental rut change (progression phase).
- All the regression results could not yield any better predictive power than assuming rutting to be changing annually with an average of 0.3 mm per year.

It should be highlighted that the analysis referred to above only included a step-wise regression for a linear model.

2.4.3   Roughness

Previous research into the prediction of roughness deterioration has yielded poor results. While we have a relatively good idea of the development direction for the rutting model, less is known for the roughness model. Some experience of the roughness model suggests the following:

- Roughness deteriorates much more slowly in New Zealand compared to the HDM default model. Calibration coefficients as low as 0.3 and 0.5 are being adopted for the environmental and pavement related calibration coefficients respectively.
- The environmental deterioration is not a gradual deterioration as is suggested in the model. It is a rapid event which may take place at any stage of the pavement life. During the stable phase, the roughness hardly ever changes, even under regular traffic loading.
- The form of the roughness model as a result of traffic-induced loading seems to be inappropriate. For example, the LTPP data confirms earlier claims that the roughness actually improves during the initial stage of pavement use.

Therefore, in terms of the future of roughness model prediction in New Zealand, it can be assumed that a new model will be required.

2.5   Research objectives

The objectives for this research are:

1. **to investigate general model formats observed from the LTPP data and confirm it by comparing it with the CAPTIF data** – this report is particularly interested in the rutting model but also tests some trends on the roughness. Previous research was unable to yield a satisfactory new model format because of some data limitations. However, some significant outcomes in terms of development direction should be considered further. Most of the data limitations were centred around the failing point of the pavement;
2. **to develop relative performance factors for different treatments and material types**, similar to the work completed in Australia (Martin 2004);
3. **to gain a better understanding of the environmental impact on pavements:** The LTPP sections were subjected to normal climatic influences whereas the CAPTIF testing was conducted under controlled conditions. It should therefore be possible to investigate the specific environmental impacts on pavement performance, something which is relatively complex to do based on LTPP work alone; and
4. c**onfirm the CAPTIF life cycle and mass limit study results** with the LTPP performance data.

2.6   Hypotheses for the prediction of rut progression

2.6.1   Rut progression stages

Based on the models developed by earlier research (Henning et al. 2006), two main differences appear between the HDM modelling approach and the actual behaviour of pavements:

- HDM's rut model consists of two phases, namely an initial densification phase and a progression phase. However, initial results based on the New Zealand study suggest three stages, namely: initial densification, progression and accelerated progression. See Figure 2.5.
- The HDM approach suggests an exponential growth of rutting, whereas New Zealand low strength pavements appear to be rutting at a constant rate until a rapid deterioration (blow-out) stage. This trend is mainly caused by relatively low trafficking during the life of the pavements.
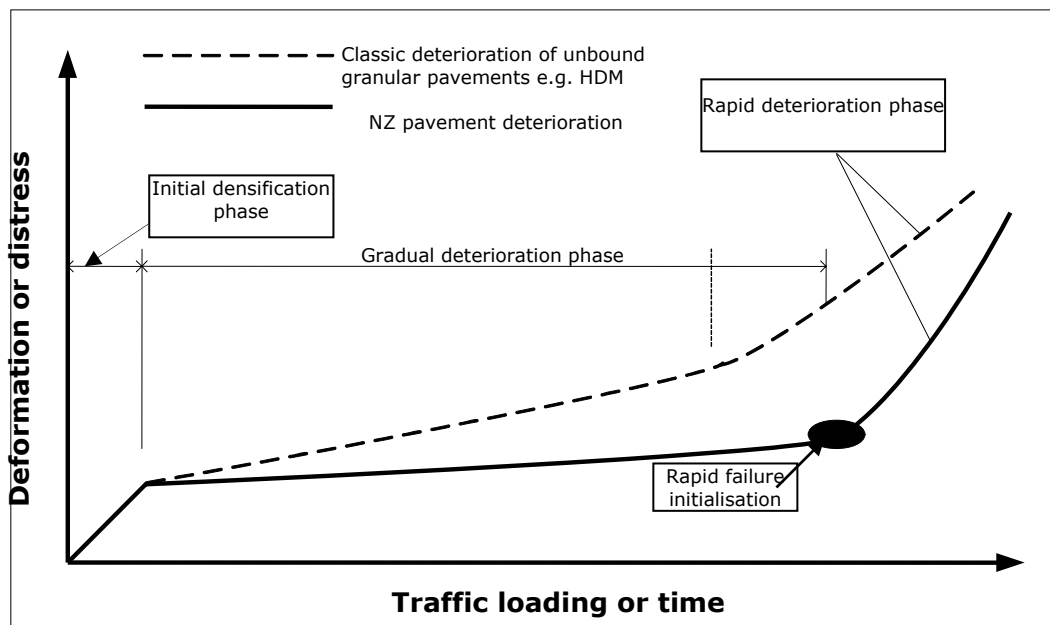
Figure 2.5   Comparing the default HDM rut model with observed rut progression in New Zealand.

Furthermore, it is strongly indicated that rut depth progression occurs at a constant rate which cannot be explained by all assumed variables. For example, having a complex model did not necessarily yield a more robust predicted rut rate than, say, just applying a constant incremental rut rate.

The first hypothesis for this research is:

Hypothesis 1: Rut rate progression has three distinct stages, namely:

- initial densification,
- stable rut rate progression, and
- failure and/or accelerated deterioration.

This hypothesis has been developed with the understanding that it may only be true for certain pavement types and associated traffic classes.

2.6.2   Predictability of rutting

Hypothesis 2: **No significant variables that can predict rut progression in a robust manner exist.**

Although this hypothesis has been addressed to a certain extent in the previous research, the data were not statistically analysed in a significant manner and not all model formats were tested.

2.6.3   Initial densification phase

It appears from network data, previous CAPTIF results and LTPP data that the initial densification differs significantly for varying environmental, pavement and traffic conditions (Arnold et al. 2005). Intuitive trends also suggest that it should be predictable. Based on practical use of the HDM-4 model, it appears that the HDM model adequately predicts this phase.

The CAPTIF experiment confirmed the initial densification to be a valid concept for given load limits (Arnold et al. 2005). However, in practice, network databases do not contain robust (if any) information on compaction; hence much of the model would be based on assumed values. This is not an ideal situation in network modelling.

Hypothesis 3: It should be possible to find an alternative model to the HDM-4 model which uses data that are more readily available in network databases.

2.6.4   Stable rut phase

Initial interpretations from the CAPTIF experiment suggest that a relationship exists between the rut rate (stable phase) and the initial densification. Figure 2.6 illustrates the relative performance of material from a strong and a weak pavement. The theory is that for strong pavements, the initial densification is relatively high, but the rut slope at a later stage of the pavement is much lower compared with weak pavements.
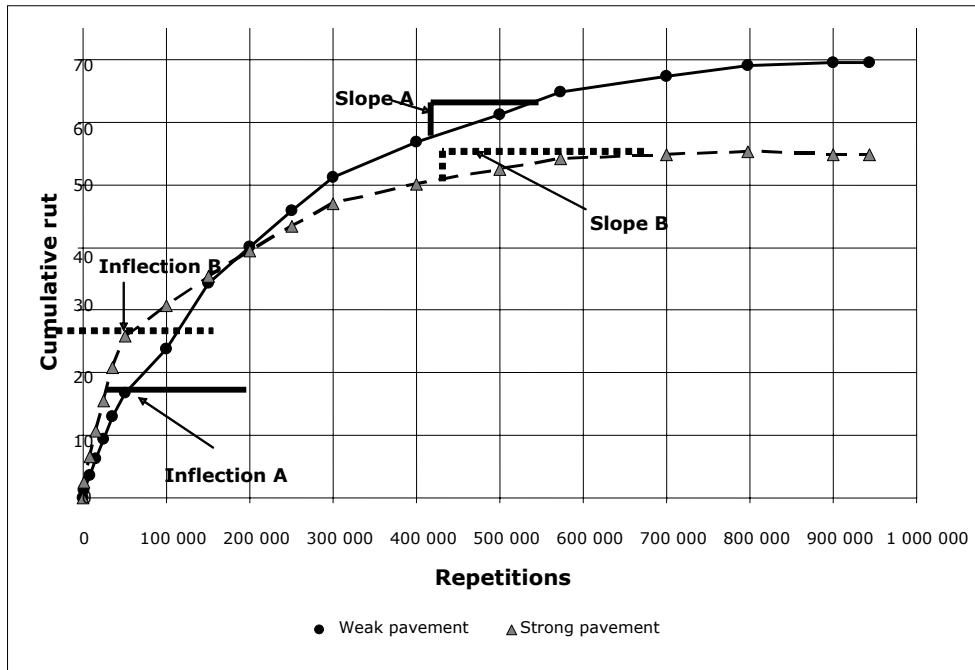
Figure 2.6   Assumed relationship between initial rut densification and rut progression.

Hypothesis 4: **A relationship between the initial densification and rate of rut change during the stable phase can be found.**

If the hypothesis is true, it would suggest that if it is possible to predict one parameter, the other can be inferred.

2.6.5   Accelerated deterioration phase

Based on the theories of pavement design behaviour, a pavement can fail according to two mechanisms specifically related to rutting, illustrated in Figure 2.7 (Visser 1999).

- In unbound pavements/low volume roads, the rutting will remain relatively low until the accelerated blow-out stage commences. During this last stage, the rutting will increase rapidly and emergency rehabilitation is imminent.
- For bound/stronger pavements, rutting will increase on a constant rate until an unacceptable rut depth is reached. No clear point of an accelerated stage could be determined, but because of safety issues, the rut simply gets too deep and a failure is accepted at this level.
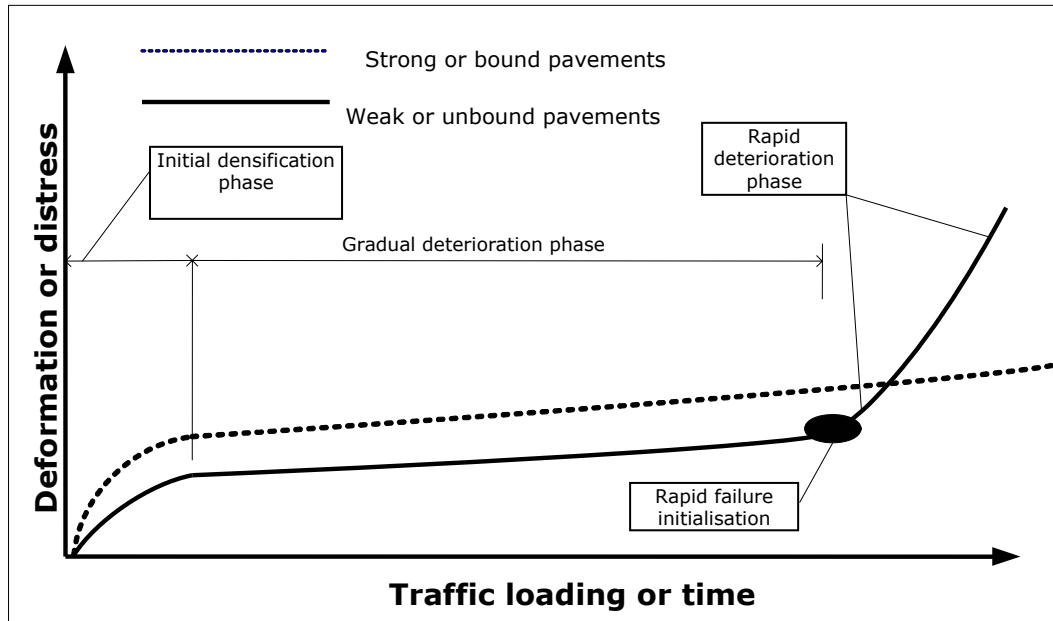
Figure 2.7   Comparing rut progression between bound (strong) and unbound (weak) pavements.

Hypothesis 5: The failure point in terms of rutting can be predicted based on two methods:

- For unbound/low volume road pavements, one can predict when the accelerated rutting will start.
- Bound and strong unbound pavements will not have an accelerated rut rate stage, but an unacceptable rut depth can be determined based on prediction outcomes (see 2.4.2 and 2.4.3).

3.   Predicting initial rut depth

3.1   Analysis process and data used

The data use and analysis process for this chapter is illustrated in Figure 3.1.
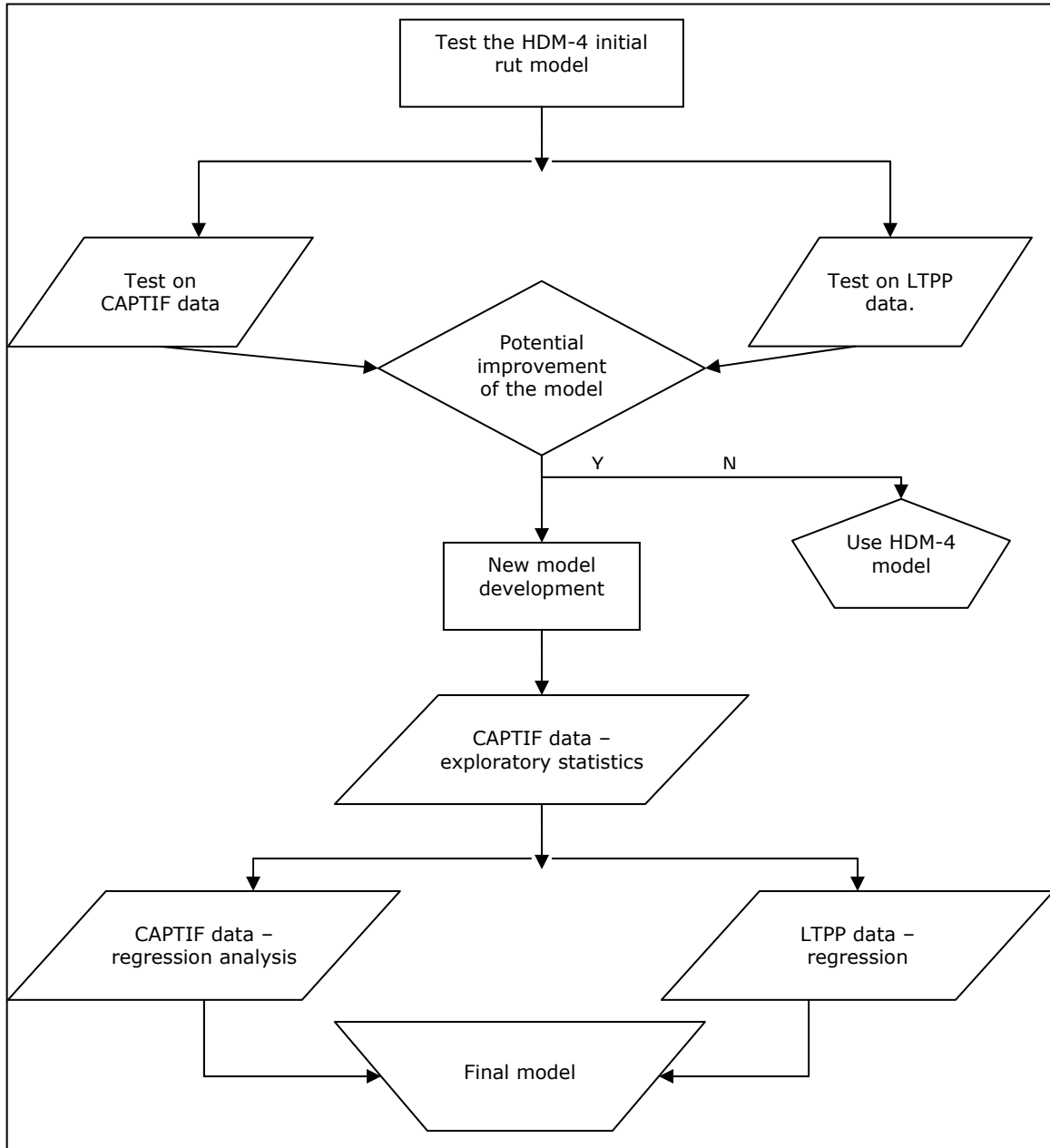

Figure 3.1   The analysis approach and data used for determining the initial rut depth.

3.2   Testing the appropriateness of the HDM initial rut model

3.2.1   Testing the HDM initial rut model on CAPTIF data

The CAPTIF data are ideal for investigating the initial densification of pavements, given the controlled conditions for constructing the pavement and monitoring its wear. Therefore, rather than using in-service pavements, the researchers have a clear understanding of the pavement make-up and the construction quality. By removing the uncertainty associated with these factors, a much better understanding can be obtained from the long term behaviour of the pavement.

The data used for the densification analysis were sourced from the PR3-0810 Fatigue CAPTIF experiment (Alabaster et al. 2006). Five pavement types were investigated; these are listed in Table 3.1 and Figure 3.2. Note that all the sections were surfaced with either Asphalt Concrete (AC) or Open-Graded Porous Asphalt (OGPA). Earlier work at CAPTIF suggested poor performance of chipseal surfaces, given the loading conditions, while the pavement behaviour was similar regardless of the surface type used.

Table 3.1   Pavement sections tested inthe CAPTIF experiment (based on Alabaster et al. 2006).

Section	Surface material	Subgrade material	Avg CBR	Min CBR	Max CBR	Base layer thickness (mm)	Pavement classification
A	AC	Tod[a] OMC[b]	7	7	8	150	thin + strong
B	OGPA	Tod OMC	9	9	10	150	thin + strong
C	OGPA	Tod OMC + 10%	2	2	2	150	thin + weak
D	OGPA	Tod OMC + 10%	3	2	4	300	thick + weak
E	OGPA	Tod OMC	8	8	9	300	thick + strong

Notes to Table 3.1:
(a)   *'This material has been named Tod Clay after the owner of the pit from which it was excavated. The soil has a workable consistency due to the mica content and has a relatively low susceptibility to shrinkage and swelling due to the predominant kaolin mineral.'* (Steven et al. 1999)
(b)   OMC = Optimum Moisture Content
(c)   CBR = California Bearing Ratio
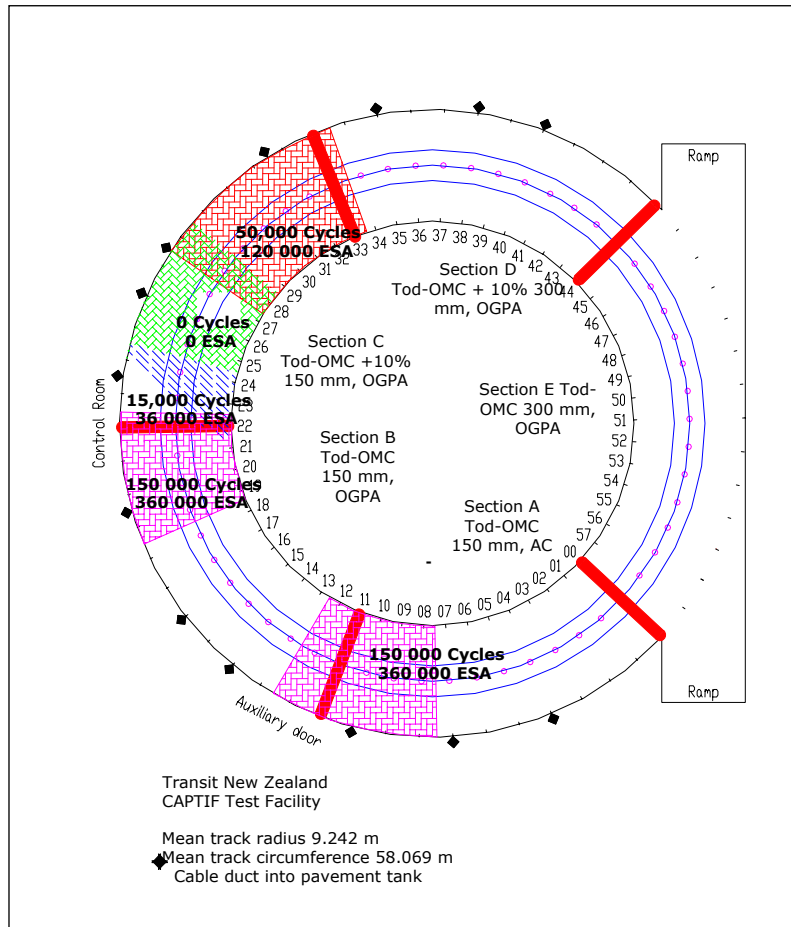
Figure 3.2   Pavement layout and failures for the PR3-0032 experiment (taken from Alabaster et al. 2006).

Notes to Figure 3.2:

- Different pavement configurations were constructed for each section (A to E).
- Each section consisted of 10 station numbers (measuring reference points).
- Sections marked in thick red represent transition stations between different pavement types.
- Failure in a section is defined as when the rut depth reaches 15 mm.

It can be observed from the layout and failure diagram that most of the early failures took place on the sections with thin base layers. It was also noted that the earliest and the most prominent failures took place in Section C (thin and weak) pavement. As a result, the data from Section C should be viewed with care, especially considering the initial densification stage.

One of the first aspects to investigate was the actual point where the initial densification is completed. The CAPTIF data was plotted using the cumulative deviation sums (CUSUM) approach. This method plots data and records the cumulative deviation from the average of each data point in much the same way as the score is kept in golf. With every significant slope change of the plots, it is expected that the trend has changed.

Figure 3.3 illustrates the CUSUM plots for the rut development in the CAPTIF experiment. Ruts develop unsteadily during the initial phases up to approximately 50 000 cycles. After 50 000 cycles, most rut development becomes stable for longer periods. The 50,000 cycles equate to approximately 100 000 ESA, which roughly equates to 12 months of

traffic for an assumed AADT of 2500 and a 15% heavy vehicle percentage. Therefore, one can expect a 6–12 month initial densification on typical state highways. This period correlates well with intuitive estimates of rut densification. For the purpose of this study, it will be assumed that the initial rut progression is completed at 50 000 cycles inthe CAPTIF experiment. The actual initial densification of in-service pavements needs to be confirmed by either the LTPP data or actual network data. An interesting conclusion from this graph is that although the sub-grade and base material differed, initial densification was achieved at a similar stage but the actual level of densification differed.
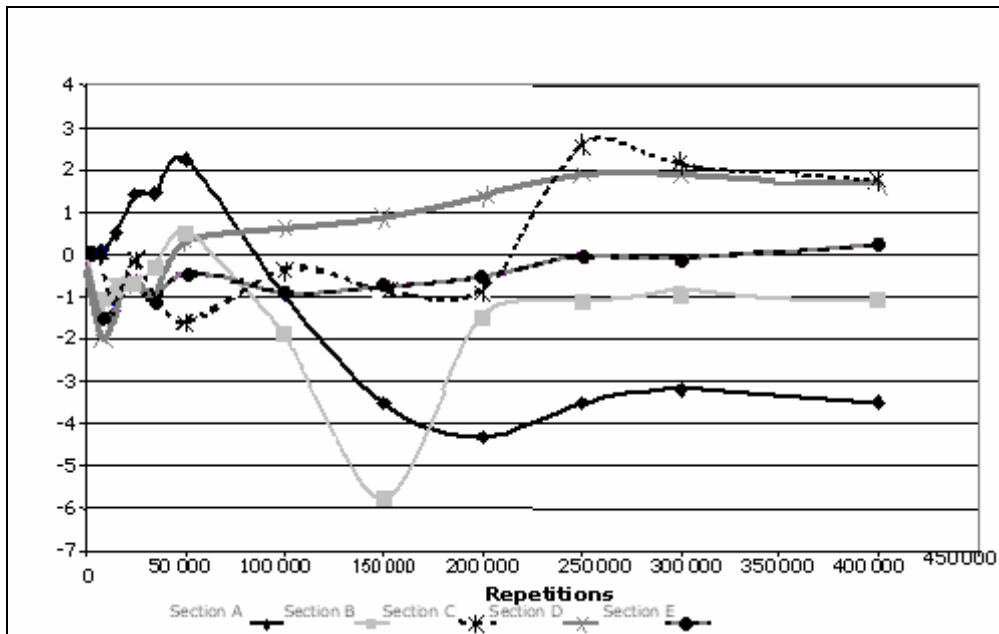
Figure 3.3   CUSUM plot for the rut development using the CAPTIF data.

Figure 3.4 compares the predicted (according to the HDM rut densification model) and actual initial densification for the five sections tested in the CAPTIF experiment. Most of the sections – except for Section C – demonstrated similar initial densification patterns. Again, the performance of Section C has led to the belief that this section should be removed from further analysis in determining initial rut depth.
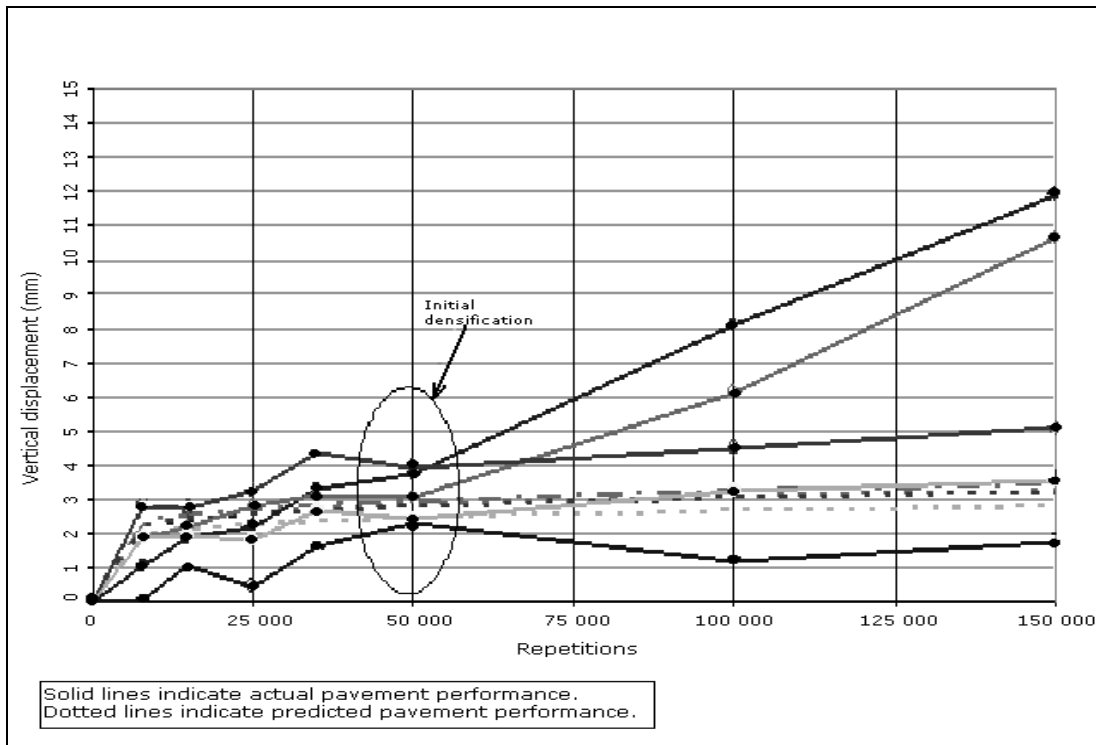
Figure 3.4 Comparing predicted and actual initial rut depth, using the CAPTIF data.
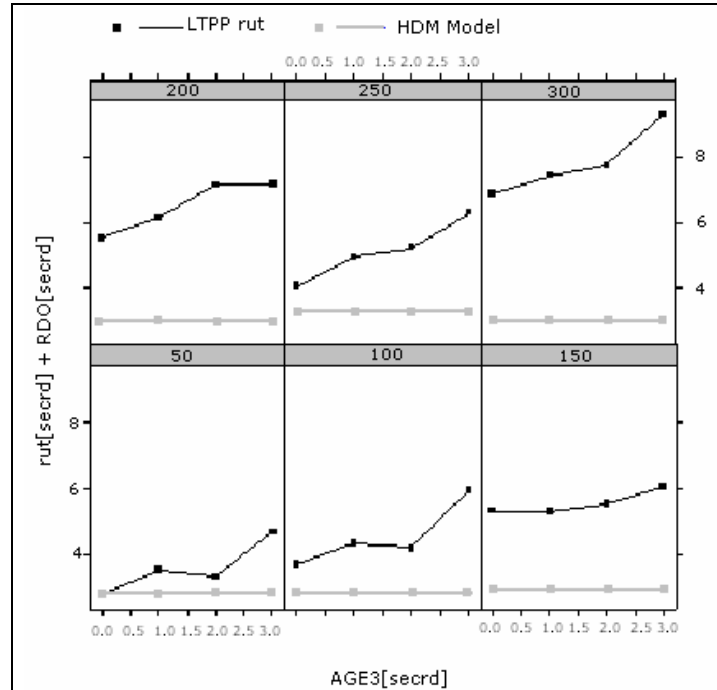
The predicted initial densification compares relatively well with the actual observations – i.e. CAPTIF data. However, the range in the predicted densification varies between three and four millimetres. The corresponding observations from the measurements varied between two and four millimetres. This difference is not considered to be too significant. However, the initial densification is used as a starting point for subsequent models and making it more accurate will ultimately contribute towards a more accurate overall outcome.

3.2.2   Testing the HDM initial rut model on LTPP data

The HDM-4 model (See Chapter 1.3.2) has been fitted and compared to the LTPP data. Six of the Transit LTPP sections have been reconstructed during the monitoring period. The survey interval on the LTPP programme is relatively infrequent compared with the CAPTIF experiment. The LTPP data survey is undertaken on an annual basis; measurements on the CAPTIF experiment roughly equate to an equivalent measurement every three months. Also, the timing of the first survey measurements after construction has varied for all the LTPP sections. For this reason, the predicted initial densification rut was compared with at least three years of measurements.

Examples of the typical outcomes of this comparison are presented in Figure 3.5, while additional outputs for the other sections are presented in Appendix A. This figure depicts the outputs of Section CAL-19 in a decreasing direction. It shows that some of the actual rutting varies significantly from the predicted initial rutting (estimated to be just under 3 mm). Some of the actual initial rutting was as high as 7 mm.

Figure 3.5   Comparing predicted versus actual initial rut depths on LTPP Section CAL-19 (decreasing chainage).
Notes to Table 3.5:
(a)   rut[secrd] is the actual rut from LTPP sections.
(b)   RDO[secrd] is the HDM predicted initial rut/initial densification.
(c)   AGE3 [secrd] is the pavement age of the LTPP section.
(d)   Each block represents the average rut depth at different pavement ages (AGE3) along a 50 m subsection of road. Each subsection is labelled by where it ends along the test section (i.e. the first 50 metres of the test section is labelled '50' and so on.
(e)   The vertical axis indicates the rut depth (predicted and actual).

Some observations from all the outputs include:

- The difference between the predicted and the actual rut depths do not show any patterns. No trends were observed in relation to assumed strong/weak pavements, and no trends were observed in relation to the left and right wheelpaths. It was somewhat unexpected to notice relatively high rut depth during initial densifications in the right wheelpaths.

- A reduction in rut depth compared to the rut depth during initial densification for some sections was not uncommon.

- Some sections have demonstrated a significant rut progression within the first three years of the section age (See the diagrams for CAL-12, CAL-19 and CAL-32 in Appendix A).

Some practical considerations during the interpretation of the rut information include the road profile changes during the initial densification period as the material settles under the movement of the traffic. The interpretation, according to the computer simulation, of the transverse profile is therefore not necessarily simulating the true rut accurately. For example, if a road is widened, a depression is often formed at the joint between the old and new pavements. Transverse measurements of this profile may indicate a rut, but it may not be a traffic-induced rut at all.

Simulations of the true rut depth at a later stage of the pavement life are expected to be much more accurate. Also, during the initial stages of pavement life, the rut depth is also influenced by the road texture. For example, Henning et al. (2006) demonstrated the influence of surface texture on rut depth trends.

3.3 New model development

3.3.1 Exploratory statistics

3.3.1.1 Variables used

Based on the CAPTIF data discussed in the previous section, a model development process was undertaken to yield the initial densification following construction. This section discusses the exploratory statistics with the aim of establishing visual trends and/or determining the factors that influence the level of initial densification. The variables available to the analysis are shown in Table 3.2.

Table 3.2   CAPTIF data variables used in model development.

| Variable	Description	Variable Type
type	Pavement type (See section description in Table 3.1)	text
DEF	Peak deflection in mm	number
SNP*	Pavement structural number	number
COMP	Relative compaction in %	number
Layer	Layer type	text
DD	Dry density	number
WD	Wet density	number
MC	Moisture content (in %)	number
PR	Density	number
%$_{SAT}$	Percent saturation	number
CBR	Californian Bearing Ratio	number
REPS	Wheel load repetitions	number

* The SNP is derived from the peak deflection using Slat's Method (HTC 1999).

3.3.1.2 Pavement strength/deflection

The previous section indicated that Section C (thin, weak pavement) may not be appropriate for use in the initial densification analysis. The rut trend on this section did not indicate a clear initial densification stage. Rather, it suggested that the section started to fail immediately, thus being unable to sustain the tested loading. In the CAPTIF

experiment, a rut was taken as a failure. This theory was tested on the initial densification data as indicated in Figure 3.6. This figure illustrates the data including and then excluding Section C for the initial rut depth as a function of SNP. Note that the initial rut depth was determined (according to Chapter 3.2.1.) at the point of 50 000 repetitions. The data that included Section C indicated some negative rut depth values, which was traced back to pavement patches following early failure as indicated in Figure 3.8. It can therefore be safely confirmed that the data from Section C is to be excluded from further analysis.

Figure 3.7 excludes Section C, and a much clearer trend is observed. In this figure, the smoothing line of the data points suggests a visible trend between the SNP and initial rut depth. As expected, the initial rut depth decreases with an increase of the SNP. It is observed, though, the data presented vary significantly. Figure 3.9 illustrates the rut depth as a function of the peak deflection.
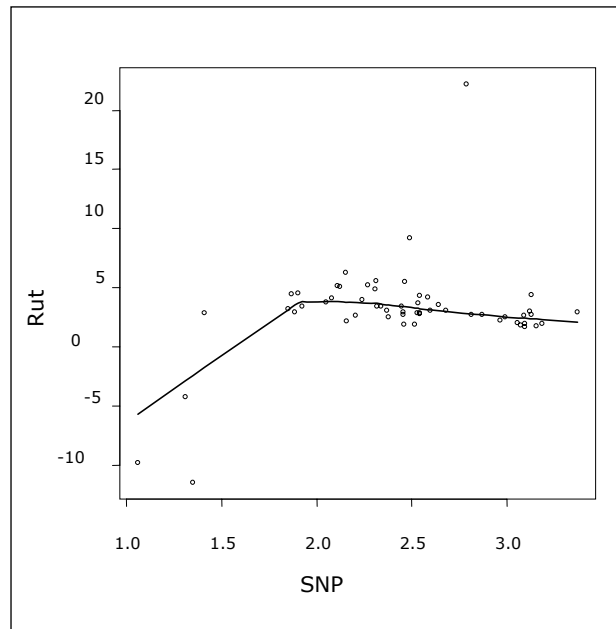
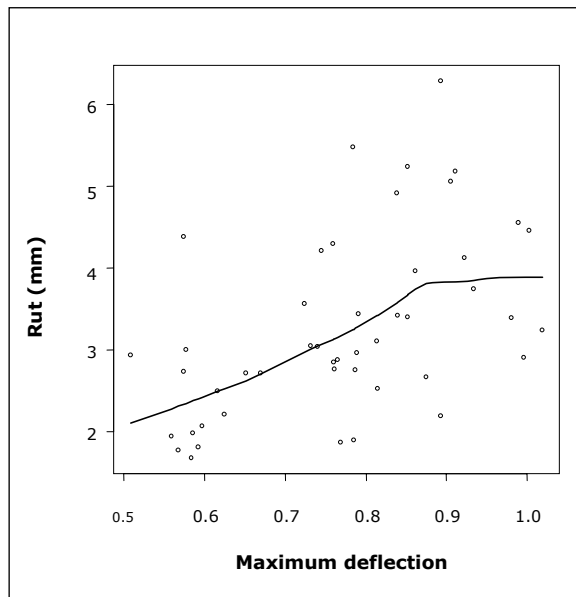**Figure 3.6   Comparing the influence of SNP on initial rut depth.**
Note: The data regarding initial rut depth included data from Section C (thin, weak pavement).
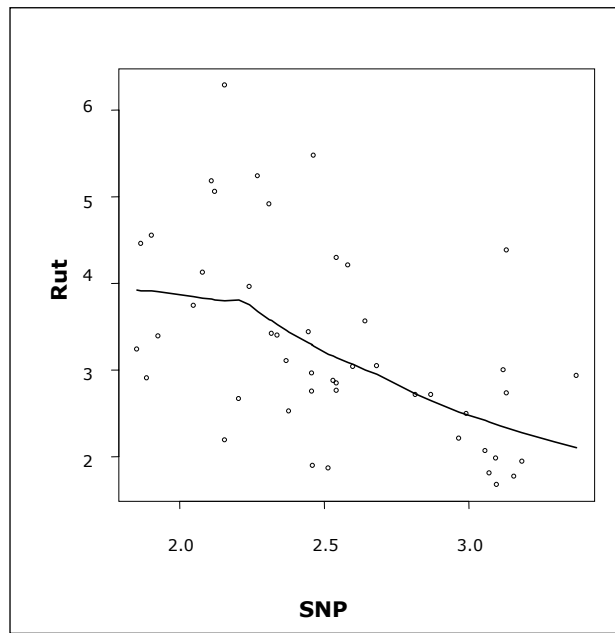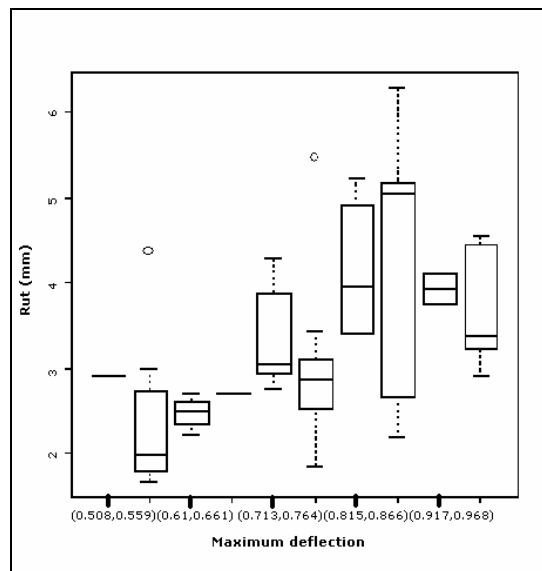
Figure 3.7   Comparing the influence of SNP on initial rut depth excluding data from Section C.

Figure 3.8   Failure at 50 000 repetitions in Section C of the CAPTIF experiment (Alabaster et al. 2006).

Figure 3.9   Initial rut densification as a function of maximum deflection.

Figure 3.10 Initial rut densification as a function of maximum deflection – scatter diagram.

The peak deflection yielded similar results to the SNP, as it was derived from the deflection data. It was therefore expected to have a similar relationship to the initial densification, with the only difference being an inverse scale (as deflection increases, SNP decreases). Figure 3.9 does show an increased initial rut depth with an increased peak deflection. In both sets of data (peak deflection and SNP), a logarithmic relationship with the initial rut depth is apparent. This trend needs to be investigated further with regression analysis. The scatter in the data was also investigated (see Figure 3.10). The scatter in the data was fairly uniform, except for the deflection ranges between 0.87 and 0.91 mm. Similar deflections were observed on totally different structural make-ups. For this range, extremely low and high initial ruts were observed.

Given that the SNP is derived from the peak deflection, these two variables are co-linear and only one was ultimately used in the final model. The more appropriate of these two was determined following the regression analysis.
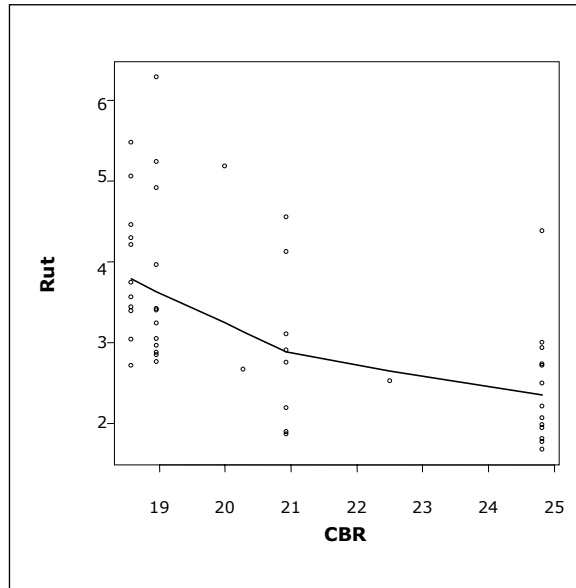
3.3.1.3 Moisture content and CBR

The impact of the moisture content and CBR on the initial rut depth is illustrated in Figure 3.11. Both these factors yielded some expected relationships with the initial rut depth, as follows:

- The maximum rut depth during the initial densification phase was noted at a moisture content of approximately 3.2. This corresponds well with the compaction theory, which states that a maximum densification will be achieved at a certain given moisture content (the optimum moisture content).
- For higher CBR values, smaller initial rut depth values were observed. It is expected that weaker sub-grades will demonstrate higher densification values.
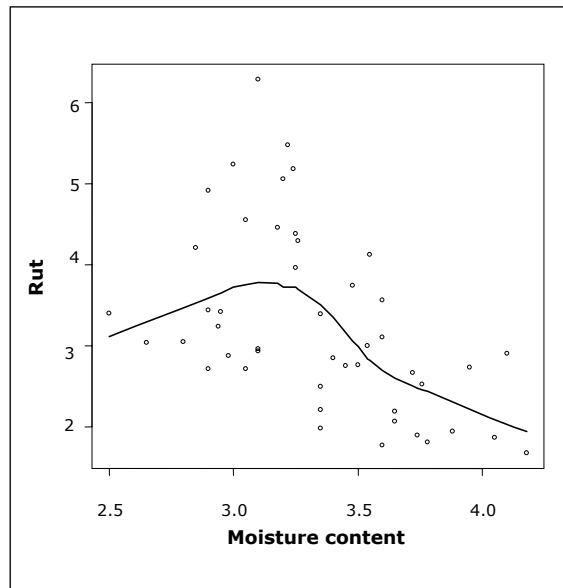
Figure 3.11 Initial rut depth as a function of moisture content.

Figure 3.12 Initial rut depth as a function of moisture content and CBR.

3.3.1.4 Other factors

Graphs depicting the relationship between initial rut depth and other factors are presented in Appendix A4. None of the other factors tested indicated conclusive relationships with the initial rut depth. These factors include:

- density,
- base layer thickness, and
- surface type.

3.3.1.5 Co-plots

Considering only a one dimensional relationship between the dependent and independent variables can sometimes be misleading. For this reason, co-plots were also depicted to test interdependent relationships. Additional plots that contributed little additional information are listed in Appendix A.

3.3.2   Regression analysis based on CAPTIF data

The regression analysis performed on the CAPTIF data yielded results which are consistent with observations made in the previous section. That is, the significant factors predicting initial rut densification are the moisture content, maximum deflection or the structural number. Table 3.3 lists the results from the step-wise model regression. The regression resulted in a relatively low Akaike's Information Criterion (AIC)[1] of 124, but further attempts are possible, lowering the AIC further and suggesting a better solution. A similar regression was also completed using SNP instead of the maximum deflection, and

---

[1] The AIC is like a fault term, with the lower values indicating a better fit with the observed data. The best model (i.e. the one with the greatest number of significant variables) is determined by finding the best combination of variables in order to minimise the AIC.

this regression had exactly the same outcome, as was expected. An explanation of the significance codes used in Table 3.3 and throughout this document is given in Table 3.4.

Table 3.3   Linear model regression for rutting initial densification.

	Estimate	Standard error	t value	Probability (>|t|)	Significance
Intercept	1.30	0.451	2.89	0.006	**
Moisture content	-0.38	0.093	-4.12	0.000	***
Max deflection	1.35	0.313	4.33	$8.70*10^5$	***
Thickness	0.13	0.085	1.50	0.14	
AIC	–	–	–	–	124.65

Table 3.4   Symbols used for the significance codes.

Value	Code
0	***
0.01	**
0.05	.
0.1	

A further analysis was completed in order to test whether to use the maximum deflection in a linear format, or to use a logarithmically transformed maximum deflection. This analysis resulted in the maximum deflection having a t value of 3.86 and a significance Pr(>\|t\|) of 0.004. Therefore, the robustness of the model was not increased by using a log-transformed maximum deflection.

Figure 3.13 illustrates the residual plots for the linear model that predicts the initial rutting densification. With these residual plots, the intention is to have a uniform distribution of the residuals (difference between predicted and actual values). If an uneven distribution is observed, it is possible to use another model format in order to improve the overall model. The histogram (Figure 3.13b) indicates a slightly uneven distribution of the residuals. In order to improve this, all the data were transformed into a logarithmic function, and a significantly better residual outcome was achieved (See Figure 3.114). Also, the overall model had an improved fit with an AIC of 4.9, suggesting a much more appropriate model format for the prediction.
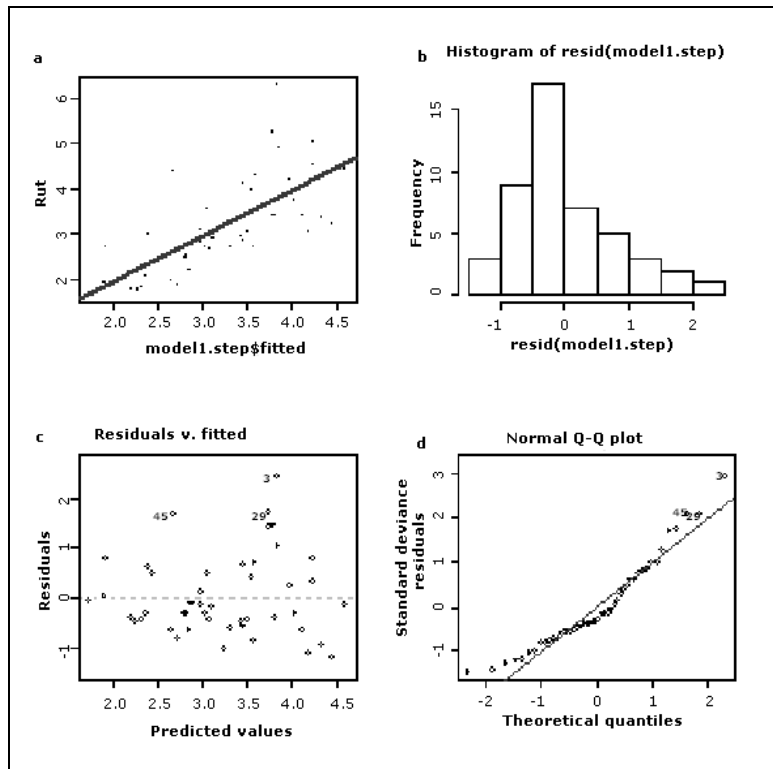
Figure 3.13 Residual plots for the linear model predicting initial densification.
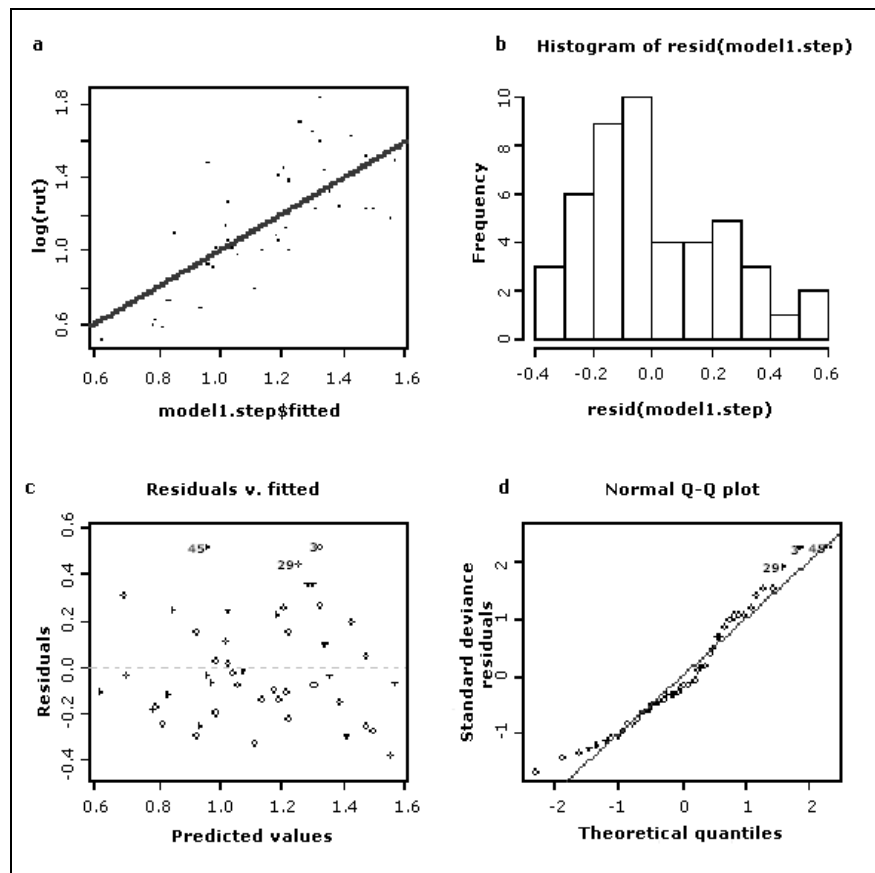

Figure 3.14 Residual plots for the linear model predicting initial densification (logarithmically transformed data).

Based on the results presented in Table 3.3, and Figures 3.13 and 3.14, two more aspects needed further investigation:

- The inclusion of the moisture content is of concern, since theory suggests that the relationship between moisture and compaction should be asymptotic. The dataset in the CAPTIF experiment therefore lacked the full range of expected moisture values, since these were not part of the experiment objectives. The moisture content only had a maximum value of 4.2 (see Figures 3.11 and 3.12). A further concern would be that the moisture content is a data item which is not readily available on network data, thus making it unsuitable for a model based on this data.
- The original HDM-4 model includes both the maximum deflection and the SNP. Both these factors and the inter-relationships between them should be investigated in the initial rutting model. However, according to this study, these two variables are co-linear and should therefore be used with care.

The model regression was repeated, testing most of the possible combinations of SNP and thickness, and excluding the moisture content as a parameter. The resulting model coefficients are listed in Table 3.5 and the residual plots are presented in Figure 3.15.

Table 3.5   Linear model regression for initial rutting densification using only SNP and thickness as predictors (based on CAPTIF data).

	Estimate	Standard error	t value	Probability (>|t|)	Significance
Intercept	2.44	0.279	8.766	3.30 e-11	***
SNP	-0.551	0.119	-4.635	3.19 e-05	***
Thickness.f300	0.161	0.099	1.633	0.11	
AIC:	–	–	–	–	18.04
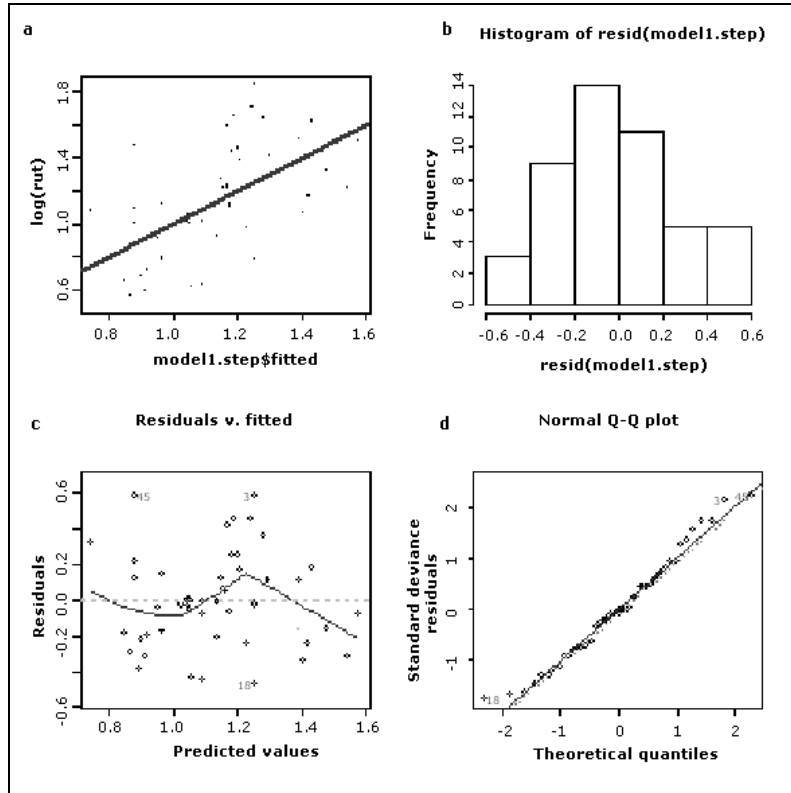
Figure 3.15 Residual plots for final outcome of the predicted initial rut depth using only SNP and thickness as predictors.

Both the table and the residual plots indicated a satisfactory model outcome. Figure 3.16 shows the model outcome for the HDM and the model derived from the CAPTIF data. Note that the model reported in Table 3.5 had to be calibrated in order to fit with the actual LTPP data.

The adjusted and final recommended model is:

$$Initial\ Rut = 3.5 + e^{(2.44 - 0.55SNP)}$$ [Equation 5]

Where:
SNP is the structural number derived from the Falling Weight Deflectometer data.

Figure 3.16 illustrates that the HDM model predictions have a larger variance in predicted initial rut depth, since they considered more factors than just the SNP. However, the general trend is very similar to the model developed on the CAPTIF data. A significant variance between the initial rut depths observed in the LTPP data and the predicted initial rut depth remains.
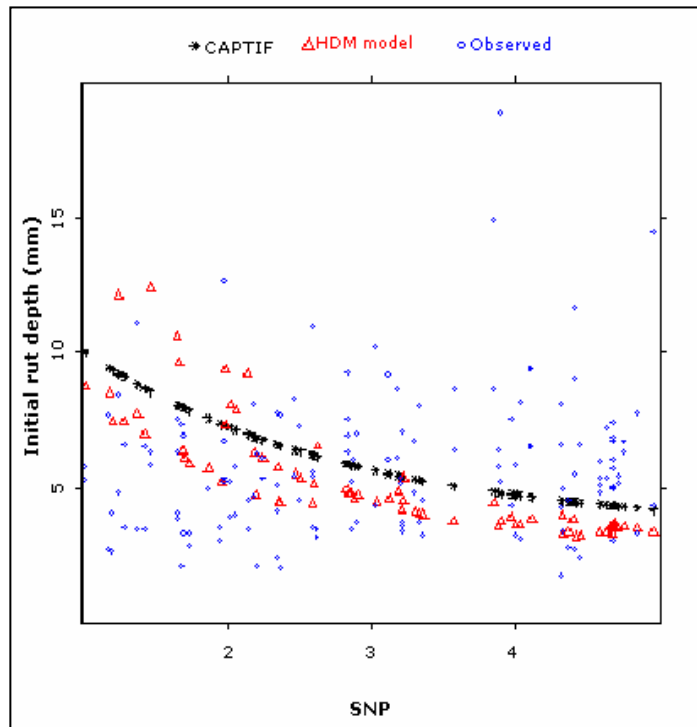
Figure 3.16 Plot of the initial rut model developed on the CAPTIF data using SNP as a predictor (plotted against LTPP observed data).

3.3.3   Regression based on the LTPP data

The regression was repeated on the six sections available from the LTPP data that were newly constructed pavements. The results obtained from this analysis had similar outcomes compared to the previous section. Again, the rainfall data (inferred moisture content) was a significant predictor of the initial rutting. However, the trend was unexpected in the sense that higher moisture content/rainfall predicted lower initial rut levels (See Figure 3.17). The rainfall was subsequently removed from the regression analysis; the resulting model outcomes are presented in Table 3.6.
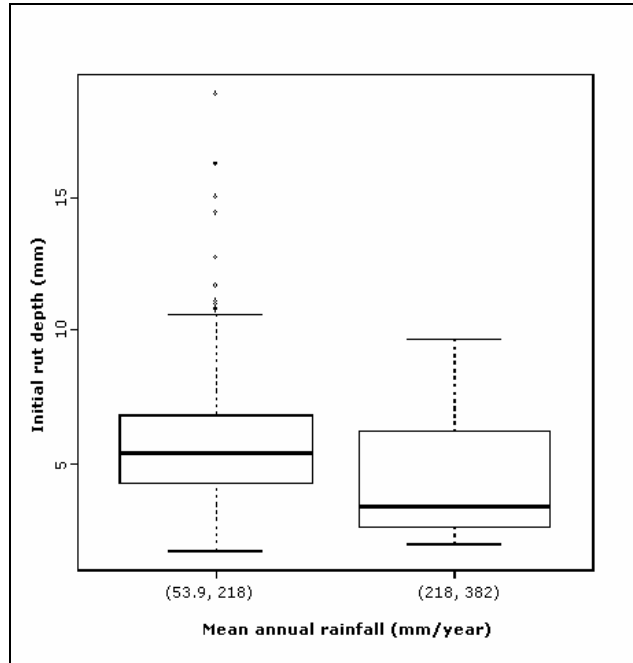
Figure 3.17 Relationship between annual rainfall and initial rut depths.

Table 3.6   Linear model regression for initial rutting densification using maximum deflection as a predictor(based on LTPP data).

	Estimate	Standard Error	t value	Probability (>|t|)	Significance
Intercept	1.61 e+00	6.12 e-02	26.32	<2 e-16	***
Maximum deflection	6.15 e-05	6.29 e-05	0.978	0.329	
AIC	–	–	–	–	233.33

The table indicates that the maximum deflection was the best predictor, yet its significance is relatively low. Also, as it has a small coefficient, the model has little predictive power, as illustrated in Figure 3.18. Therefore, the model developed on the CAPTIF data delivered a more robust model.
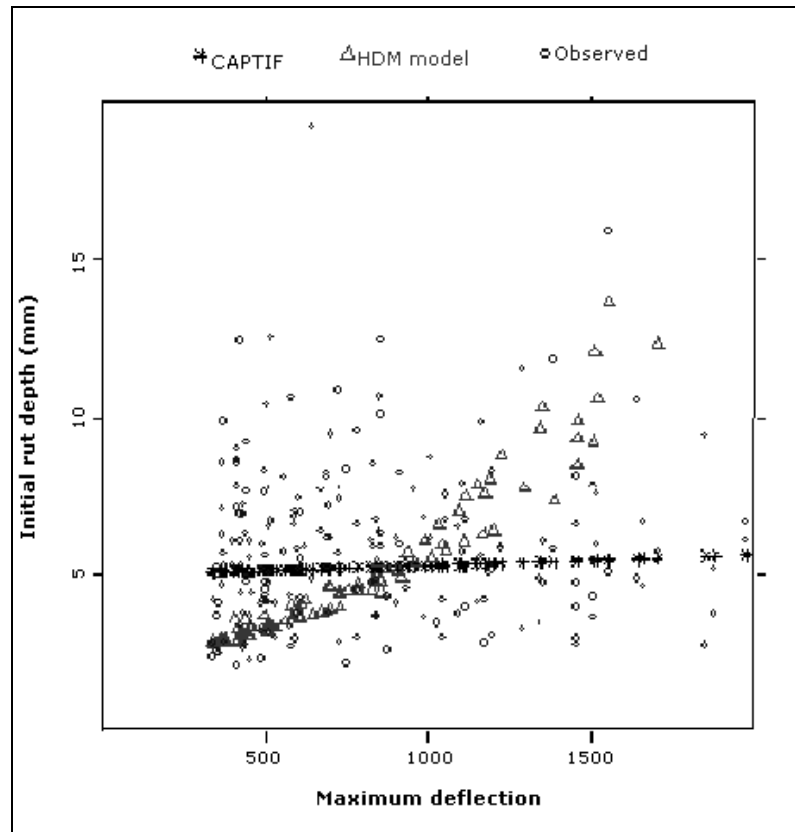
Figure 3.18 Plot of the initial rut model using maximum deflection as a predictor (developed on the LTPP data).

3.4   Discussion

The objective of the analysis work documented in this chapter was to develop a model to predict the rut depth during initial densification. This considered exploratory statistics, applied the HDM model to the existing data and developed an initial rut depth model from first principles. Some general observations are:

- The significant factors for predicting initial rutting included deflection, structural number and moisture content.
- Models developed based on first principles all had a logarithmic relation with the initial rutting.
- All the models, including the HDM model, showed a significant variation in predicted versus actual rut observations.

From the regression analysis, it became evident that many other factors contribute towards the initial densification and these are not available in the databases. Some of these factors may include:

- the material properties of the layers, such as angularity or plasticity;
- the loading of the pavement, including actual axle mass and wandering effect of the vehicles;
- moisture conditions during construction, plus prevailing moisture during the initial densification stage; and
- the road's transversal profile.

It is therefore accepted that with the data we have available, a perfect model would be an unrealistic expectation.

The next issue is to compare the HDM model with the model developed on the CAPTIF data. The main difference between the model formats is that the HDM model considers more variables. In the application of the model in New Zealand conditions, the deflection and structural numbers are co-linear variables because most of the structural numbers would be based on deflection data. The second difference is that the HDM model includes a traffic loading variable, which suggests that different traffic loadings will result in a different level of initial rut depth. However, both the CAPTIF and the LTPP data suggest that the time taken for the initial rut to develop would be a function of the traffic level, but the traffic level will not influence the initial rut depth value. Arnold et al. (2005) indicated that the initial rut depth will only vary for different mass loadings per vehicle.

The HDM-4 model and the CAPTIF model did not yield significantly different results in predicting the initial rut depth. Therefore, both models should be tested on a network level in order to establish the most robust outcome.

4. Testing Hypothesis 2: predicting rut progression as a constant rate based on LTPP data

4.1 Analysis process and data used

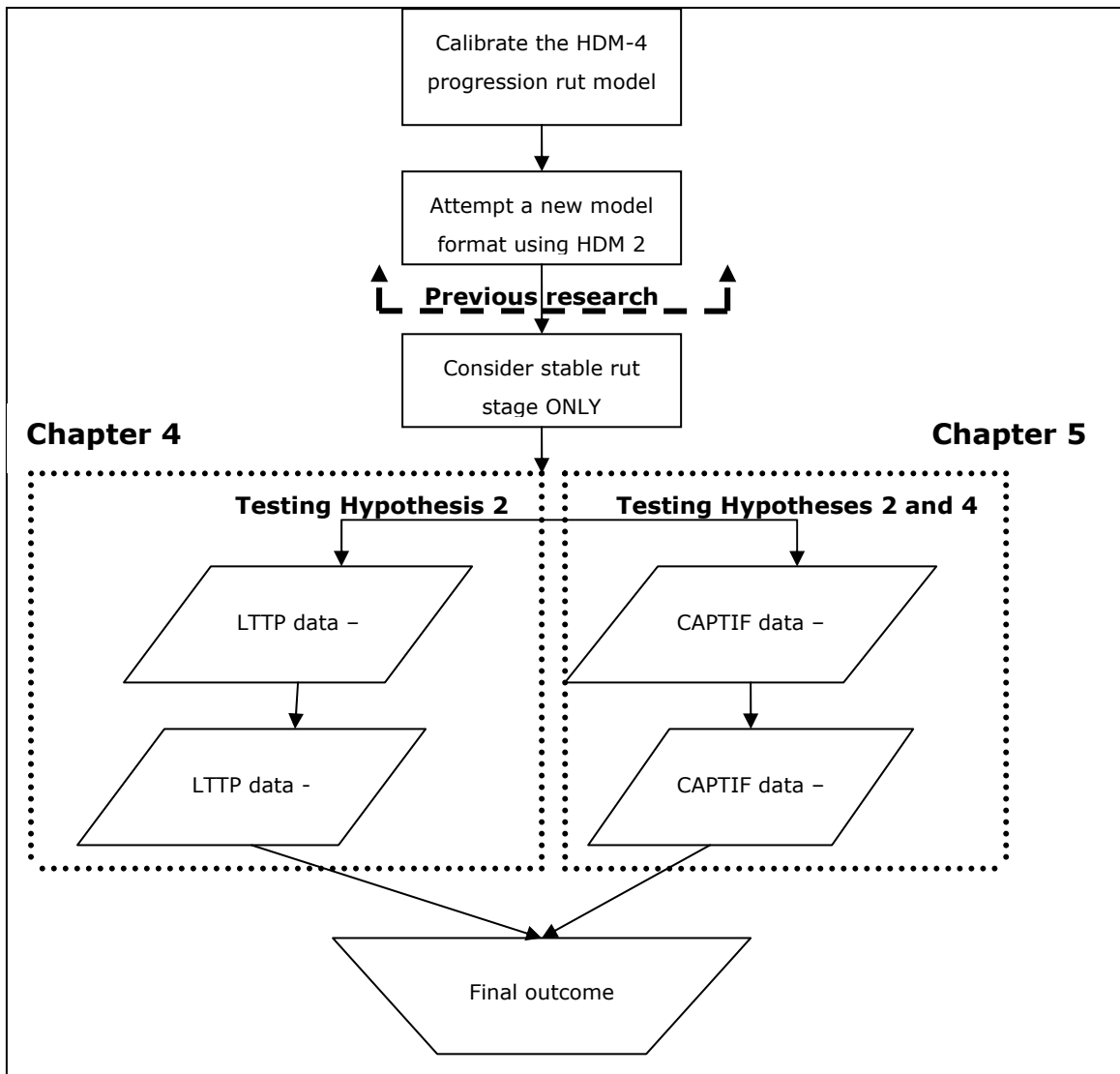The analysis process and data used in Chapters 4 and 5 are illustrated in Figure 4.1.

Figure 4.1   Analysis process and data used for predicting rut progression.

4.2   **Exploratory statistics**

4.2.1   **Considering the stable rut rate stage in isolation**

This section refers to analysis performed on the LTPP data from the past six years (i.e. 2000–2006). The data were filtered in order to exclude any data point that had originated from early periods following construction or any periods that may have indicated accelerated deterioration. This filtering was based on a combination of age data plus actual performance data.

Earlier attempts have targeted establishing the significant variables that may influence the rate of rut progression. These analyses found none, accepting that the analysis considered a full dataset and a full deterioration curve.

One aspect which was not considered before was splitting the data into the three rut progression stages. This section documents the outcome of exploratory statistics on the stable rut progression stage.

The factors considered during the exploratory statistics are listed in Table 4.1.

Table 4.1   Variables considered for predicting rut progression.

Variable	Description	Variable type
AADT	Annual average daily traffic	Continuous
YE4	Annual number of ESA (millions/lane)	Continuous
SNP	Structural number of the pavement	Continuous
MMP	Mean monthly precipitation	Continuous
wpiri	Wheelpath IRI[a] (mm/km)	Continuous
HTOT	Total surface thickness (in mm) of all the layers	Continuous
Sens	Climatic sensitivity area	Factor
AGE3	Age of the pavement (years)	Continuous
AGE2	Age of the surface	Continuous
OTCI	Time until crack initiation	Continuous
Stat.crx	Cracked status	Binary
D0-D9	(FWD[b]) – Deflections for given geophones (micro mm)	Continuous
maxdef	FWD – Maximum deflection from all geophones (micro mm)	Continuous
SF1 & SF2	FWD – Deflection shape factors 1 and 2	Continuous
SCI	FWD – Surface curvature index	Continuous
BCI	FWD – Base curvature index	Continuous
BDI	FWD – Base damage index	Continuous

Notes to Table 4.1
a   IRI = International Roughness Index in mm/km
b   FWD = Falling Weight Deflectometer

Appendix B lists some of the outputs based on the statistical analysis which are similar to earlier results. The explanatory results did not yield any significant factor for predicting rut progression. For example, Figure 4.2 illustrates the influence of surface age (AGE2) and climatic sensitivity area on the rut progression.
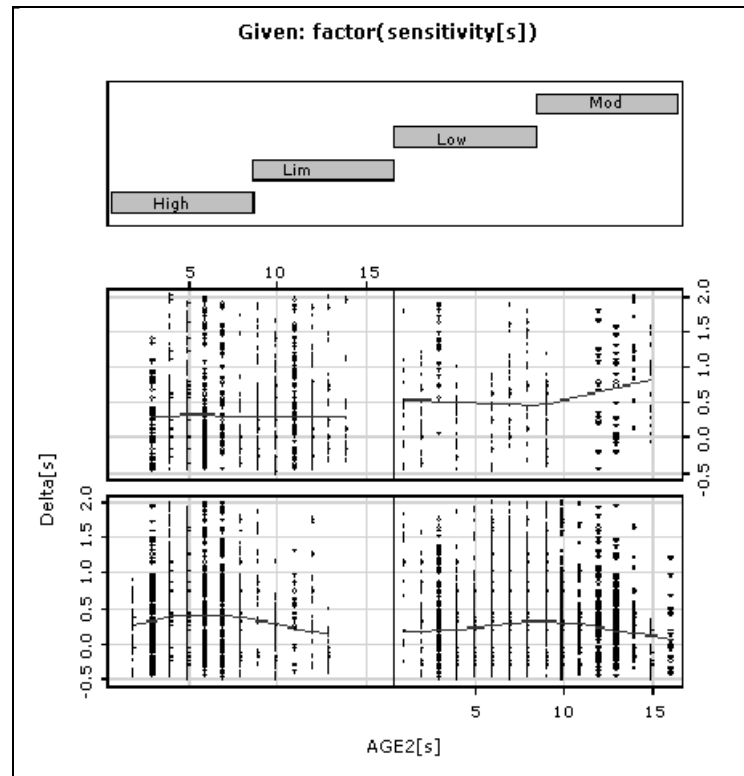
**Figure 4.2   Influence of surface age and climate on rut progression.**

The figure illustrated the delta rutting as a function of the surface age (AGE2) and four climate/moisture sensitivity regions – as described in Henning et al. (2004a). It would have been expected that older pavements (older than AGE2) and pavements in a high and moderate climatic/soil sensitivity area would have demonstrated higher rut rates. However, no clear trend based on any of the factors was observed. Likewise, no clear trend was observed in all the additional outputs depicted in Appendix B, including total surface thickness, traffic, structural number, peak deflection, traffic and pavement age.

4.2.2   Considering single and multiple layered surfaces separately

Based on results obtained for the crack initiation model development, the data have been split further into pavements with a total surface thickness of more than 30 mm and pavements with a total surface thickness less than this. Exploratory statistical results for this analysis showed more promising results, especially for pavements with total surfaces greater than 30 mm. A potential relationship may exist between rutting and the following factors:

- the presence of cracking,
- the base layer index,
- the pavement age (AGE3), and
- traffic.

None of these parameters seemed to have an influence on rut rate for pavements that are less than 30mm of total surface thickness. All the outputs are presented in Appendix B. Figure 4.3 and 4.4 illustrate a typical example of the output.
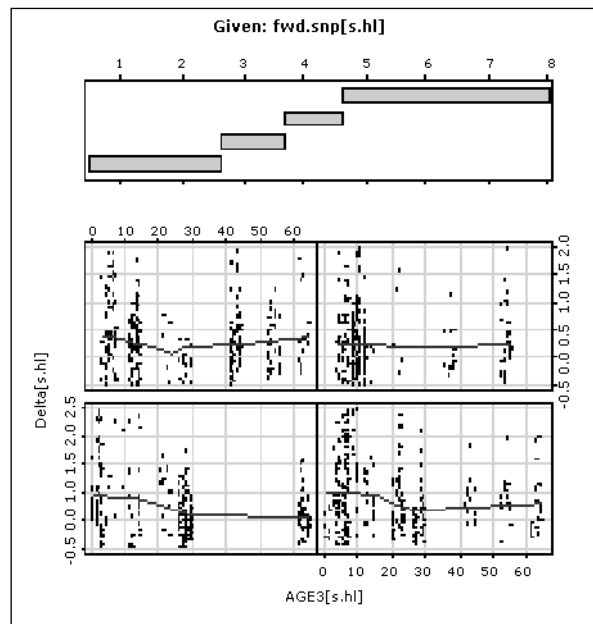
Figure 4.3   Influence of pavement strength and pavement age (AGE3) in pavements with surfaces less than 30 mm thick.
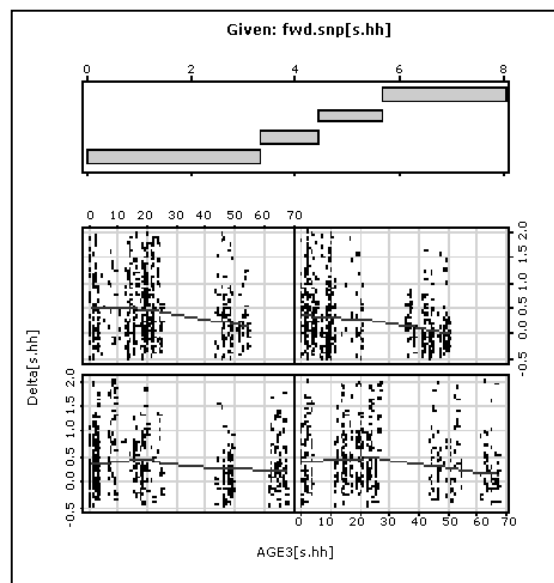
Figure 4.4   Influence of pavement strength and pavement age (AGE3) for pavements with surfaces more than 30 mm thick.

Observations from Figure 4.4 indicate that for pavements with a total surface thickness of more than 30 mm:

- the rutting progression decreases with pavement age; and
- no significant trend for the pavement strength (SNP) is apparent.

As opposed to this, the pavements with a total surface thickness of less than 30 mm (Figure 4.3) show no clear trend for either pavement strength or pavement age.

4.3   Model regression analysis

Based on results presented in Chapter 3, it was doubtful whether the regression analysis would yield any better results. However, for the sake of completeness, a full series of regression analysis was completed on the data. Some regressions and model formats tested include:

- step-wise regression of a linear model, and
- the General Additive Model (GAM).

The results from the regression analysis were consistent with previous findings where a relatively good fit was established, but the resulting model outcome was little more than a predictor of the average outcome (also see Henning et al. 2006). Appendix B depicts the resulting residual plots of the linear model outcomes for the absolute and incremental rutting model. From the residual plots, it can be concluded that the linear model format is appropriate for the predicted rut progression. However, consistent with earlier results, the model consists of an addition of all the possible variables, with hardly any of the variables being more significant than any other. Also, Appendix B listed very low R^2 values in both the absolute and incremental rut predictions (0.24 and 0.07 respectively).

The attempt to use an alternative model format such as the general additive model yielded equally poor results. Table 4.2 illustrates typical results obtained for this model format in an attempt to predict the incremental rut progression for the LTPP sections. Similar to the results obtained for the linear model, all variables appear to be significant, but the overall fit of the model is poor, with a R^2 of only 0.05. This value is even less than the outcome of the linear model predictions.

Table 4.2   Regression results obtained for the GAM model on the LTPP data.

Variable	Estimate	Standard Error	t value	Probability (>|t|)	Significance
Intercept	0.84	0.20	4.126	3.76 e-05	***
HTOT.class: Thick surface	0.48	0.08	5.728	1.09 e-08	***
crkTRUE	-0.07	0.04	-1.905	0.0569	.
AGE3	-0.01	0.001	-7.165	9.17 e-13	***
AGE2	0.06	0.006	10.235	<2 e-16	***
log(YE4)	0.10	0.024	3.912	9.31 e-05	***
log(mmp)	-0.05	0.038	-1.431	0.1526	
fwd.snp	-0.08	0.012	-6.929	4.88 e-12	***
HTOT.class: Thick surface:log(YE4)	0.24	0.037	6.345	2.47 e-10	***

Notes to Table 4.2:
(a) R^2.(adjusted)   = 0.0522
(b)   Deviance explained   = 5.4%
(c)   GCV score   = 1.1186
(d)   Scale estimation   = 1.1162
(e)   n   = 4 188
(f)   fwd.snp is the Structural Number (SNP) derived from FWD results
(g)   crkTRUE is a binary number that indicates whether a section has cracked

4.4   Discussion

This section has presented a comprehensive statistical analysis of the LTPP data. The exploratory statistics have indicated that no significant variable determines the rut progression.

The regression analysis has further investigated the possible predictability of rut rate according to traditional means. In both the model formats tested (Linear Model and GAM) it was concluded that these model formats yielded poor results.

It can therefore be concluded that Hypothesis 2 (which states that no significant variables can predict a rut progression in a robust manner) is true.

5.   Testing Hypothesis 4: predicting rut progression as a constant rate – based on CAPTIF data

5.1   Exploratory statistics

All calibration work completed on rutting to date has suggested that rut progression cannot be modelled by any better method than to simply apply a constant rate of change. Also, none of the analysis completed to date has suggested any significant variable that reliably indicates rut progression.

According to the hypothesis of this report (See Chapter 2.6), rutting can be divided into three stages:
1.   initial rut densification,
2.   stable rut progression, and
3.   accelerated rut progression.

This chapter attempts to establish possible relationships between some descriptive variables and a constant rate of rut progression. Underlying this analysis is the assumption that during the stable rut phase, the rut progression occurs according to a constant rate.

The first aspect investigated was the relationship between the initial rut depth and the rut progression slope (See Figure 5.1). A strong relationship appeared between the initial densification and the rut progression slope. It suggests that on a pavement with higher initial rut depths, one can expect a faster rut progression rate. This phenomenon is in agreement with expected trends, but contradicts earlier suspicions about the relationship between initial rut depth and rut progression (as illustrated in Figure 2.6).
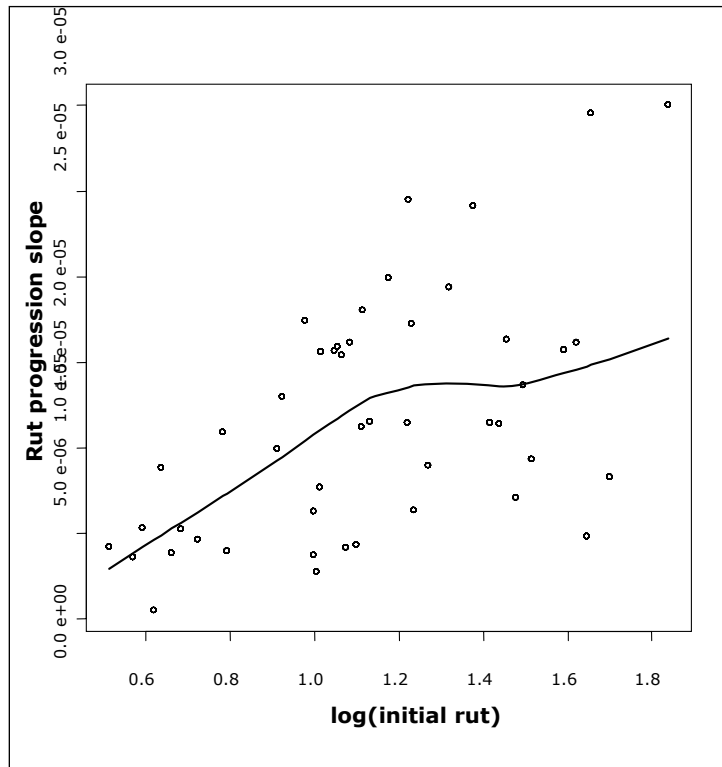
Figure 5.1   The relationship between the initial rut depth and the slope of rut progression.

Figure 5.2 and 5.3 illustrate the relationship between rut rate (in mm/repetition) and the structural number (SNP). Figure 5.2 shows this relationship with the data in a raw format, whereas Figure 5.3 shows the same relationship with the rut rate data being log transformed. A strong relationship appears between the rut progression and the SNP, especially in a log transformed format.
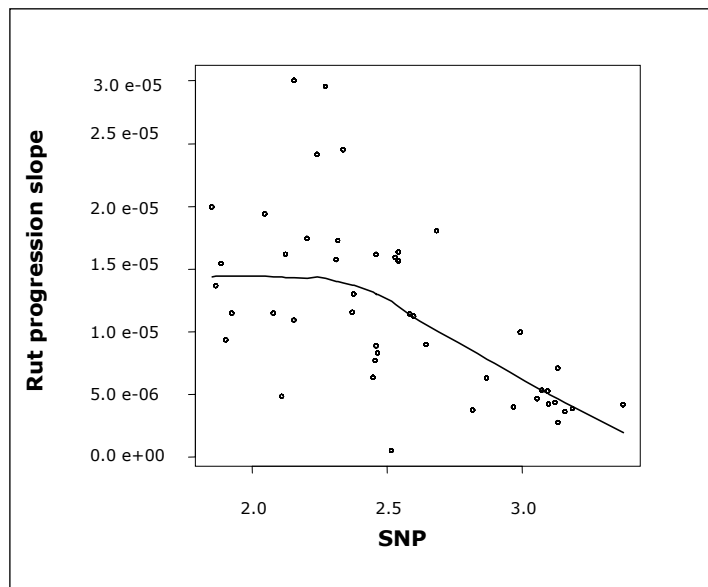
Figure 5.2   Rut progression slope as a function of SNP (raw format).
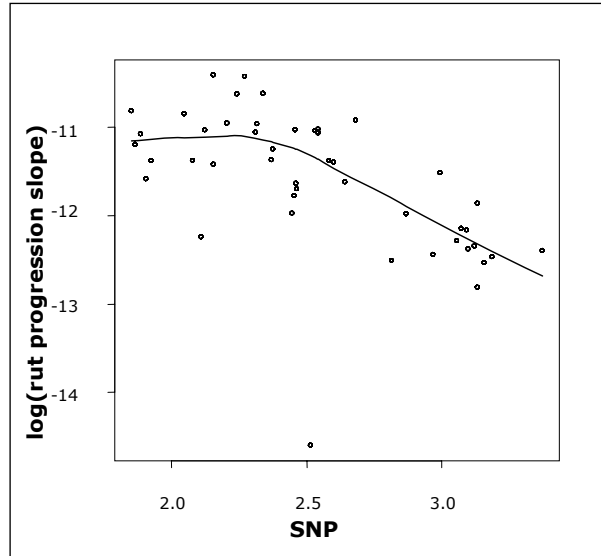
Figure 5.3   Rut progression slope as a function of SNP (log transformed format).

The rut rate was also investigated as a function of the base layer thickness, as illustrated in Figure 5.4. It is noted that the rut rate for the thicker pavement is significantly less than the thin layer pavement. The data used for this analysis excluded any early failures that were noticed on the thinner pavements.
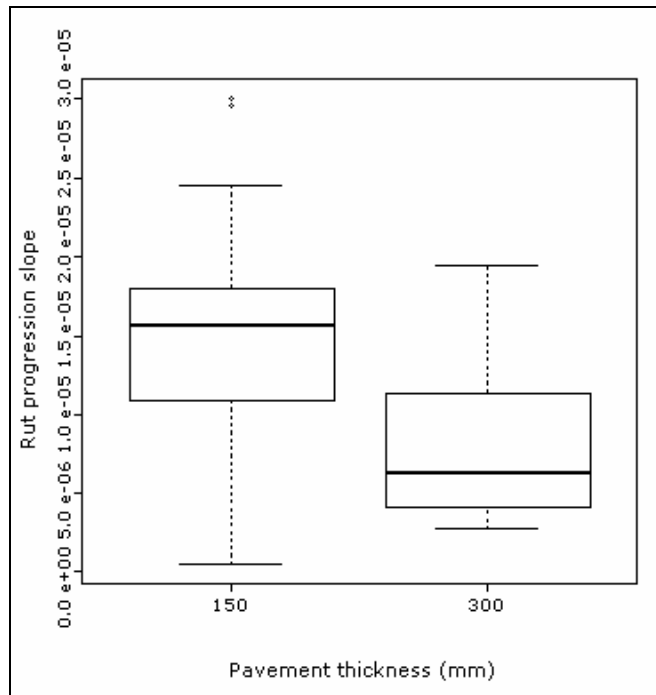
Figure 5.4   Rut progression slope for different pavement thicknesses.

Figure 5.5 and 5.6 illustrate the inter-relationship between the rut rate, the layer thickness, the initial densification and the SNP. The co-plots confirmed the observations made earlier, but the observed trends are much stronger for the deeper pavements. It seems that the shallower pavements are more erratic in behaviour compared with the deeper pavements.
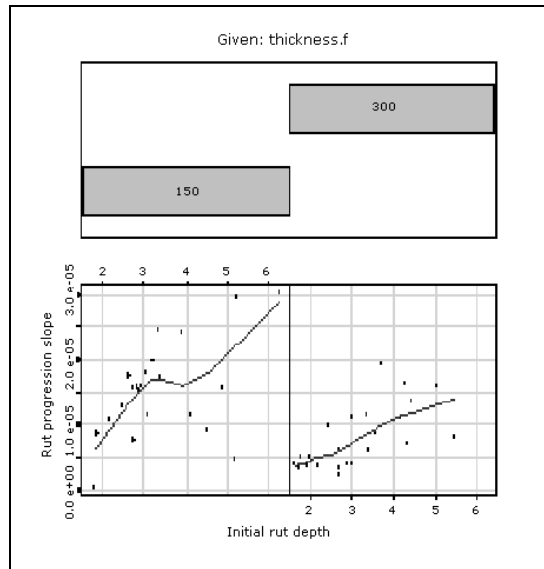
Figure 5.5   Rut progression slopes for different pavement thicknesses and initial rut values.
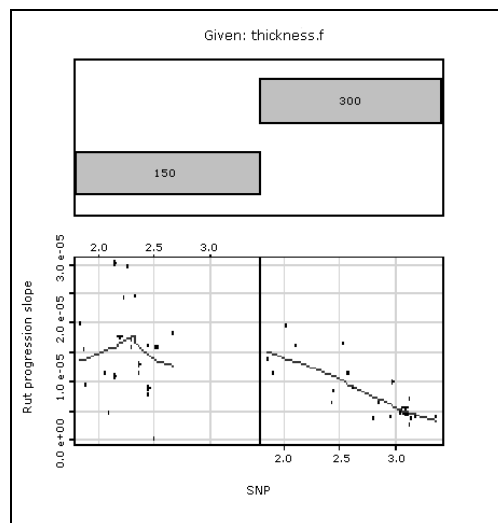
Figure 5.6   Rut progression slopes for different pavement thicknesses and structural numbers.

From the exploratory statistics, it can be concluded that the rut rate during the stable progression is a function of the SNP and the thickness of the base layer.

5.2 Regression analysis

As a first attempt, the regression on the rut rate slope was performed to include all possible variables. This yielded results that were similar to the results obtained in Chapter 4.3 (see also Appendix C). Most of the variables resulted in being significant in an additive format. Therefore, none of the variables stood out as an independent variable.

The next step was to undertake a regression on the variables identified in the exploratory statistics. Table 5.1 lists the results from this analysis and Figure 5.7 depicts the residual plots.

Table 5.1   Regression results obtained for the linear model on the CAPTIF rut rate data.

	Estimate	Standard error	t value	Probability (>|t|)	Significance
Intercept	2.26 e-05	2.71 e-06	8.31	3.75 e-16	***
SNP	-3.14 e-06	1.18 e-06	-2.66	0.008	**
thickness.f300	9.66 e-06	3.18 e-06	3.03	0.003	**
SNP:thickness.f300	-5.63 e-06	1.32 e-06	-4.26	2.25 e-05	***

Notes to Table 5.1:
(a)   Residual standard error = 5.286 e-06 on 842 degrees of freedom
(b)   Multiple R^2 = 0.43,
(c)   Adjusted R^2 = 0.43
(d)   F-statistic: 211.1 on 3 and 842 degrees of freedom
(e)   p-value: <2.2 e-16
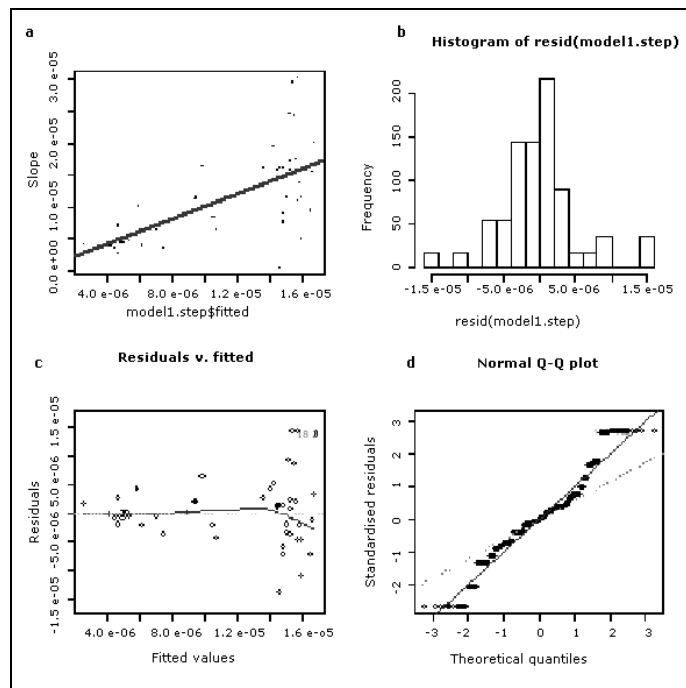
Figure 5.7   Residual plots for the rut progression slope linear regression using CAPTIF data.

Observations from the regression results are as follows:

- The overall fit of the model to the observed point were not strong. An R^2 of 0.42 is acceptable within the modelling of road pavements, but it should be viewed bearing in mind that the CAPTIF experiment is tested under controlled conditions.
- The residual plots indicated the model to be unstable on the extreme point of the data. Normally, this phenomenon indicates that the model format is incorrect.

Given these observations, the logarithmic model format was attempted. Poorer results were obtained. The resulting R^2 from this analysis was 0.35 and, as illustrated in Figure 5.8, the residuals are not normally distributed, again suggesting the model to be in the wrong format. Note the influence of the extreme points of the data is more prominent in this figure (see the Q-Q plot, labelled (d) in Figure 5.8).

It should also be noted that the results in this section also did not include any SNP values higher that 3.5, which makes any extrapolation of the model above these values dangerous.
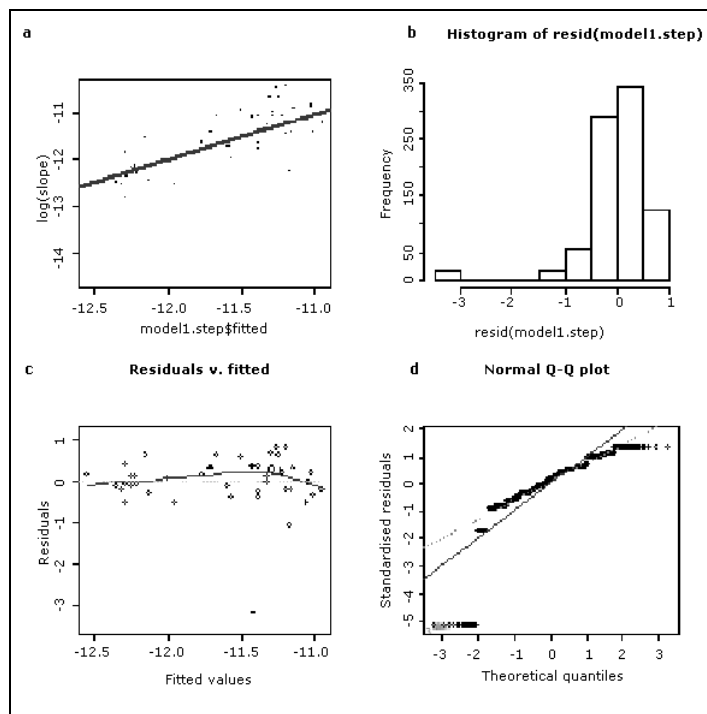
Figure 5.8   Residual plots for the logarithmic regression of the rut progression slope.

5.3 Discussion

Various attempts have been made to model rut progression over time:

- Based on the LTPP data, rut progression was modelled according to a two-phase process (initial densification and rut progression) similar to the HDM-4 approach (this work was completed in earlier research (Henning et al. 2006).
- The LTPP data was also used in a similar regression, but splitting the data into thick and thin surfaces (See Chapter 4).
- Based on the CAPTIF data, the regression was undertaken for a three-phase model (initial densification, stable rut progression and accelerated rut progression). This chapter has outlined some analysis that considers the stable rut phase.

Only the last regression showed some potential, since it indicated some significant independent variables (structural number and base layer thickness). However, the regression results did not have a strong correlation and excluded the full range of expected strength numbers.

Considering these facts, it can be safely concluded that rut progression is a high variable mechanism that cannot be predicted with confidence for the data that was available for this study. However, it was also demonstrated that annual rut progression is quite small, being in the range of approximately 0.3–0.6 mm per year. It is therefore recommended that the progression of rutting be taken as a constant rate within this range, as appropriate to the layer thickness.

6. Accelerated rut progression

6.1 Analysis process and data used

The analysis process and data used are illustrated in Figure 6.1.
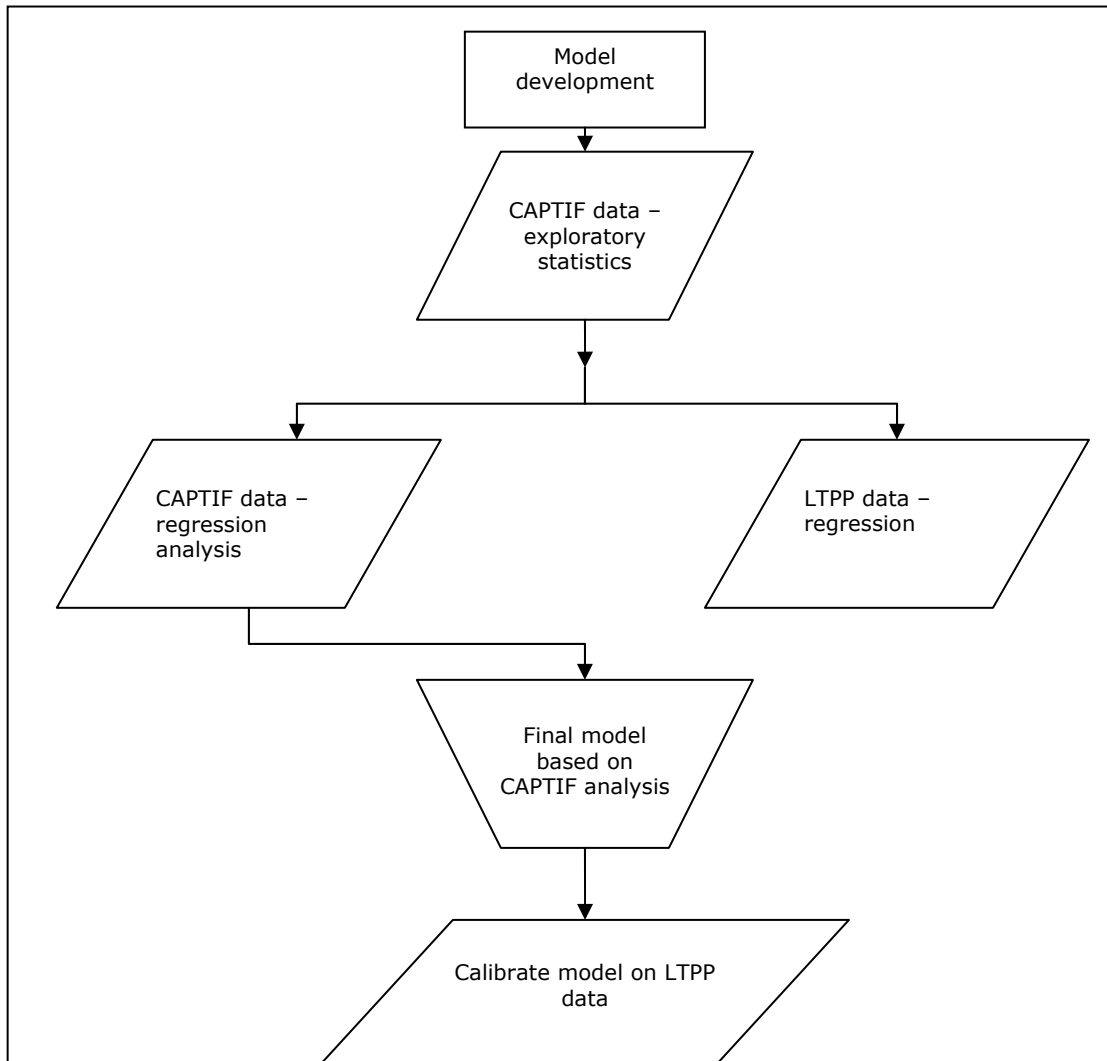
Figure 6.1   The analysis process and data used to determine accelerated rutting.

6.2   **Exploratory statistics**

So far, this study has indicated that the initial rut depth can be predicted relatively accurately. However, the rut progression cannot be predicted more accurately than by simply assuming an average rut rate. For the purpose of road maintenance planning, it is crucial to be able to predict the rut depth at intervention levels, which is typically when ruts are between 15 and 20 mm deep. This chapter attempts to predict the stage at which accelerated rut progression takes place for road pavements with different strength and traffic loading configurations.

The normal exploratory statistics were performed on the accelerated rut progression data based on the CAPTIF experiment. In the first instance, the accelerated rut progression was taken as an absolute point of traffic loading (repetitions as per CAPTIF).

Appendix D lists the resulting figures, with the general observed trends being:
- Only pavements with base layer thicknesses of ≤150 mm demonstrated an accelerated rut rate.
- The relationship between the actual commencement of the accelerated rut rate and the structural number increases – this trend is inverse for maximum deflection.
- The accelerated rut starts sooner for pavements with a higher moisture content.
- Accelerated rut progression will start later for higher compaction levels.
- No clear relationship was observed between the absolute accelerated rut progression point and any of the independent variables.

All of the above observations were consistent with expected outcomes, but again, no clear trends emerged from the data in a raw format.

As a second attempt, all the data were translated into a logistic format. Translating data into a logistic format assigns a true or false data item to each section for when it is still in a stable rut progression (false) or when it goes into an accelerated rut progression (true). The trends for the logistic data are presented in Figure 6.2 to 6.5.
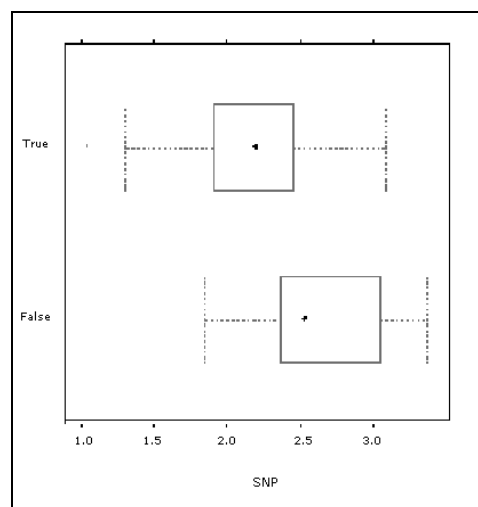
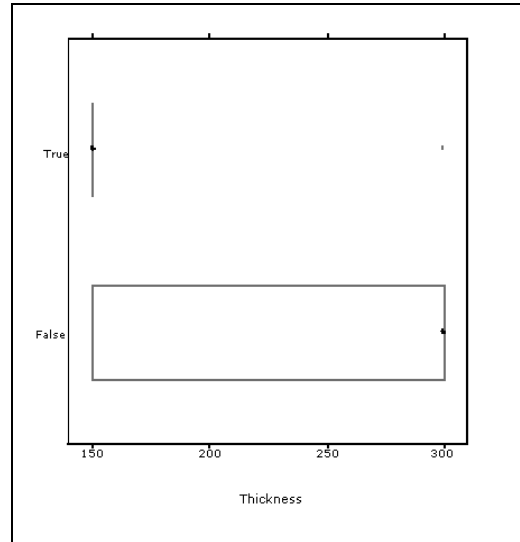**Figure 6.2   Plotting the occurrence of an accelerated rut progression versus SNP.**
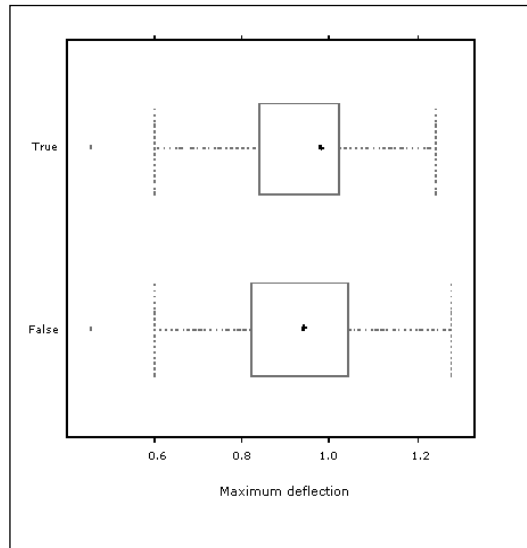
Figure 6.3   Plotting the occurrence of an accelerated rut progression versus maximum deflection.
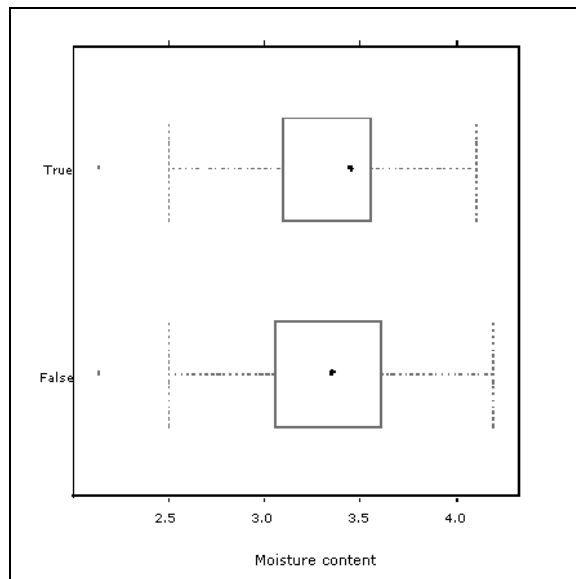
Figure 6.4   Plotting the occurrence of an accelerated rut progression versus moisture content.

Figure 6.5   Plotting the occurrence of an accelerated rut progression versus base layer thickness.

Observations from the figures include:

- Most of the accelerated rut progression took place on pavements with an SNP number lower than 2.4 and a maximum deflection greater than 0.8 mm.
- The moisture content did not reveal any clear trends.
- Accelerated rut progression only took place on pavements with layer thicknesses of ≤150 mm.

6.3   Regression analysis

With normal regression functions, it is assumed that a dependent variable (e.g. y) will change as the independent variable(s) (e.g. x) changes. The relationship between x and y can then be represented in a number of formats including linear, logarithmic, exponential, etc. However, the assumption of this type of relationship is that the dependent and independent variables are related to each other in a continuous format.

An alternative statistical method of predicting an outcome is by turning the result into a discrete outcome. For example, the outcome can be defined according to either a binary (0 or 1) or a logistic (true or false) format. Once the outcome is defined in this format, the probability of the result can be determined according to the population distribution of the observed outcomes.

Figure 6.6 illustrates an example of a logistic model. For this example, a large number of people were measured and their gender was recorded against their height. A logistic model was derived based on the data, which return the probability of gender as a function of a given height. For example, if someone is 67 inches tall, the probability that this person is male is 70%.
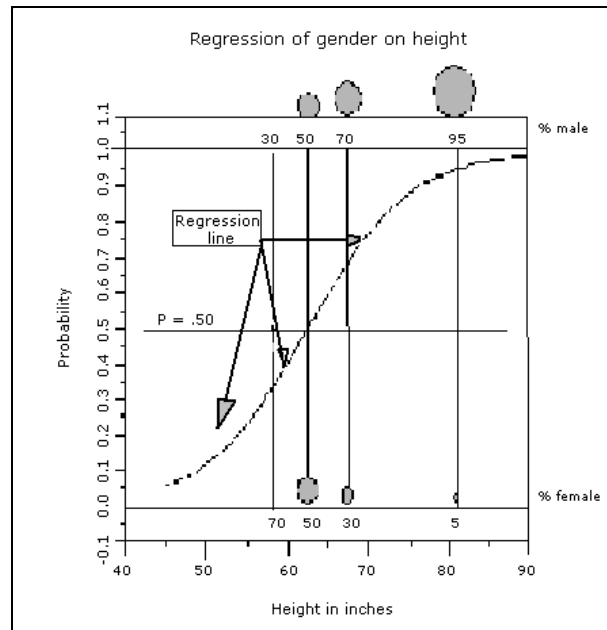
Figure 6.6   Example of a logistic model that predicts gender based on height (Brannick 2000).

The rut data was transformed into a logistic format where 'true' represented the traffic loading at which a particular section started to display accelerated rut progression. Various different logistic regressions were performed on the data, with the most successful outcome being presented in Table 6.1,and the residual plots presented in Figure 6.7 and 6.8.

Table 6.1   Accelerated rut rate regression results obtained for the logistic model based on the CAPTIF rut rate data.

	Estimate	**Standard Error**	**z value**	**Probability (>|z|)**	**Significance**
Repetitions	3.78 e-06	3.73 e-07	10.145	< 2 e-16	***
SNP	-2.43 e+00	2.91 e-01	-8.362	< 2 e-16	***
Thickness.f150	4.43 e+00	6.54 e-01	6.771	1.28 e-11	***
Thickness.f300	4.74 e-01	7.63 e-01	0.621	0.534	

Notes to Table 6.1:
(a)   Null deviance: 1369.66 on 988 degrees of freedom
(b)   Residual deviance: 635.93 on 984 degrees of freedom
(c)   AIC: 643.93
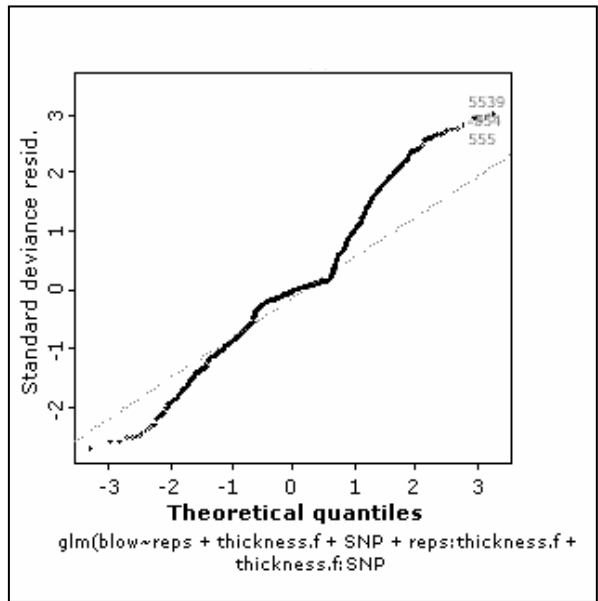
Figure 6.7   Residual plot (Normal Q-Q) for the accelerated rut progression according to a logistic model.
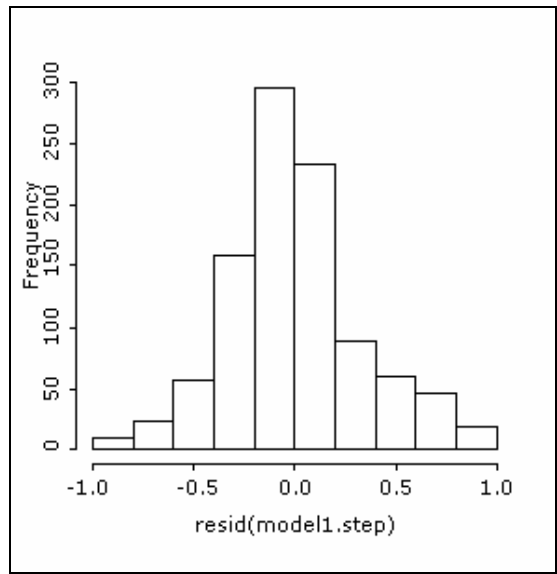
Figure 6.8   Residual plot (histogram of resid(model1.step) for the accelerated rut progression according to a logistic model.

The model outcome from the regression analysis was consistent with the findings and observations of the exploratory statistics. The results further illustrated that the chosen factors (pavement thickness, structural number and traffic loading) are significant in predicting the outcome. The residuals plots were not problematic, since the residuals are normally distributed. It should be noted, though, that the AIC (643) is still relatively high.

The final model for predicting the initiation point of accelerated rut progression is:

$$p(Rutaccel) = \frac{1}{1 + e^{\left(-3.784 \times 10^{-6} \times reps + 2.434 \times snp - \left[(4.426, 0.4744) \text{ for thickness} = (0,1)\right]\right)}}$$

[Equation 6]

or translating the same expression from rep (CAPTIF) to ESA would be:

$$p(Rutaccel) = \frac{1}{1 + e^{\left(-7.568 \times 10^{-6} \times ESA + 2.434 \times snp - \left[(4.426, 0.4744) \text{ for thickness} = (0,1)\right]\right)}}$$ [Equation 7]

Where:

ESA	Equivalent Standard Axles
SNP	Pavement strength Structural Number
Thickness	0 for base layer thickness <150 mm; 1 for base layer thickness >150 mm
thickness =(0,1)	for thin pavements (i.e. *thickness* =0), the first value in brackets is used as a constant e.g. 4.426

The graphical presentation of the model is illustrated in Figure 6.9. For this figure, a SNP of 3 was assumed. The graph shows the increase in probability of the pavement initiating an accelerated rut depth at different loading cycles. The probability of a thick pavement going into an accelerated rut progression stays relatively low.
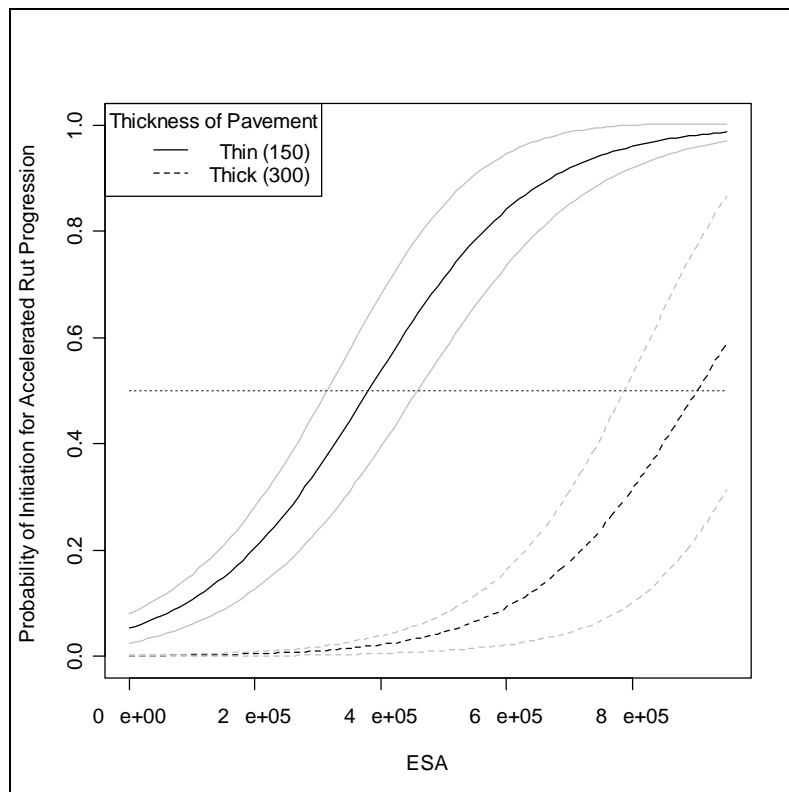
Figure 6.9   Final logistic model for predicting the initiation point of accelerated rut progression (SNP = 3).

64

6.4   Discussion

It is a well accepted fact that rutting is one of the best indicators of pavement deterioration. This chapter has presented outputs related to the accelerated rut progression towards the end of the expected pavement life. It is evident that pavement rutting indicates pavement wear caused by:

- fatigue considerations, or
- (sometimes) rapid shear failure that occurs as a result of overloading a pavement.

Earlier chapters indicated that no clear independent variables influence the rate of rutting during the stable rut phase. For the initial point of accelerated rutting, the reverse was true: significant variables were observed, indicating that when the accelerated rut progression begins is predictable. These factors included the total thickness of the pavement, traffic loading and the SNP.

With the regression analysis, a linear logistic model was fitted to the data and a relatively good statistical outcome was achieved. The overall model fit was good and the residual plots have indicated the model format to be appropriate. The model was tested further by plotting it onto the LTPP data, and actual initiation points for accelerated rut progression were equally distributed around the 50th percentile point. This suggested that the model is valid on the actual pavement data.

The logistic model format has a number of advantages in its application, since the predicted output is expressed in terms of a percentage rather than an absolute value. Therefore, it allows for intervention strategies to be considered at profiles with different probabilities of failure or risk. It is also much more effective in demonstrating the impact of different scenarios such as investment levels because an immediate impact is observed in the probabilities. However, this model format is a data driven model, and it has to be tested before applying to areas it was not developed for.

7. Recommendations

7.1 Summary of the results

The results from this research are summarised in Table 7.1. Note that the results are presented in relation to the original expected outcome during the initial stages of the project.

Table 7.1 Summary of results from this research.

Hypothesis	Outcome from this study
Hypothesis 1: Three distinct stages of rut rate progression exist: • initial densification, • stable rut rate progression, and • failure and/or accelerated deterioration.	**True.** The three phases were identified and used effectively in this study. However, bound and strong pavements have only two phases, initial densification and progression.
Hypothesis 2: No significant variables can predict rut progression in a robust manner.	**True**. Rut progression analysis was intensively investigated in this report and no satisfactory outcome was achieved with the current data.
Hypothesis 3: It is possible to find an alternative model to the HDM-4 model for predicting initial densification that uses data which are more readily available on network databases.	**True.** A simpler alternative model was established.
Hypothesis 4: A relationship between the initial densification and rate of rut change exists during the stable phase.	**False.** A relationship was noticed but no robust model could be developed that could predict the rate of rut change.
Hypothesis 5: The failure point in terms of rutting can be predicted based on two methods: • For unbound/low volume pavements, the point of commencement of the accelerated rutting can be predicted. • Bound and strong unbound pavements will not have an accelerated rut rate stage, but an unacceptable rut depth can be determined based on predictions from the rate of rutting.	**True**. A linear logistic model that yielded satisfactory results was developed.

The models that were developed for predicting rutting include:

- **Predicting the initial densification rut:**

$$Initial\ Rut = 3.5 + e^{(2.44 - 0.55SNP)}$$ [Equation 5]

Where:

SNP is the structural number as derived from the Falling Weight Data

- **Predicting the rut progression**
  - For thin pavements (total layer thickness <150 mm), the rate is 0.5 mm per year.
  - For thick pavements (total layer thickness ≥150 mm), the rate is 0.3 mm/year.

- **Predicting the initiation of accelerated rutting:**

$$p(Rutaccel) = \frac{1}{1 + e^{\left(-7.568\times10^{-6}\times ESA + 2.434\times snp - \left[(4.426, 0.4744) for\ thickness=(0,1)\right]\right)}}$$ [Equation 7]

Where:

ESA   Equivalent Standard Axles

SNP   Pavement strength Structural Number

Thickness   0 for base layer thickness <150 mm; 1 for base layer thickness >150 mm

7.2   Further work

As with many research projects, this research was also limited to achieving outcomes for which sufficient data were available. However, much was achieved. Using both the LTPP data and the CAPTIF data in the model development work gave excellent outcomes. But some remaining holes in the data prevented all the objectives from being achieved. In addition to this, the research work needs to continue in order to test and expand the applicability of the model developed. A summary of the recommended further work is presented in Table 7.2.

Table 7.2   Summary of recommended further work arising from this study.

Topic Area	Description of recommended further work
General applicability of models	The models are data-driven models and should therefore be tested on other data in New Zealand, such as network data.
Relative performance of different material types	This study only included thin surfaced unbound pavements. Some work still needs to be completed in order to understand the difference in behaviour between different material types such as dense graded and open graded porous asphalt pavements.
Urban environment	Most of the data included in the current research represented pavements from the rural environment. As the data become available on the Land Transport New Zealand and Local Authority LTPP database, these models should be tested for local urban pavements.
Operational research	It should be realised that the LTPP programmes delivered a wealth of data for research into practical aspects such as data collection and maintenance practices. For example, the data can be used to validate some maintenance practices to address rutting. Similarly, a number of aspects can be investigated regarding the data collection of rutting etc. These research areas should be encouraged in order to get the full benefit from the data collected so far.

8. References

Alabaster, D., Fussell, A. 2006. Fatigue design criteria for low noise surfacings. *Land Transport New Zealand Research Report 307*. Wellington: Land Transport New Zealand.

Arnold, G., Steven, B., Alabaster, D., Fussell, A. 2005. Effect on pavement wear of increased mass limits for heavy vehicles – concluding report. *Land Transport New Zealand Research Report number 281.* Wellington: Land Transport New Zealand.

Brannick, M.T. 2000. Logistic regression lecture notes – University of South Florida, USA. *http://luna.cas.usf.edu/~mbrannic/files/regression/ Logistic.html.*

Henning, T.F.P., Costello, S.B., Watson, T.G. 2006. A review of the HDM/dTIMS pavement models based on calibration site data. *Land Transport New Zealand Research Report 907.* Wellington: Land Transport New Zealand.

Henning, T.F.P., Dunn, R.C.M., Costello, S.B., Hart, G., Parkman, C.C., Burgess G. 2004. *Long term Pavement Performance (LTPP) Studies in New Zealand – Lessons, the Challenges and the Way Ahead.* Paper presented at the 6th International Conference for Managing Pavements, Brisbane, Australia.

Henning, T.F.P., Costello, S.B., Dunn, R.C.M., Parkman, C.C., Hart, G. 2004. The establishment of a long-term pavement performance study on the New Zealand State Highway network. *Australian Road Research Board Journal* Vol 13 No 2.

HTC. 1999. Pavement strength software manual. *Report DT99/12.* Auckland: HTC Infrastructure Management Ltd.

Martin, T. 2003. Pavement performance prediction deterioration model development: data review and calibration of HDM-4 road deterioration models. *AUSTROADS Project No: BS.AN.552.* Australia: Australian Road Research Board.

Martin, T.C., Toole, T., Oliver, J.W.H. 2004. *The Development of HDM-4 Technology Road Deterioration Models for Australia's Sealed Granular Pavements*. Paper presented at the 6th International Conference for Managing Pavements, Brisbane, Australia.

NDLI. 1995. Modelling road deterioration and maintenance effects in HDM-4. *Final Report ADB BETA 5549.* Vancouver, B.C.

Steven, B.D., de Pont, J.J., Pidwerbesky, B.D., Arnold, G. 1999. *Accelerated Dynamic Loading of Flexible Pavements at CAPTIF.* Paper presented at the International Conference on Accelerated Pavement Testing.

Vissser, A.T. 1999. *Siviele Ingenieursmateriale en Plaveiselontwer (Civil Engineering Materials and Pavement Design).* Civil Engineering Course SGM 220, University of Pretoria, South Africa.

Appendix A: Additional results for initial rut depth densification

A1   LTPP Section 12
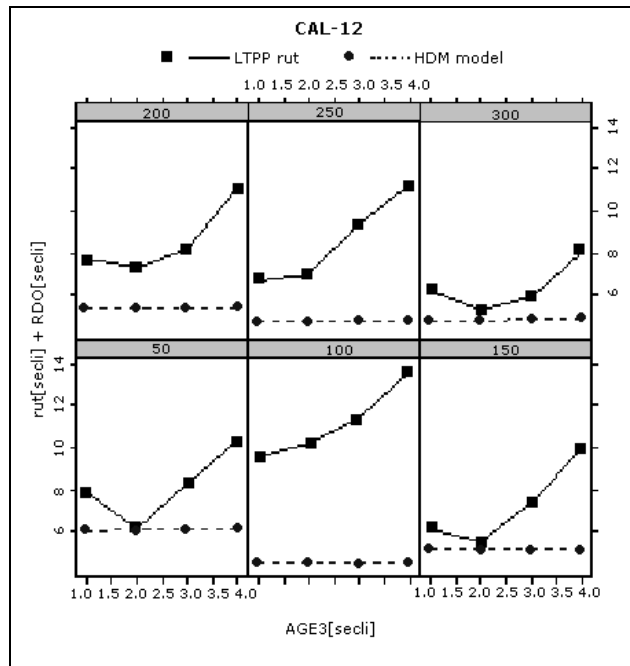
Figure A1   Comparing predicted and actual initial rut depths on LTTP Section 12, left wheelpath increasing.
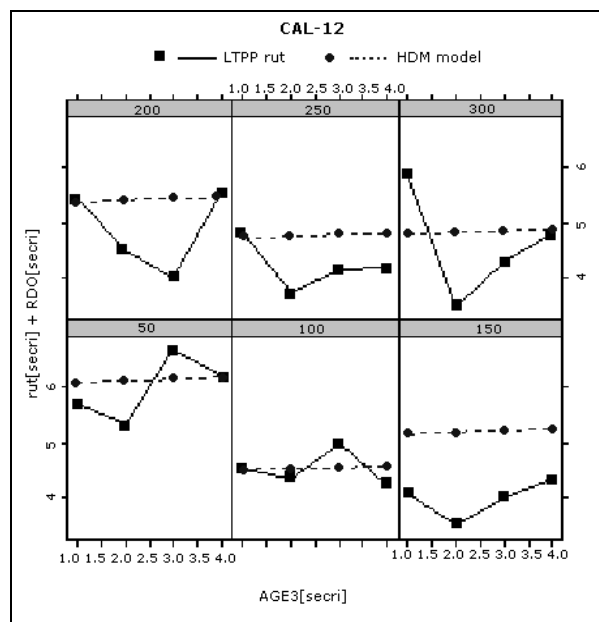
Figure A2   Comparing predicted and actual initial rut depths on LTTP Section 12, right wheelpath increasing.

69

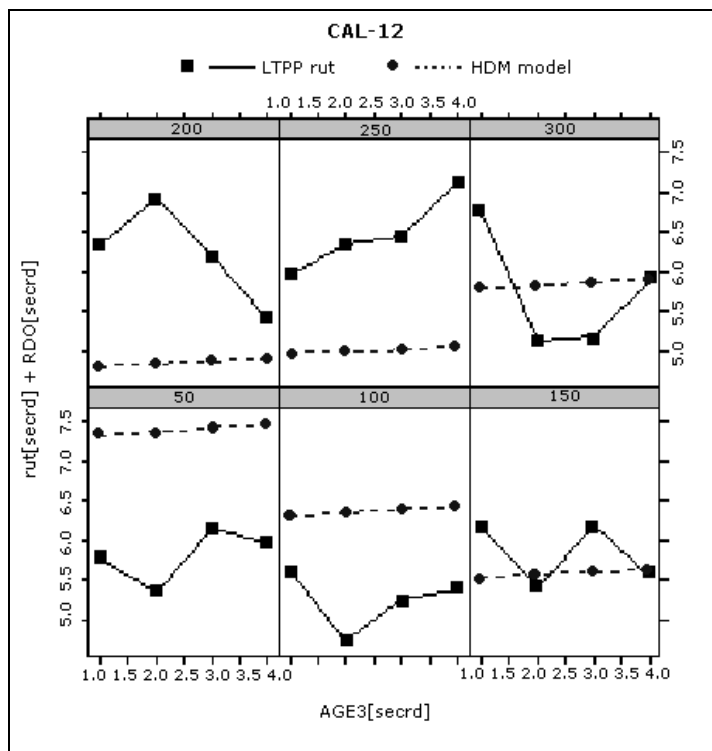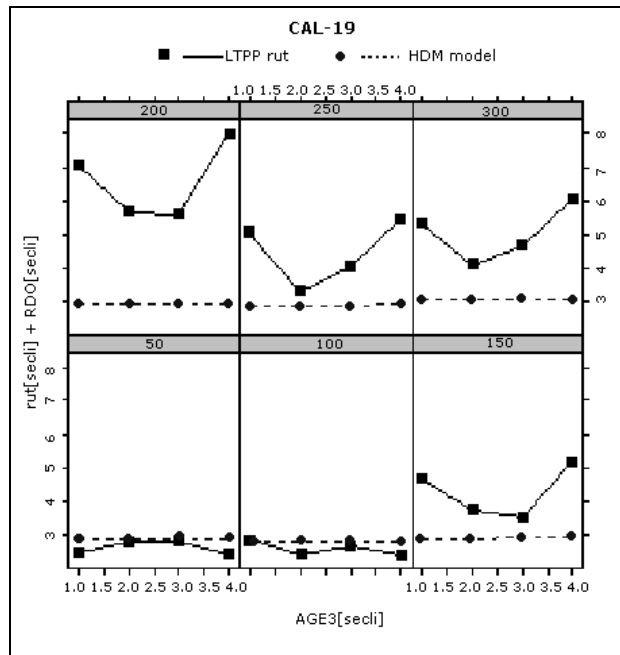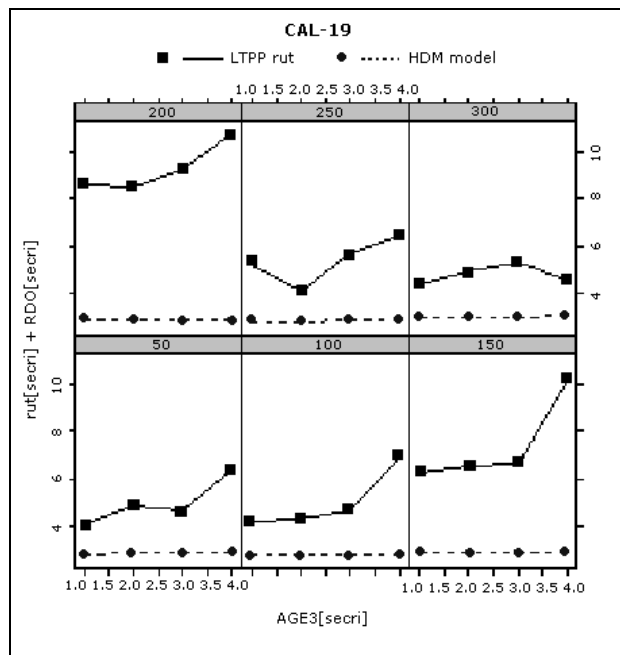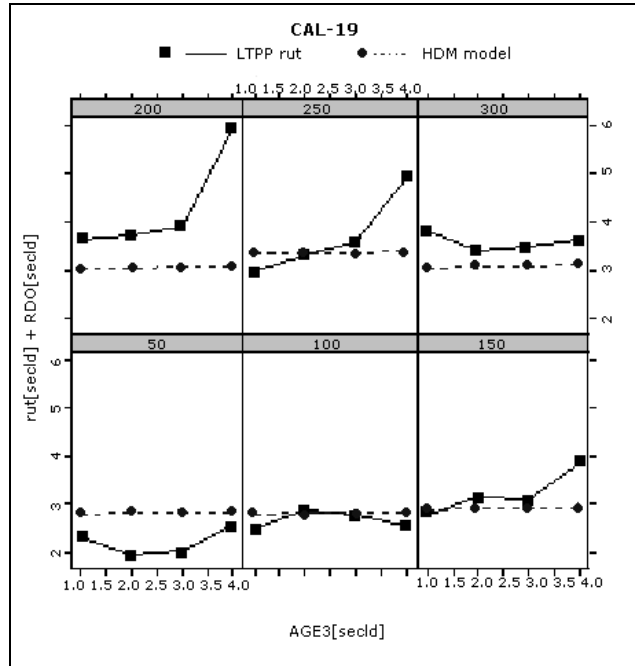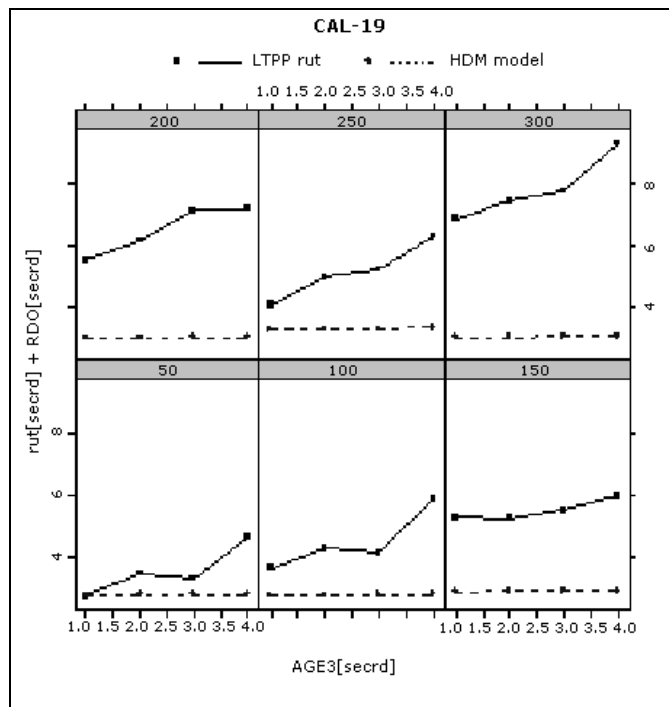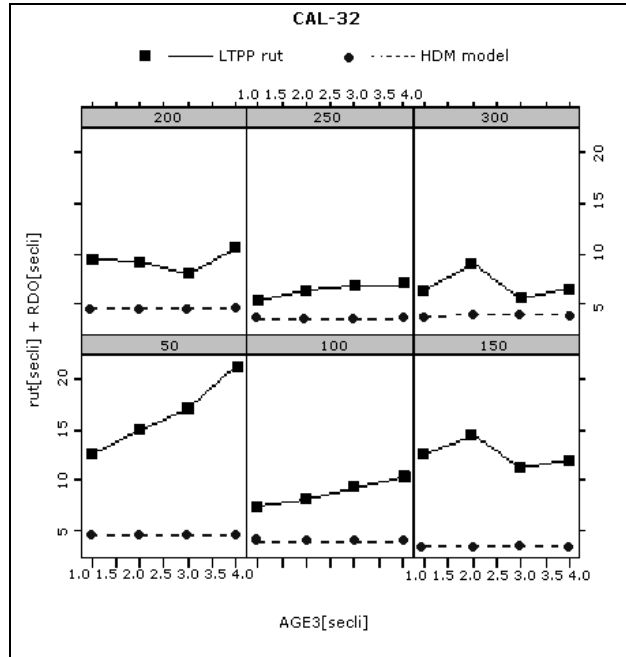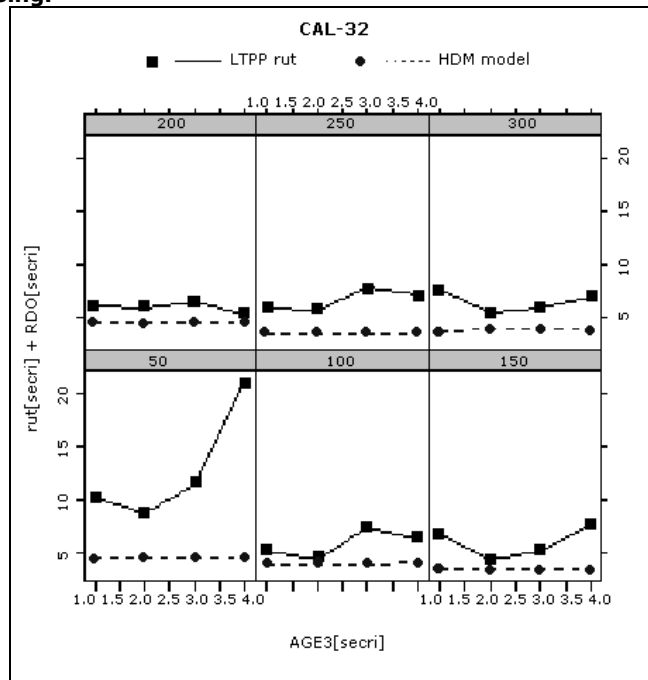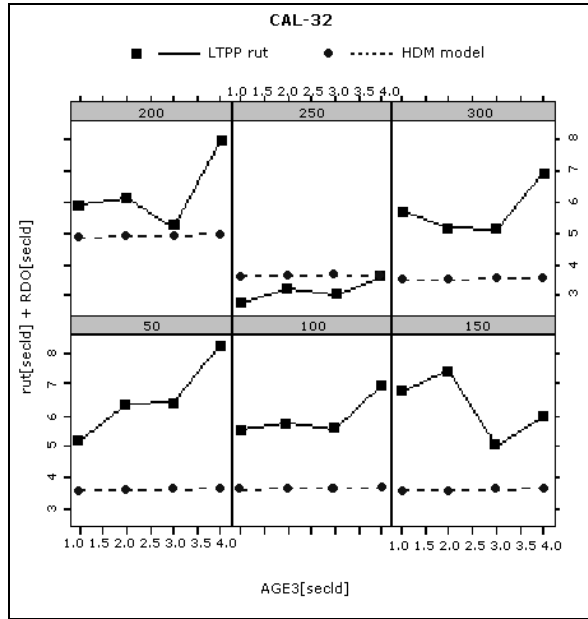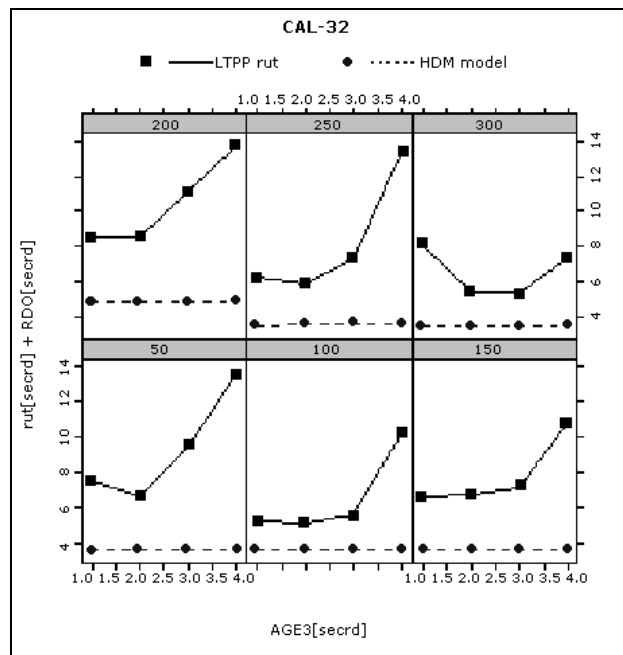**Figure A3   Comparing predicted and actual initial rut depths on LTTP Section 12, left wheelpath decreasing.**

Figure A4   Comparing predicted and actual initial rut depths on LTPP Section 12, right wheelpath decreasing.

A2   LTPP Section 19

Figure A5   Comparing predicted and actual initial rut depths on LTPP Section 19, left wheelpath increasing.

Figure A6   Comparing predicted and actual initial rut depths on LTPP Section 19, right wheelpath increasing.

Figure A7   Comparing predicted and actual initial rut depths on LTPP Section 19, left wheelpath decreasing.

Figure A8   Comparing predicted and actual initial rut depths on LTPP Section 19, right wheelpath decreasing.

A3   LTPP Section 32

Figure A9   Comparing predicted and actual initial rut depths in LTPP Section 32, left wheelpath increasing.

Figure A10   Comparing predicted and actual initial rut depths in LTPP Section 32, right wheelpath increasing.

Figure A11   Comparing predicted and actual initial rut depths in LTPP Section 32, left wheelpath decreasing.

Figure A12   Comparing predicted and actual initial rut depths in LTPP Section 32, right wheelpath decreasing.

74

A4   Relationships between the various factors

In Figures A13 and A14, rutting (in mm) is displayed for different compaction levels (pr). Figure A13 indicates the individual sections, while Figure A14 groups these values for the categories indicated.
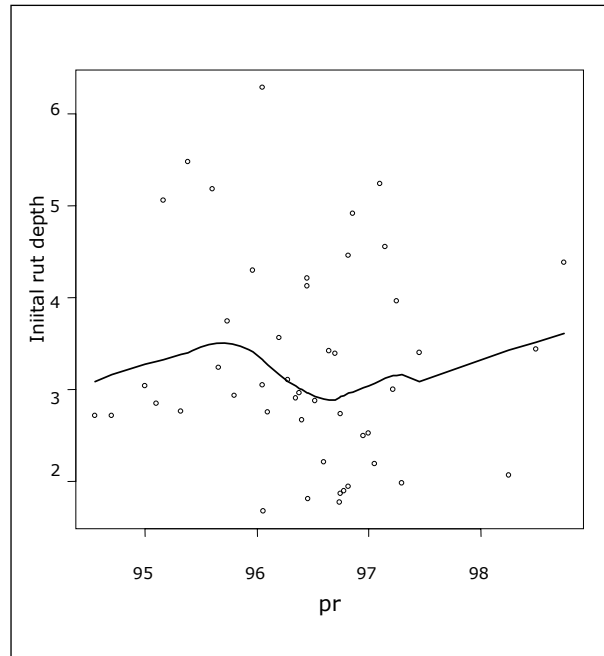
Figure A13   Initial rut depth as a function of the density.
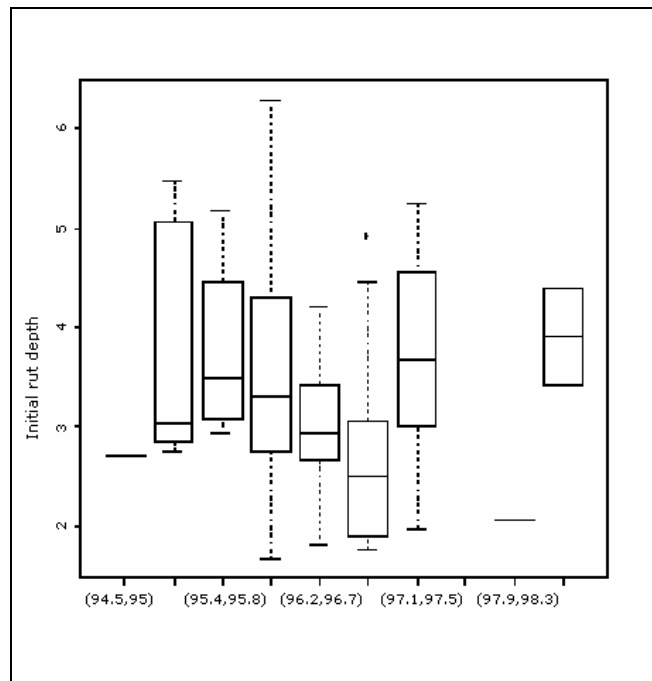
Figure A14   Initial rut depth as a function of the density (scatter diagram).
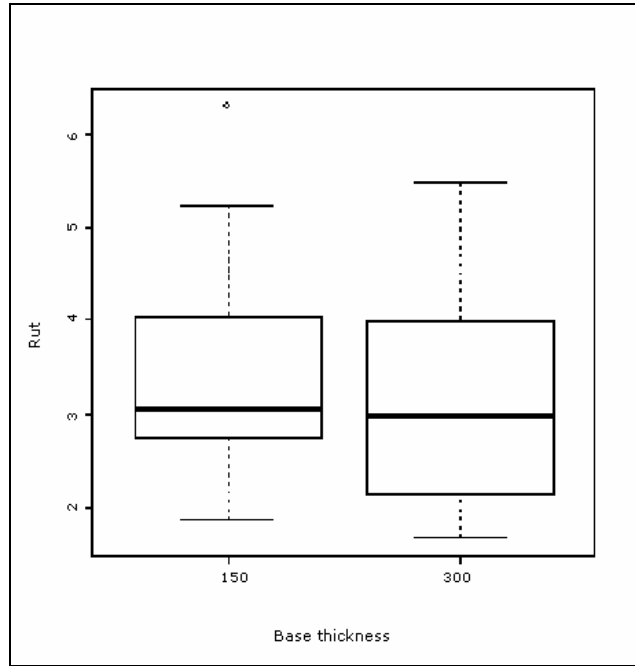
Figure A15   Box and whisker diagram showing initial rut depth (in mm) as a function of base layer thickness in mm.
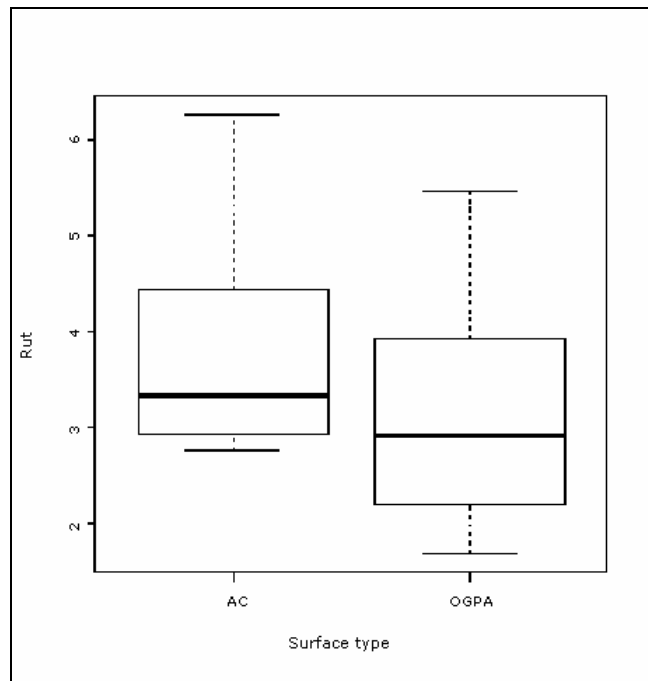
Figure A16   Box and whisker diagram showing initial rut depth in mm as a function surface type.
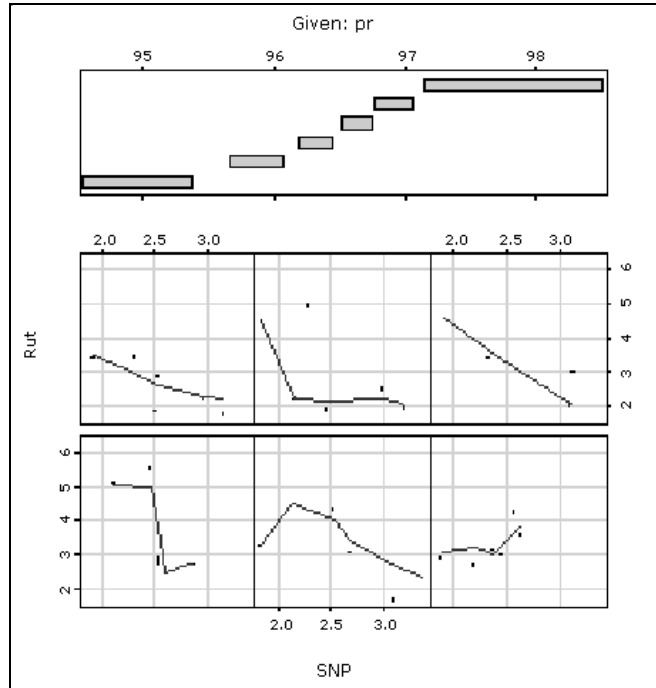
Figure A17 Testing the relationship of initial rut depth and SNP with compaction.
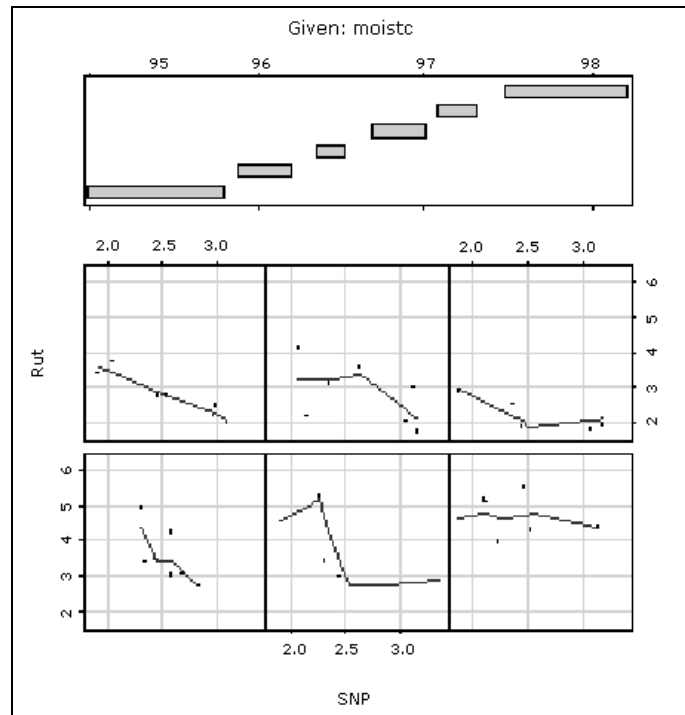
Figure A18 Testing the relationship of SNP and initial rut depth with moisture.
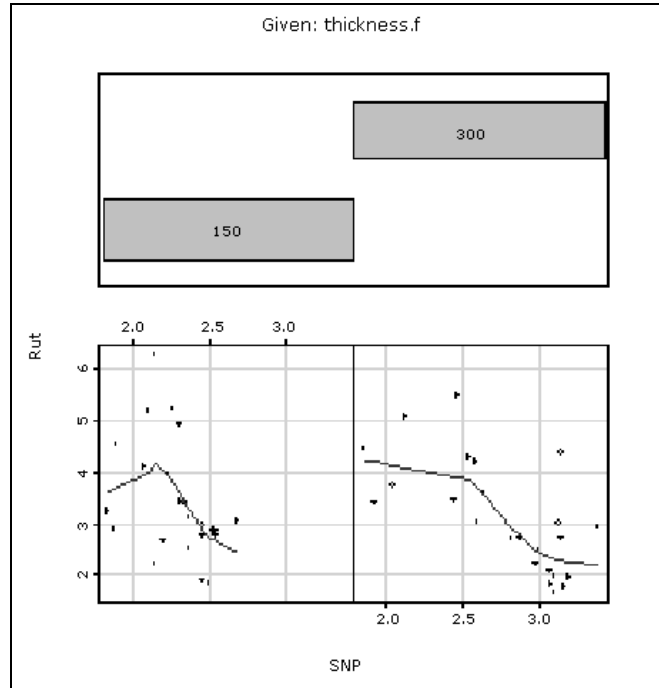
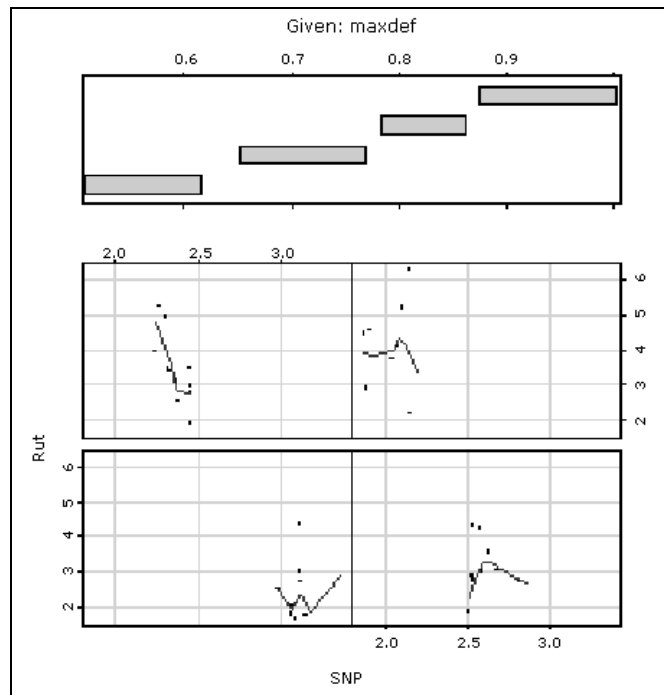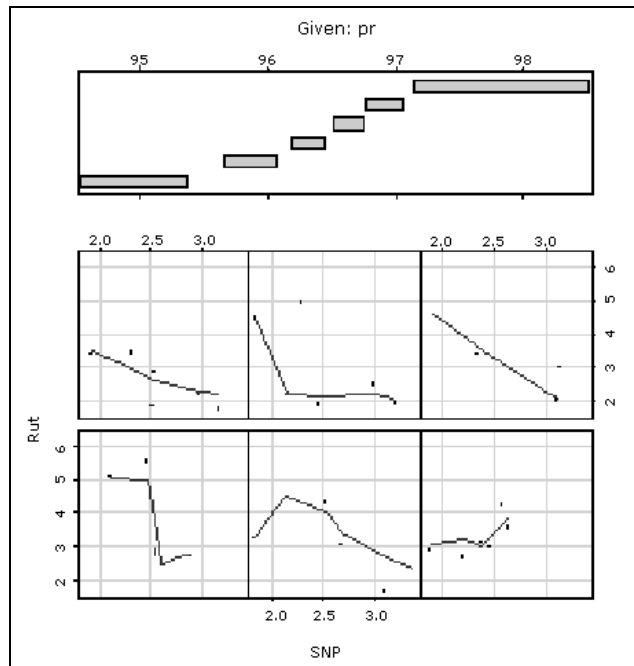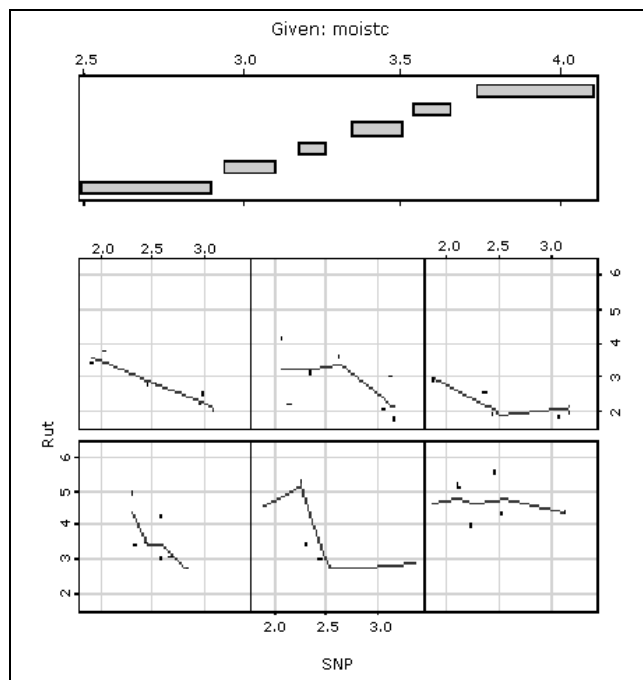**Figure A19   Testing the relationship of SNP and initial rut depth with layer thickness.**

Figure A20   Testing the relationship of SNP and initial rut depth with maximum deflection.

Figure A21   Testing the relationship between SNP and compaction (pr).

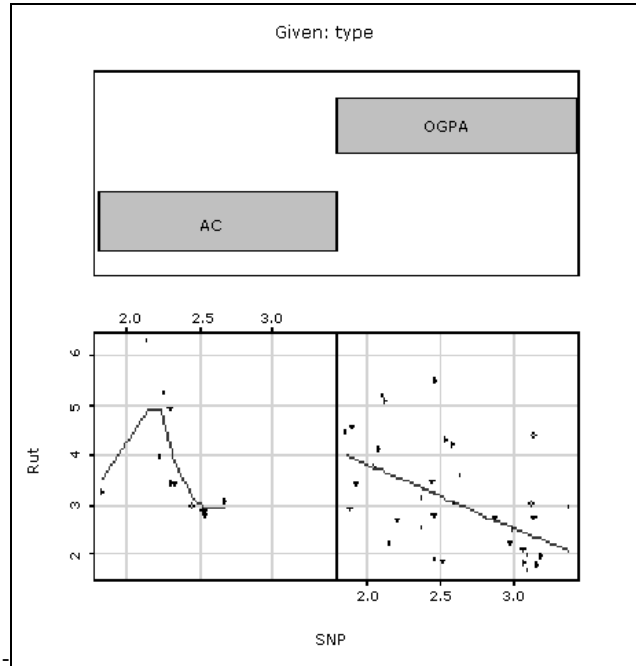**Figure A22   Testing the relationship between SNP and moisture content.**

Figure A23   Testing the relationship of SNP and initial rut depth with surface type.
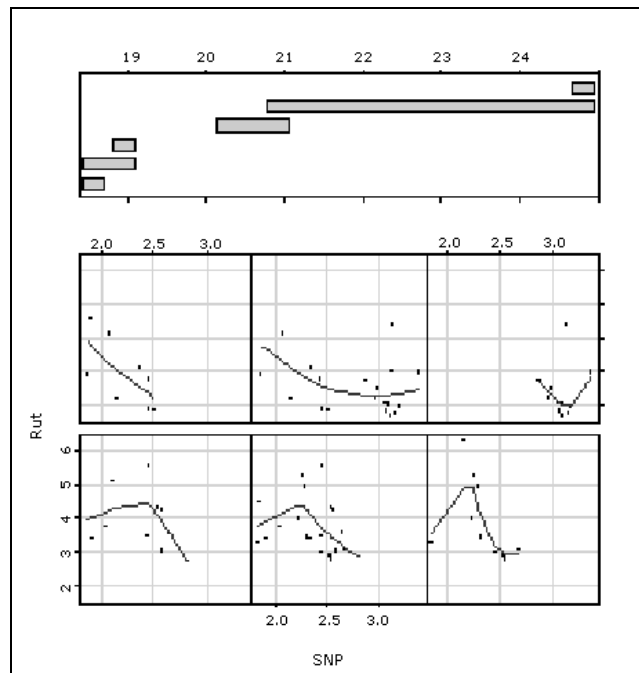

Figure A24   Testing the relationship of SNP and initial rut depth with CBR.

Appendix B: Additional results for exploratory and regression analysis for rut progression – LTPP data
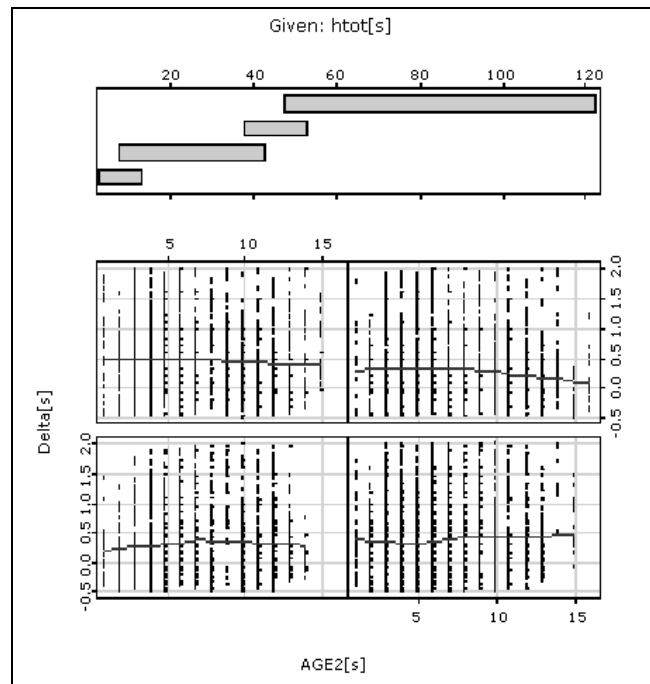

Figure B1   Incremental rutting as a function of surface age (AGE2) and total surface thickness.
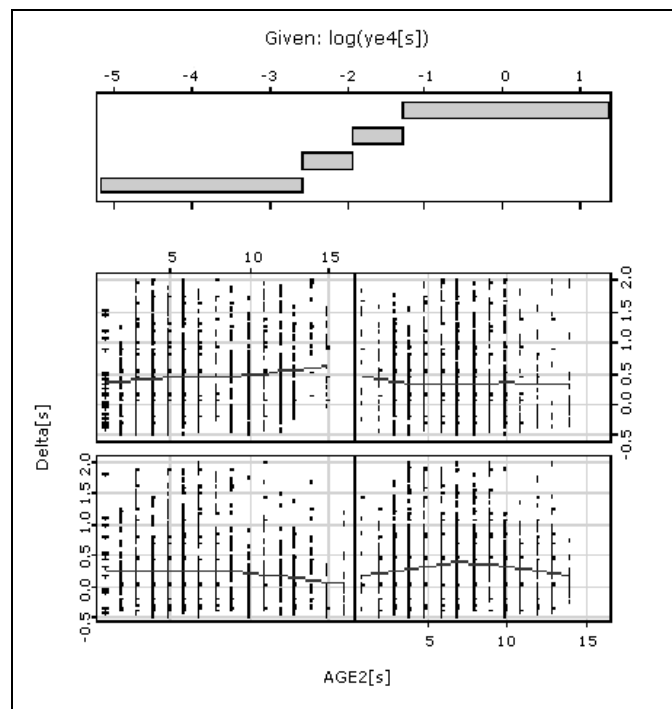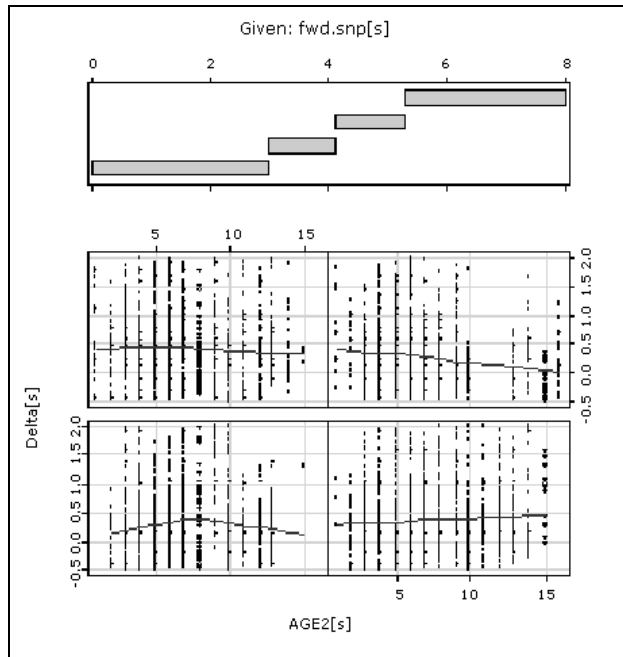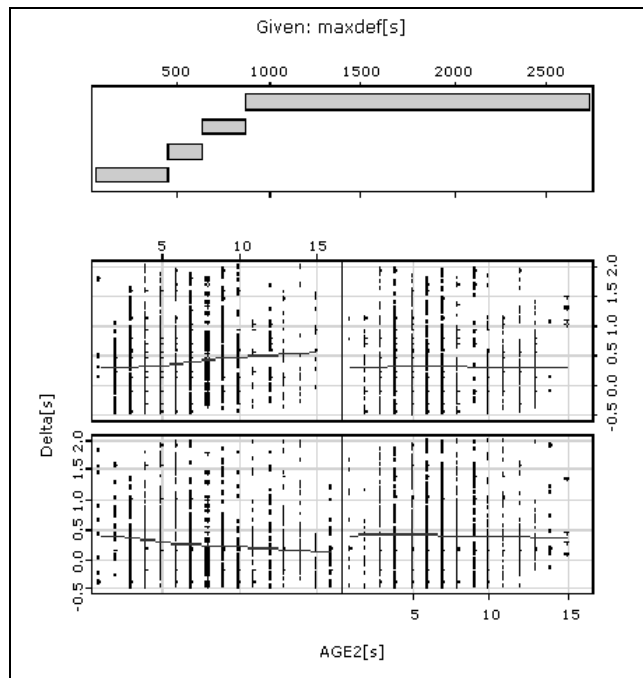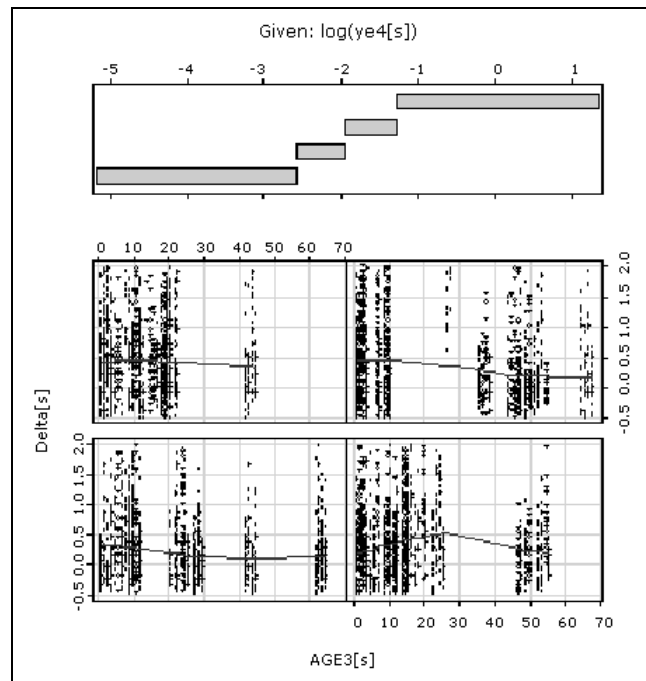

Figure B2   Incremental rutting as a function of surface age (AGE2) and log traffic loading (YE4).

Figure B3   Incremental rutting as a function of surface age (AGE2) and the SNP as inferred from the FWD.
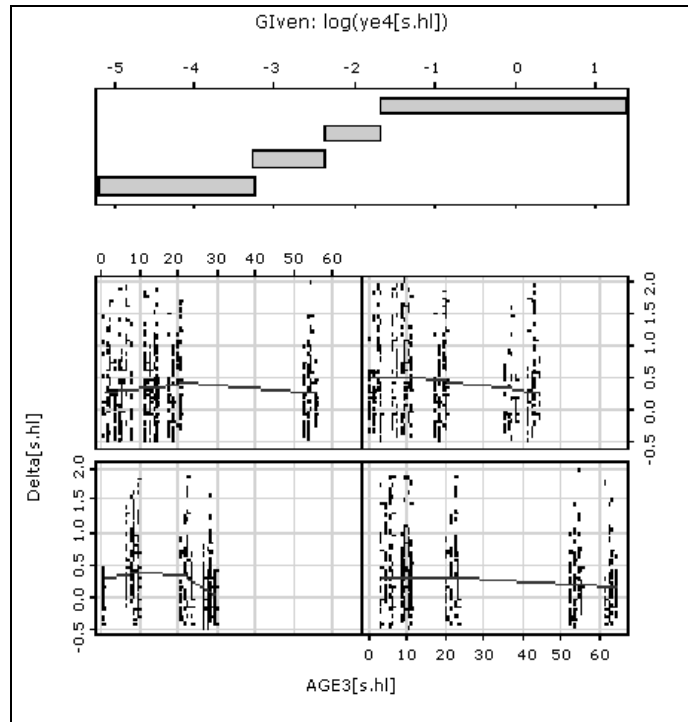

Figure B4   Incremental rutting as a function of surface age (AGE2) and FWD maximum deflection.

Figure B5   Incremental rutting as a function of pavement age (AGE3) and log total traffic loading (YE4).
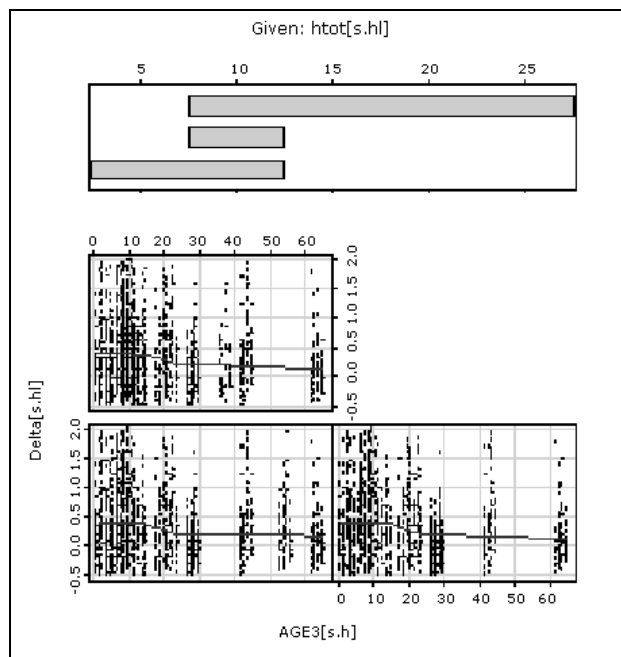
Figure B6   Incremental rutting as a function of pavement age (AGE3) and total surface depth (htot).

Figure B7   Comparing incremental rut rate for pavement thickness ≤150 mm as a function of pavement age (AGE3) and log total traffic loading (YE4).
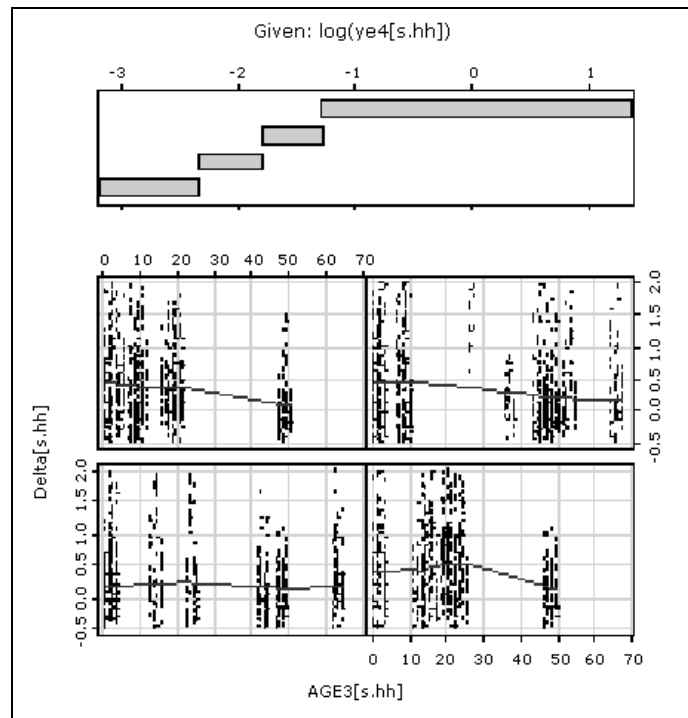
Figure B8   Comparing incremental rut rate for pavement thickness >150 mm as a function of pavement age (AGE3) and log total traffic loading (YE4).
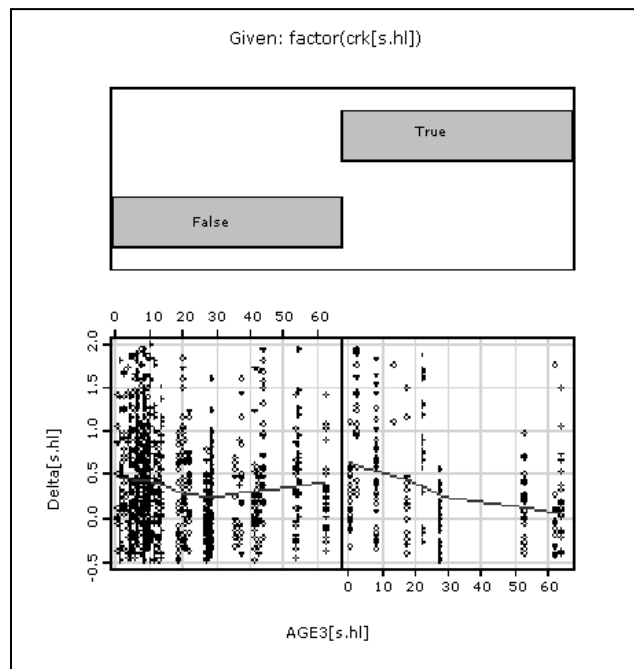
Figure B9 **Comparing incremental rut rate for pavement thickness ≤150 mm as a function of pavement age (AGE3) and log total surface thickness (htot).**
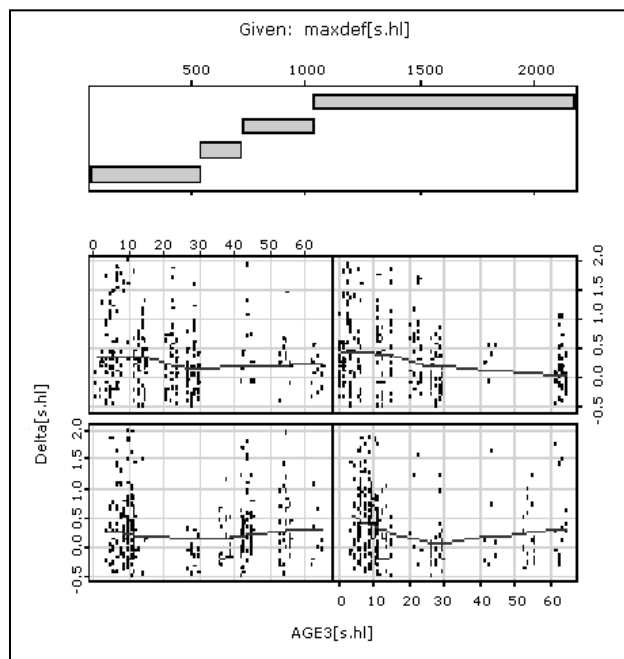
Figure B10 **Comparing incremental rut rate for pavement thickness >150 mm as a function of pavement age (AGE3) and log total surface thickness.**
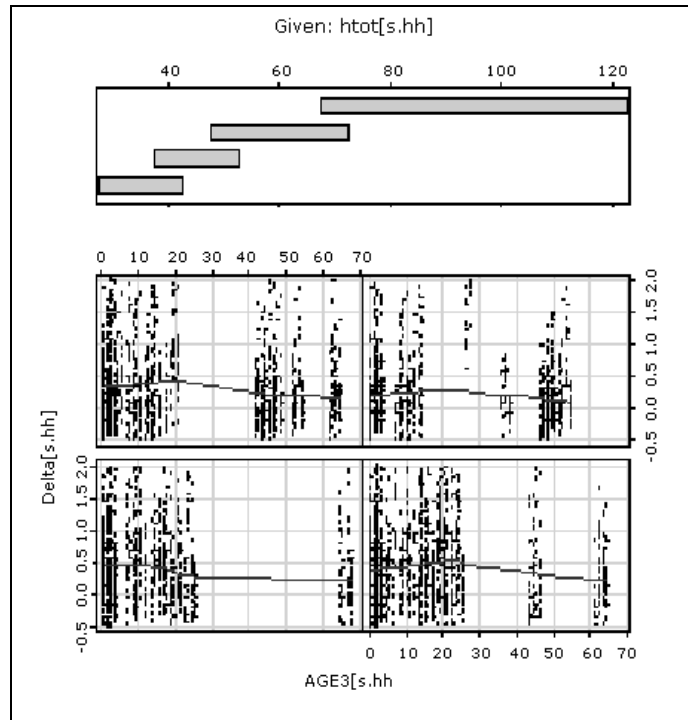
Figure B11   Comparing incremental rut rate for pavement thickness ≤ 150 mm as a function of pavement age (AGE3) and maximum deflection (maxdef).
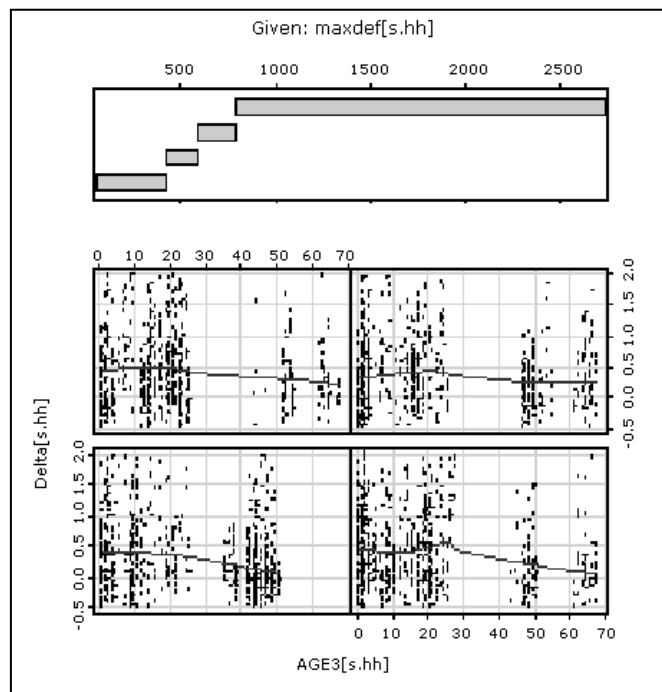
Figure B12   Comparing incremental rut rate for pavement thickness >150 mm as a function of pavement age (AGE3) and maximum deflection (maxdef).
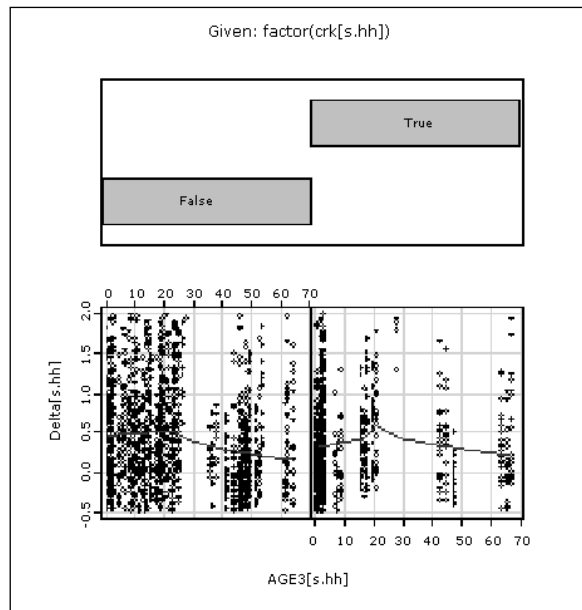
Figure B13   Comparing incremental rut rate for pavement thickness as a function of pavement age (AGE3) and cracked status of the surface.
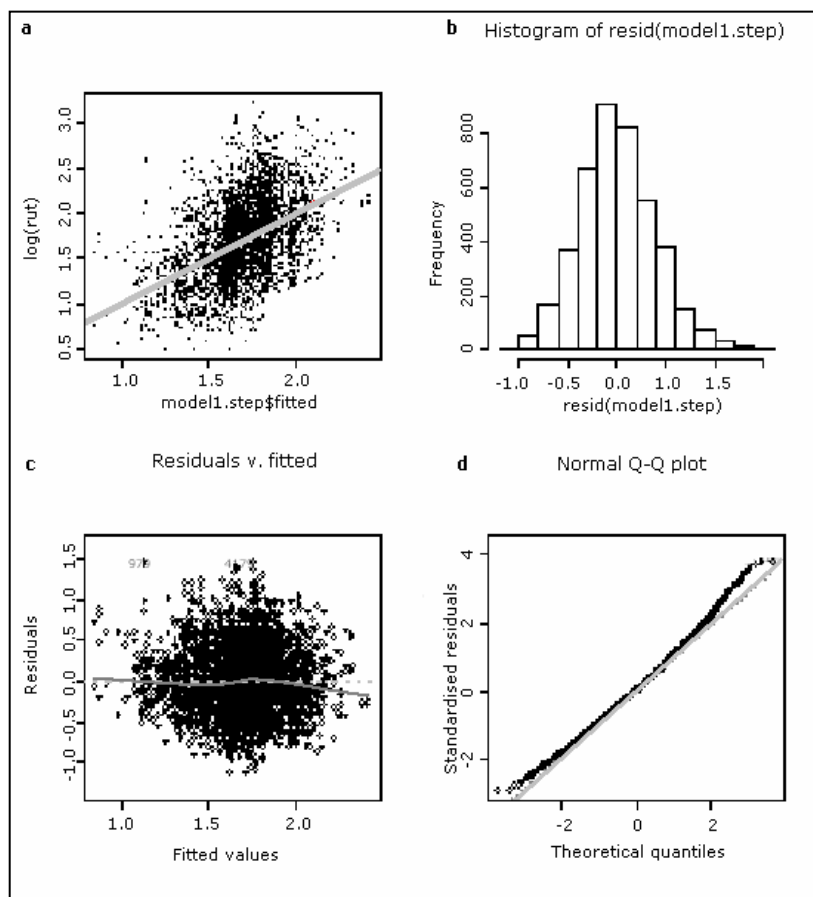
Figure B14   Predicting absolute rutting – residual plots for linear regression model based on the LTPP data.

Notes to Figure B14:
Residuals:

- Minimum   -1.15744
- First quartile   -0.25998
- Median   -0.01652
- Third quartile   0.23740
- Maximum   1.45406

Table B1   Model outcome statistics used to predict absolute rutting as shown in Figure B14.

| Coefficients:	Estimate	Std Error	t value	Pr(>|t|)	Significance
Intercept	-0.1263230	0.5697587	-0.222	0.824548	
AGE3	0.0169183	0.0047186	-3.585	0.000340	***
fwd.snp	0.0785535	0.0603471	1.302	0.193093	
log(ye4)	-0.4137261	0.1344762	3.077	- 0.002108	**
log(mmp)	0.3699118	0.1153410	3.207	0.001351	**
AGE2	0.2082950	0.0351116	5.932	3.23 e-09	***
htot.class: Thick Surface	1.4824972	0.1899374	7.805	7.46 e-15	***
crkTRUE	0.2879655	0.1649694	1.746	0.080960	.
fwd.snp:log(ye4)	-0.0581627	0.0036721	-15.839	<2 e-16	***
AGE3:log(ye4)	0.0063066	0.0007448	8.468	<2 e-16	***
fwd.snp:AGE2	-0.0181501	0.0020368	-8.911	<2 e-16	***
AGE3:log(mmp)	0.0037685	0.0010752	3.505	0.000462	***
log(ye4):AGE2	0.0218455	0.0033784	6.466	1.12 e-10	***
AGE3:fwd.snp	0.0005313	0.0003511	1.513	0.130332	
log(mmp): htot.class: Thick Surface	-0.2733493	0.0378736	-7.217	6.27 e-13	***
log(mmp):AGE2	-0.0134648	0.0067773	-1.987	0.047017	*
AGE2:htot.class Thick Surface	-0.0251453	0.0050656	-4.964	7.18 e-07	***
fwd.snp:htot.class Thick Surface	0.0191666	0.0106790	1.795	0.072758	.
AGE3:crkTRUE	0.0026143	0.0008544	3.060	0.002229	**
htot.class Thick Surface: crkTRUE	-0.1987098	0.0321242	-6.186	6.78 e-10	***
fwd.snp:crkTRUE	0.0142477	0.0096329	1.479	0.139198	
log(mmp):crkTRUE	-0.0778663	0.0328309	-2.372	0.017750	*
fwd.snp:log(mmp)	-0.0373158	0.0117812	3.167	-0.001549	**
log(ye4):log(mmp)	0.0915533	0.0284722	3.216	0.001312	**
AGE3:AGE2	0.0002880	0.0001345	2.142	0.032231	*
AGE2:crkTRUE	0.0084921	0.0050828	1.671	0.094848	.

Notes to Table B1:

- Residual standard error   0.3871 on 4162 degrees of freedom
- Multiple R^2 0.2373
- Adjusted R^2 0.2327
- F-statistic   51.79 on 25 and 4162 degrees of freedom
- p-value   <2.2 e-16
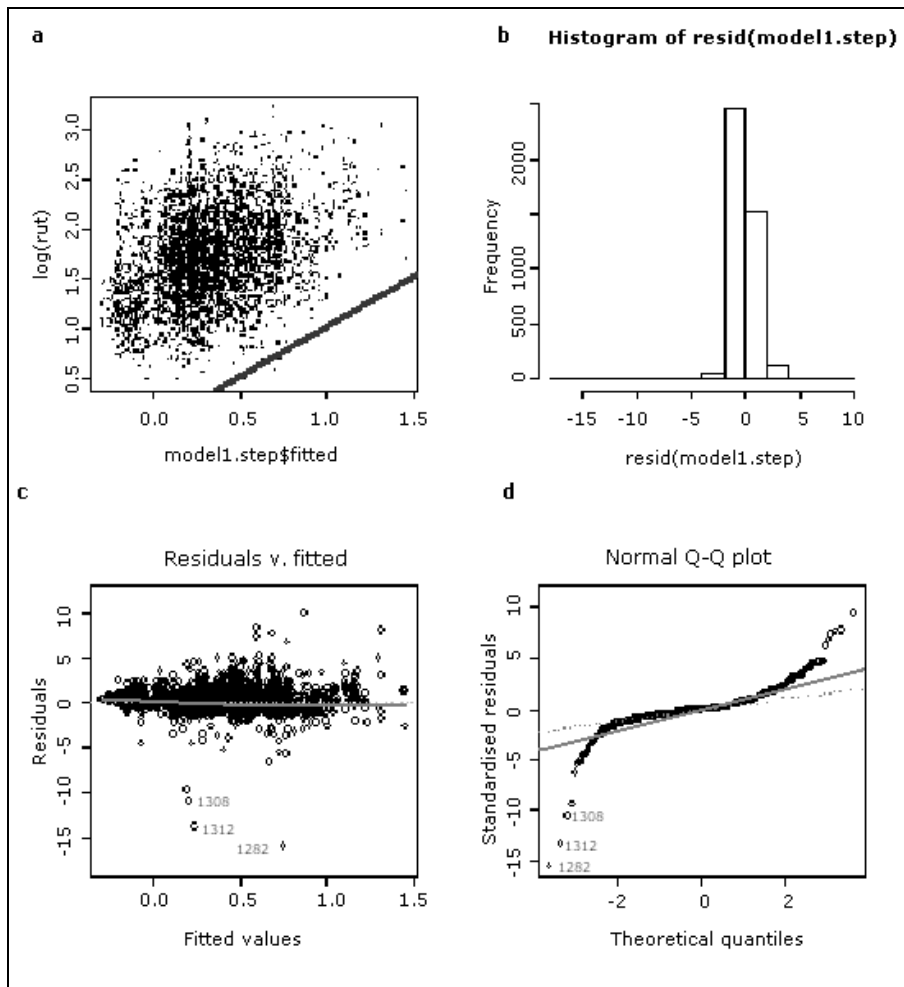
Figure B15   Predicting incremental rutting – residual plots for linear regression model (based on the LTPP data).

Notes to Figure B15:
lm(formula = delta ~ log(ye4) + age2 + fwd.snp + age3 + log(mmp) + log(ye4):age2 + log(ye4):fwd.snp + age2:age3 + age2:fwd.snp + log(ye4):age3 + age2:log(mmp) + age3:log(mmp))
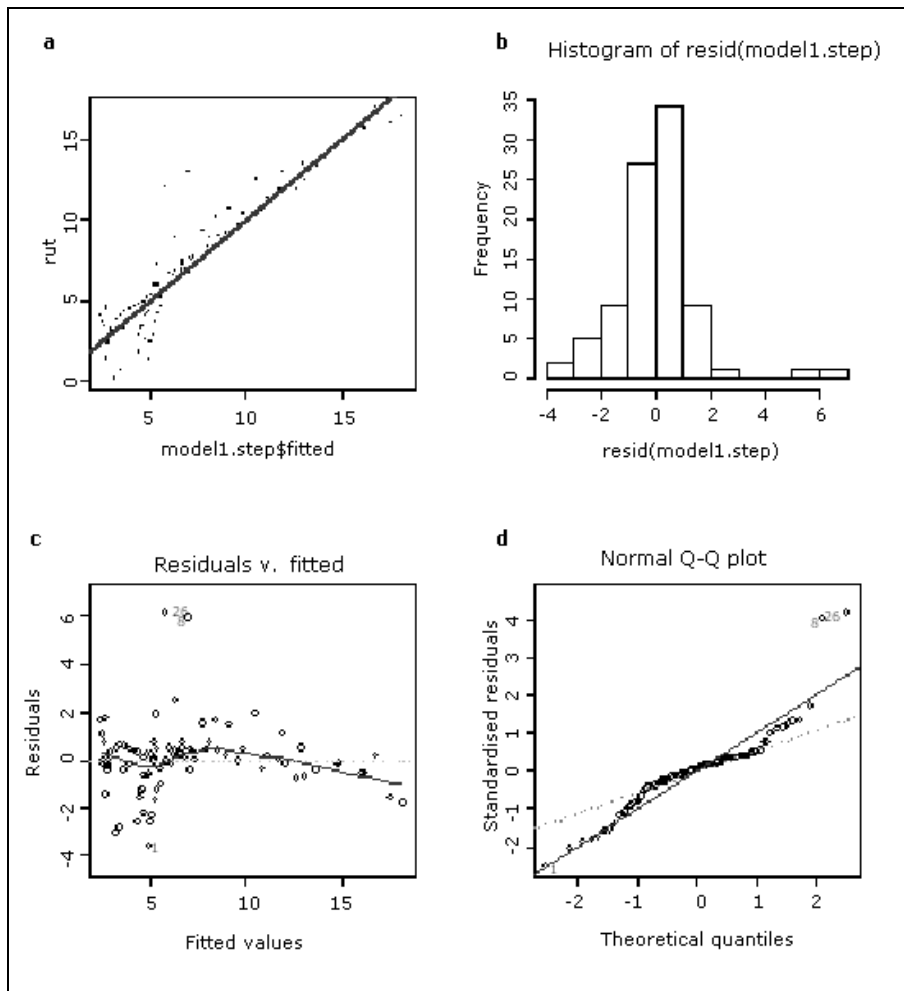
Residuals:

- Minimum   -16.1924
- First quartile   -0.4612
- Median   -0.1395
- Third quartile   0.3134
- Maximum   9.7941

Table B2   Model outcome statistics used to predict absolute rutting as shown in Figure B15.

Coefficients	Estimate	Standard error	t value	Probability (>|t|)	Significance
(Intercept)	-0.5162607	0.3887401	-1.328	0.18424	
log(ye4)	0.0985964	0.0554598	1.778	0.07551	.
AGE2	0.6403647	0.0842511	7.601	3.62 e-14	***
fwd.snp	-0.0379018	0.0270472	-1.401	0.16119	
AGE3	-0.0503622	0.0108565	-4.639	3.61 e-06	***
log(mmp)	0.0944936	0.0751051	1.258	0.20841	
log(ye4):AGE 2	0.0214097	0.0082714	2.588	0.00968	**
log(ye4):fwd.snp	-0.0450530	0.0087414	-5.154	2.67 e-07	***
AGE2:AGE 3	-0.0015290	0.0003282	-4.658	3.29 e-06	***
AGE2:fwd.snp	-0.0180834	0.0038786	-4.662	3.22 e-06	***
log(ye4):AGE 3	0.0047087	0.0015342	3.069	0.00216	**
AGE2:log(mmp)	-0.0936187	0.0164865	-5.678	1.45 e-08	***
AGE3:log(mmp)	0.0142727	0.0025456	5.607	2.19e-08	***

Notes to Table B2:

- Residual standard error   1.049 on 4175 degrees of freedom
- Multiple R^2 0.06795
- Adjusted R^2 0.06527
- F-statistic   25.36 on 12 and 4175 degrees of freedom
- p-value   < 2.2 e-16

Figure B16   Predicting absolute rutting – residual plots for the linear regression model based on the CAPTIF data.

Notes to Figure B16:
- Call: lm(formula = rut ~ reps + d.factor + type + reps:d.factor + reps:type)
- Residuals:
    - Minimum   3.6414
    - First quartile   -0.5632
    - Median   0.0561
    - Third quartile 0.4955
    - Maximum   6.1394

91

Table B3   Model outcome statistics used to predict absolute rutting as shown in Figure B16.

Coefficients	Estimate	Standard error	t value	Probability (>|t|)	Significance
Intercept	3.293 e+00	9.053 e-01	3.637	0.000489	***
reps	9.673 e-06	1.972 e-06	4.905	4.9 e-06	***
d.factor1.34	1.652 e+00	7.392 e-01	2.235	0.028254	*
d.factor1.63	1.999 e+00	7.392 e-01	2.704	0.008376	**
d.factor2.31	-2.923 e-01	7.555 e-01	-0.387	0.699899	
type: OGPA	-5.134 e-01	7.392 e-01	-0.695	0.489370	
reps:d.factor1.34	4.316 e-06	1.610 e-06	2.681	0.008941	**
reps:d.factor1.63	7.828 e-06	1.610 e-06	4.862	5.8 e-06	***
reps:d.factor2.31	3.591 e-08	1.623 e-06	0.022	0.982399	
reps:typeOGPA	-4.834 e-06	1.610 e-06	-3.003	0.003583	**

Notes to Table B3:
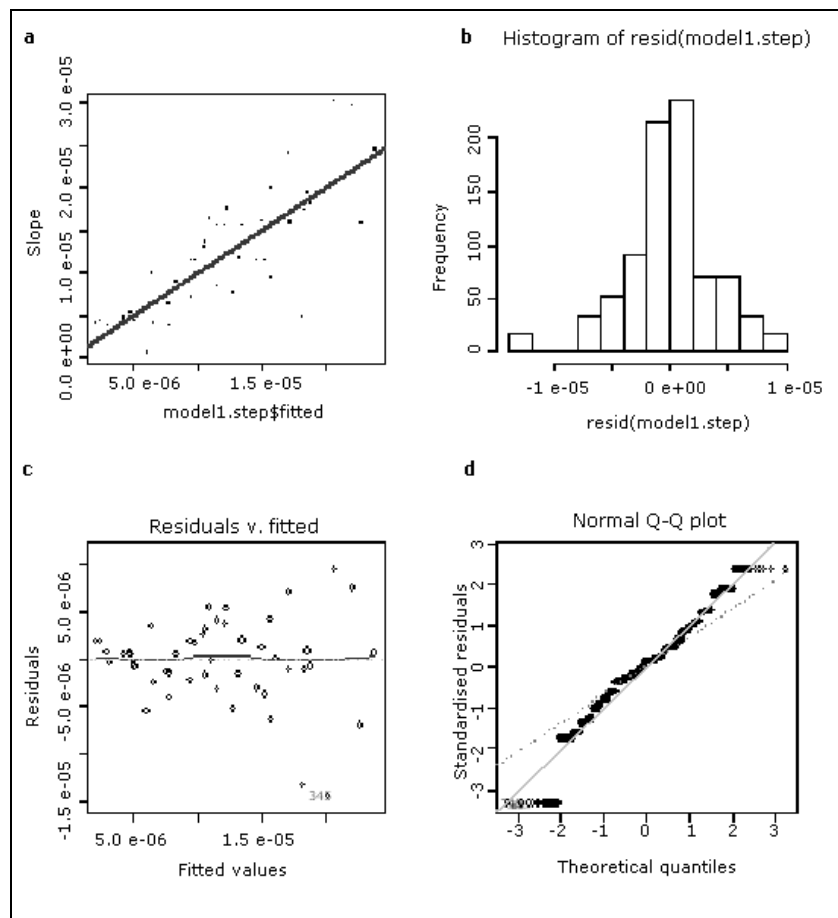
- Residual standard error   1.539 on 79 degrees of freedom
- Multiple R^2 0.8775
- Adjusted R^2 0.8636
- F-statistic   62.88 on 9 and 79 degrees of freedom
- p-value   <2.2 e-16

1.1   Appendix C: Additional results for exploratory and regression analysis for rut rate progression
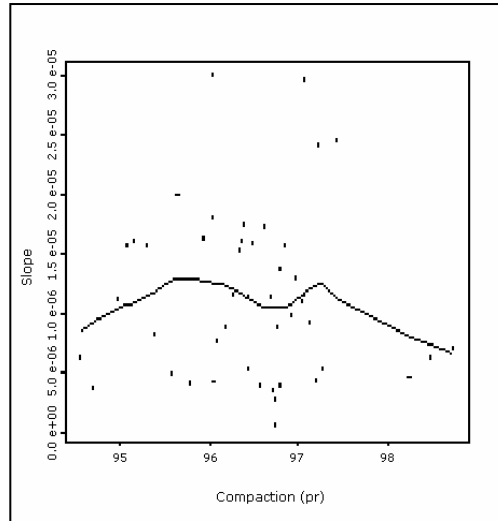
Figure C1   Relationship between rut rate (slope) and the compaction (pr).

Figure C2   Residual plots for the regression outcome performed on the stable rut rate progression.

Table C1   Model result statistics used to regress the stable rut rate progression as shown in Figure C2.

Coefficients	Estimate	Standard error	t value	Probability (>|t|)	Significance
Iintercept	1.40 e-04	1.95 e-04	0.715	0.474728	
SNP	-4.31 e-04	6.63 e-05	-6.499	1.39 e-10	***
Moisture content	2.75 e-04	6.66 e-05	4.127	4.05 e-05	***
thickness.f300	3.27 e-04	5.78 e-05	5.665	2.03 e-08	***
log(rut50k)	-1.88 e-06	7.68 e-06	-0.244	0.807006	
Compaction (pr)	-1.89 e-06	2.06 e-06	-0.917	0.359647	
moistc:thickness.f300	1.08 e-05	1.56 e-06	6.956	7.07 e-12	***
SNP:moistc	-9.94 e-06	1.94 e-06	-5.133	3.55 e-07	***
SNP:thickness.f300	-1.12 e-05	1.38 e-06	-8.116	1.73 e-15	***
moistc:log(rut50k)	-6.32 e-06	2.04 e-06	-3.101	0.001995	**
thickness.f300:log(rut50k)	-1.48 e-05	2.04 e-06	-7.261	8.86 e-13	***
SNP:log(rut50k)	1.33 e-05	2.43 e-06	5.459	6.31 e-08	***
SNP:pr	4.67 e-06	6.70 e-07	6.966	6.65 e-12	***
thickness.f300:pr	-3.34 e-06	5.56 e-07	-5.999	2.97 e-09	***
moistc:pr	-2.60 e-06	7.04 e-07	-3.694	0.000235	***

Notes to Table C1:

- Residual standard error   4.037 e-06 on 831 degrees of freedom
- Multiple R^2 0.6713,
- Adjusted R^2 0.6658
- F-statistic   121.2 on 14 and 831 degrees of freedom
- p-value   <2.2 e-16

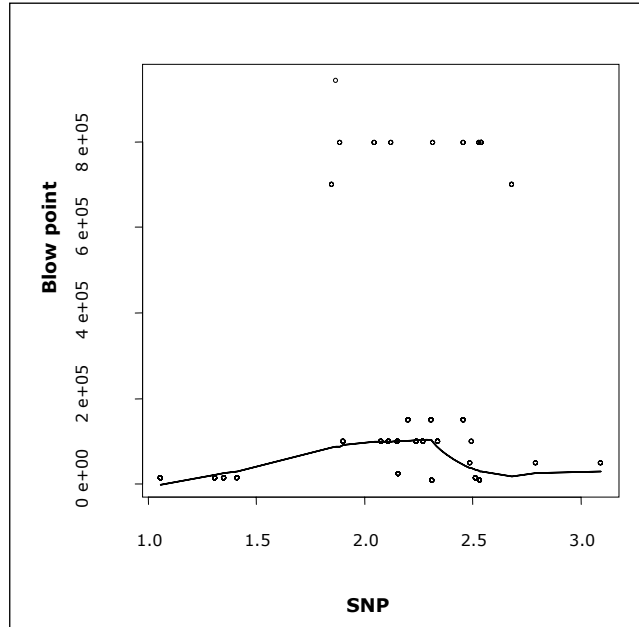# Appendix D: Additional outputs for accelerated rut progression

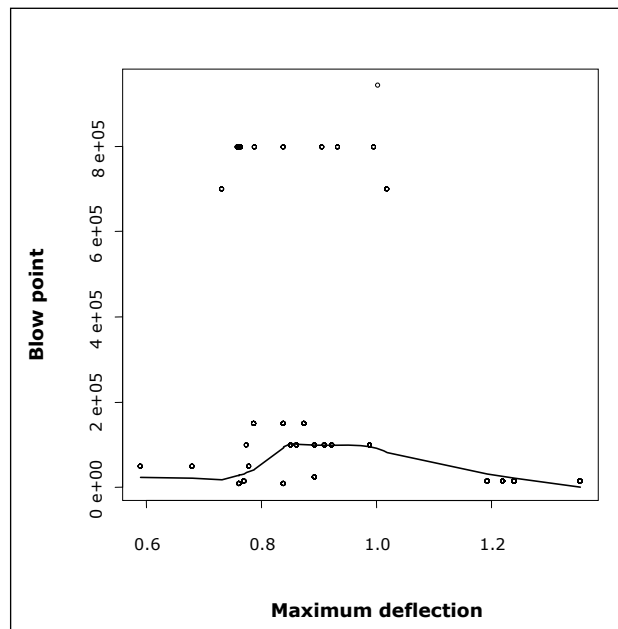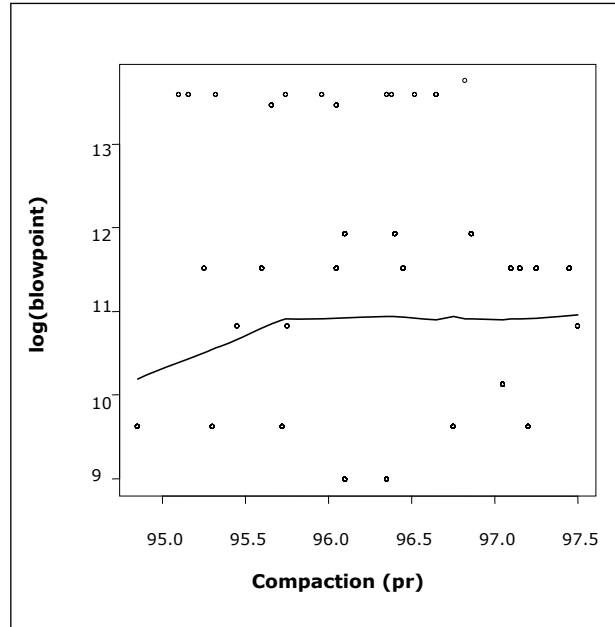**Figure D1   Relationship between the accelerated rut stage (blow point) and SNP.**
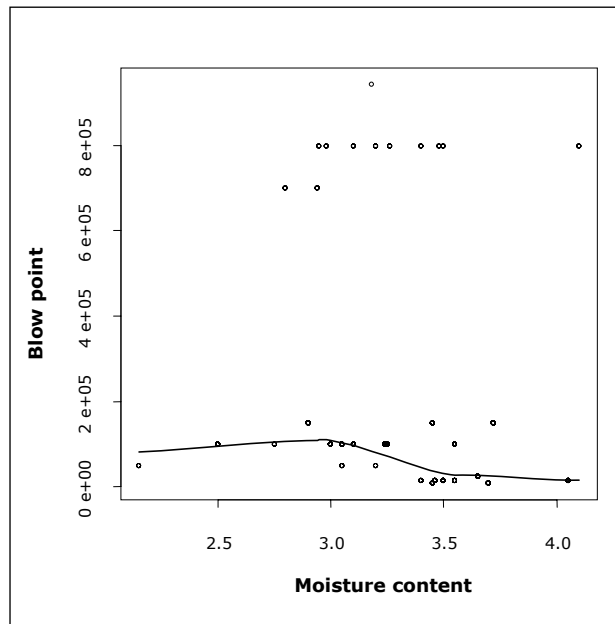

Figure D2   Relationship between the accelerated rut stage (blow point) and deflection compaction (pr).

Figure D3 **Relationship between the accelerated rut stage (blow point) and compaction (pr).**

Figure D4 **Relationship between the accelerated rut stage (blow point) and moisture content.**

Appendix E   Glossary and abbreviations

AADT: Annual Average Daily Traffic volume

AC: Asphalt Concrete

AGE2:   Age of the surface

AGE3:   Age of the pavement

AIC: Akaike's Information Criterion

BCI: FWD (q.v.) Base Curvature Index

BDI: FWD (q.v.) Base Damage Index

CAPTIF: Canterbury Accelerated Pavement Testing Indoor Facility

CBR: Californian Bearing Ratio

CUSUM: **Cum**ulative deviation **Sum**s

D0–D9:   FWD (q.v.) Deflections for given geophones.

dTIMS: pavement deterioration modelling system

ESA: Equivalent Standard Axles

FWD: Falling Weight Deflectometer

GAM: General Additive Model

HTOT: Total surface thickness of all layers in a pavement

IRI: International Roughness Index (measured in mm/km)

LTPP: Long Term Pavement Performance

maxdef: Maximum Deflection from all geophones

MMP: Mean Monthly Precipitation

OMC: Optimum Moisture Content

OGPA: Open-Graded Porous Asphalt

OTCI: Time to Crack Initiation

SCI: FWD (q.v.) Surface Curvature Index

Sens: Climatic **Sens**itivity Area

SF1 and SF2: FWD (q.v.) deflection Shape Factors 1 and 2

SLAVE: Simulated Loading And Vehicle Emulator

SNP: Structural Number of the Pavement

Stat.crx: Cracked status

wpriri: Wheelpath IRI (q.v.)

YE4:   annual number of ESA (q.v.)

Benchmarking Pavement Performance between Transit's LTPP and CAPTIF Programmes

Land Transport New Zealand
Research Report 319